

STUDY OF WELD JOINT CHARACTERIZATION USING MICROWAVE HYBRID HEATING

THESIS

Submitted to

DELHI TECHNOLOGICAL UNIVERSITY

For the award of the degree of

DOCTOR OF PHILOSOPHY

IN

MECHANICAL ENGINEERING

By

UMA GAUTAM

(2K16/Ph.D/ME/54)

Under the supervision of

PROF VIPIN

(Department of Mechanical Engineering, DTU)



**DEPARTMENT OF MECHANICAL ENGINEERING
DELHI TECHNOLOGICAL UNIVERSITY
(Formerly Delhi College of Engineering)
Main Bawana Road, Shahabad Daultpur, Delhi - 110042, India**

2023

CERTIFICATE

This is to certify that the thesis entitled “**Study of Weld Joint Characterization using Microwave Hybrid Heating**” submitted to the Delhi Technological University, Delhi -110042, is fulfilment of the requirements for the award of degree of Doctorate in Philosophy in Mechanical Engineering embodies the original research work carried out by **Mrs. UMA GAUTAM**, Enrollment No: 2K16/Ph.D/ME/54 under my supervision. This work has not been submitted in part or full for any other degree or diploma of this or any other University.

Prof. VIPIN

Department of Mechanical Engineering

Delhi Technological University, Delhi.

DECLARATION

I certify that the work which is being presented in this thesis entitled “**Study of Weld Joint Characterization using Microwave Hybrid Heating**” in the partial fulfilment of requirement for the award of degree of Doctorate in Philosophy submitted in the Department of Mechanical Engineering at Delhi Technological University, is an authentic record of my own work carried out during a period from August 2016 to March 2023, under the supervision of **Prof. VIPIN**, Department of Mechanical Engineering, Delhi Technological University, Delhi. The matter presented in this thesis has not been submitted in any other University/Institute for the award of any degree or diploma.

(UMA GAUTAM)

Roll No: 2K16/Ph.D/ME/54

ACKNOWLEDGEMENT

With great pleasure, I wish to express my deep gratitude to my supervisor, Prof. Vipin, Department of Mechanical Engineering, Delhi Technological University, for providing tremendous direction, insight, constructive comments, encouragement, and support during my research project. I have the utmost respect for him and am really thankful to him for providing me with the materials, tools, and information I needed. He is a wonderful thinker who is constantly seeking fresh perspectives and new approaches to comprehend the world around us. For my research, I could not have hoped for a greater mentor and advisor.

I humbly express my gratitude to Chairman of DRC committee, Dean and Head of Department of Mechanical, Production, Industrial, and Automobile Engineering, for his wise advice and ongoing support. Thanks to the SRC Committee and the Professors of Delhi Technological University's Department of Mechanical Engineering for their advice and encouragement throughout the research process. The technical personnel at DTU, particularly Mr. Sandeep for his assistance in carrying out the XRD investigations and Mr. Tek Chand for his assistance in disclosing the microstructures, deserve a special word of thanks as well.

I would like to thank Dr. Dheeraj Gupta, Professor and Head in the central workshop at the Thapar Institute of Engineering & Technology, Patiala, for his invaluable guidance, numerous suggestions and continued support throughout this research work. I am profoundly grateful to Dr Kanwarjeet Singh, Assistant Professor in Mechanical Engineering at DSEU Okhla-II, with reverence for helping me with necessary information.

I owe a great deal of gratitude to my husband, Er. P.D. Kabeer, and my son, Chaitanya Kabeer, for their support and love in helping me achieve higher goals in life. Without their inspiration and encouragement, pursuing my Ph.D. work would not have been feasible. I appreciate their concern and support while I worked on my studies.

UMA GAUTAM

ABSTRACT

One of the connecting processes that have the most potential that has developed is welding. Throughout their growth, many welding techniques have been developed. Any nation's manufacturing industry is crucial to its economic growth, but it also uses more than 30% of the nation's energy resources. Technologists, researchers, and academics are always trying to process materials efficiently in order to lower manufacturing costs and conserve energy in order to tackle such scenarios. Due to increased energy use, pollution levels, low productivity, and the production of more flaws in manufactured components, traditional manufacturing techniques are becoming obsolete. To lower production or manufacturing costs, processing times, and to improve product quality, alternative processing methods are necessary.

The development of sustainable, green, and energy-efficient processing techniques is the main emphasis at the moment. Therefore, it is crucial for researchers to look for alternate processing methods and procedures that might potentially compensate for or lessen the shortcomings of current ones. The established procedures are anticipated to generate better-quality goods at an efficient processing cost while reducing CO₂ or other undesired hazardous gas emissions and improving energy efficiency.

There has been a lot of work published on the microwave joining of bulk metals and the coating of metallic-based powders on metallic surfaces. The researchers were inspired to investigate the possibilities of microwave heating in powdered metal joining techniques since the joining and cladding were accomplished with partial melting of metallic powders. However, the majority of the research focused on the sintering of metallic powders and gave researchers a chance to explore the possibility of using microwaves to melt metallic-based powders.

In the current study, stainless steel 304 (40x20x3) mm is joined using microwave radiation, and the impact of various process parameters on the mechanical characteristics of welded butt joints is examined. As a microwave applicator, a domestic IFB microwave oven operating at 2.45 GHz and 900 W of fixed frequency and power respectively is employed with hybrid heating technique.

Tensile strength, microhardness, and surface temperature were chosen as the output process parameters that are to be optimised, while varied sizes of nickel powder, variation in slurry by weight, and welding time were chosen as the input process parameter. Response surface methodology (RSM), which is based on statistics, was used to conduct the tests, evaluate the findings, and improve the settings. The design matrix for welding the butt joints was created using rotatable central composite design with face centered (CCDFC). The matrix was created using three factors, each with three levels. Twenty trials in all, including the centre points, were carried out using a standard microwave oven.

An ANOVA (analysis of variance) was used to analyse how the process factors affected the weldments mechanical characteristics. The relationship between the input parameter and the outcomes has been demonstrated empirically. This model is capable of predicting both the primary impacts and the combined effects of the two elements that make up the selected welding process parameters.

The X-Ray Diffraction patterns (phase analysis), mechanical characteristics (microhardness, tensile strength), microstructural characterizations (using optical microscope and field emission scanning electron microscopy), and surface temperature measurement were all used to evaluate the generated joints. Optical microscopy and a field emission scanning electron microscope (FESEM) are used for microstructural characterization. Tensile testing and microhardness testing were done for mechanical characteristics. An infrared gun is employed to determine the surface temperature of the joint region.

Overall, the findings supported the assertion that metal components were effectively joined using microwave radiation. Using the CCDFC approach, the ideal values for the input variables welding time, particle size, and slurry weight were found. The impact of welding time (microwave) was greatest, followed by powder particle size and weight of the slurry material. As welding time and slurry weight increases, tensile strength, microhardness, and surface temperature of the welded material all increase, but as particle size increases, all three output variables decreases.

The greatest values of tensile strength (501MPa), microhardness (454Hv), and surface temperature (932⁰C) in the welded region are obtained using experimental settings of 13 min. of welding time, 3 g of slurry weight, and 5 μm of powder size.

The high microwave heating caused different intermetallic phases to develop, as demonstrated by the XRD examination of welded joint. Formation of Carbides (Cr₃C₂ and Fe₂C) and phases of iron and nickel (NiSi and FeSi) are detected at peak in the research.

Microstructure and FESEM study findings showed that microwave processing generates superior microstructures for the highest values of welding time and slurry weight and the lowest value of powder size with fewer flaws when compared to other input values. Absolute fusion of flaring surfaces and appropriate metallurgical bonding with metal are achieved by volumetric and uniform heating throughout the joint. Both brittle and ductile modes of failure were seen during the joint fracture. According to the Energy Dispersive Spectroscopy (EDS) analysis, the joint section contains higher chromium and carbon content for the maximum output values.

TABLE OF CONTENTS

CERTIFICATE	i
DECLARATION	ii
ACKNOWLEDGEMENT	iii
ABSTRACT	iv
TABLE OF CONTENTS	vii
LIST OF FIGURES	xii
LIST OF TABLES	xvii
NOMENCLATURE	xviii
LIST OF SYMBOLS	xix
CHAPTER 1: INTRODUCTION	1
1.1 Introduction	1
1.2 Metal Joining Process	2
1.2.1 Types of joining process.....	2
1.3 Introduction of Microwave	6
1.3.1 Development of Microwaves	7
1.3.2 Mechanisms of Heating by Microwaves	8
1.3.3 Microwave – Material Interactions	13
1.4 Application of Microwaves	16
1.4.1 Communications.....	16
1.4.2 Radio Detection and Ranging (Radar).....	16
1.4.3 Electronic Warfare.....	17
1.4.4 Medical Applications.....	17
1.4.5 Scientific Applications	17
1.4.6 Industrial and Commercial Applications.....	18
1.4.7 Potential Applications	19
1.4.8 Microwave Heating/Processing of Materials	19
1.5 Characteristics of Microwave Heating	19
1.5.1 Penetrating Radiation	20

1.5.2 Rapid Heating	22
1.5.3 Controllable Field Distributions	22
1.5.4 Selective Heating of Materials.....	23
1.5.5 Self-limiting Characteristic	23
1.6 Microwave Heating Types.....	23
1.6.1 Microwave Assisted Processing of Materials.....	24
1.6.2 Selective Heating.....	25
1.7 Development of Microwave Heating	26
1.8 Overview of the thesis	30
1.9 Summary	31
CHAPTER 2: LITERATURE REVIEW.....	33
2.1 Introduction	33
2.2 Thermal Application of Microwaves	33
2.2.1 Food Processing.....	33
2.2.2 Ceramic Processing	35
2.2.3 Polymer Processing	37
2.2.4 Microwave Processing of Composites	38
2.2.5 Microwave joining of ceramic and polymer composites	40
2.2.6 Environmental Applications:.....	41
2.3 Specimen Based Developments	42
2.4 Susceptors Based Developments	49
2.5 Interface Powders Based Developments	50
2.6 Experimental Set-up Based Developments	54
2.7 Power Consumption in Microwave Processing of Materials	56
2.8 Microwave Materials Sintering Processing	58
2.9 Microwave Drilling	63
2.10 Microwave-Processed Coatings/Claddings.....	64

2.11 Microwave Melting of Metals	71
2.12 Microwave Joining of Bulk Materials	72
2.13 Some Industrial Applications of Microwaves	79
2.14 Future Perspective of Microwave Materials Processing	82
2.15 Research Gap	82
2.16 Motivation	83
2.17 Research Objectives	83
2.18 Scope of the Work	84
2.19 Flow Chart of the Present Work	85
2.20 Summary	86
CHAPTER 3: EXPERIMENTAL SETUP	87
3.1 Microwave Oven	87
3.2 Tensile Testing	88
3.3 Microhardness	90
3.4 Optical Microscopy	92
3.5 FE-SEM	95
3.6 XRD	97
3.7 Surface Temperature Measurement	99
3.8 Summary	100
CHAPTER 4: METHODOLOGY	101
4.1 Material Selection	101
4.1.1 Substrate / Base Material	102
4.1.2 Refractory Brick	105
4.1.3 Interfacing Material	106
4.1.4 Separator Sheet	108
4.1.5 Susceptor Powder	109

4.2 Process Parameter	109
4.2.1 Limits of the Process Parameter and Design Matrix.....	111
4.2.2 Optimization of Process Parameters.....	112
4.2.3 Response Surface Methodology.....	112
4.3 Experimental Setup	113
4.3.1 Trial Runs.....	116
4.3.2 Final Experiment.....	117
4.4 Sample Preparation for Testing	122
4.4.1 Macrostructure Characterization.....	122
4.4.2 Microstructure Characterization.....	123
4.4.3 Microhardness.....	124
4.4.4 Tensile Testing.....	125
4.5 Summary	126
CHAPTER 5: RESULTS & DISCUSSIONS	128
5.1 Introduction	128
5.2 Optimization of Process Parameters	129
5.3 Experimental Results for Tensile strength	131
5.3.1 Mathematical Model Equation of Tensile strength.....	133
5.3.2 Checking the adequacy of the model for tensile strength.....	133
5.3.3 Effect of process parameter on tensile strength.....	137
5.4 Experimental Results for Micro hardness	142
5.4.1 Mathematical Model Equation for Microhardness.....	144
5.4.2 Checking the adequacy of the model for Micro hardness.....	144
5.4.3 Effect of process parameter on Microhardness.....	147
5.5 Experimental Results for Surface Temperature	151
5.5.1 Mathematical Model Equation for surface temperature.....	152
5.5.2 Checking the adequacy of the model for surface temperature.....	152

5.5.3 Effect of process parameter on surface temperature	155
5.6 X-Ray Diffraction	159
5.7 Microstructural Characterization of Welding	161
5.8 Field Emission Scanning Electron Microscope Analysis	163
5.9 Energy X-Ray Dispersive Spectroscopy Analysis	168
5.9 Summary	170
CHAPTER 6: CONCLUSIONS AND SCOPE FOR FUTURE WORK	172
6.1 Conclusions	172
6.1.1 Mechanical Characterizations of Microwave Processed welding	173
6.1.2 Effects of Process Parameter on Tensile Strength.....	173
6.1.3 Effects of Process Parameter on Microhardness	174
6.1.4 Effects of Process Parameters on Surface Temperature.....	175
6.1.5 Characterizations of the Microwave-Processed Welded Joint by XRD, Microstructure, FESEM and EDS	175
6.2 Scope for Future Work	177
REFERENCES	178
LIST OF PUBLICATIONS	195

LIST OF FIGURES

Fig 1.1: Types of joining process.....	2
Fig 1.2: Classification of electromagnetic waves.....	8
Fig 1.3: Interaction of electromagnetic field with materials.....	15
Fig 1.4: Characteristics of Microwaves Heating.....	20
Fig 1.5: Heat distribution during Conventional and Microwave heating.....	22
Fig 1.6: Temperature distribution in conventional, microwave, and microwave hybrid heating.....	25
Fig 1.7: Developments in the field of microwave materials processing in chronological order.....	28
Fig 1.8: Chronological developments in microwave processing of metallic materials.....	29
Fig 2.1: Temperature versus time profiles for austenitic stainless steel grades 316L and 434L when heated using a microwave and traditional heating methods.....	57
Fig 2.2: Comparison of power consumption and heating time for conventional and microwave sintering.....	58
Fig 2.3: Theoretical W-Cu composite sintered densities (in percent) after microwave and traditional sintering are compared.....	59
Fig 2.4: SEM of W–Cu composite subjected to conventional and microwave heating.....	61
Fig 2.5: SEM micrographs of (a) microwave and (b) conventional.....	61
Fig 2.6: 316L and 434L steel compacts' optical microstructure after being sintered for 1 hour at 1400 ⁰ C in a conventional furnace and a microwave furnace.....	62
Fig 2.7: Potential areas of surface engineering technologies.....	65
Fig 2.8: Flow chart of Present Work.....	85

Fig 3.1: Microwave oven.....	87
Fig 3.2: Tensile machine.....	89
Fig 3.3: Microhardness machine.....	91
Fig 3.4: Optical microscope.....	93
Fig 3.5: Field emission scanning electron microscope.....	95
Fig 3.6: XRD machine.....	97
Fig 3.7: Infrared gun.....	100
Fig 4.1: Base metal SS 304.....	103
Fig 4.2: Microstructural images by optical microscope (a) & (c) Base Metal SS 304, (b) & (d) Magnified view of marked section.....	103
Fig 4.3: Stress strain curve of base metal.....	104
Fig 4.4: XRD of base metal.....	104
Fig 4.5: FE SEM of base metal.....	105
Fig 4.6: Refractory brick.....	105
Fig 4.7: a) Nickel powder, b) Nickel powder mixed with epoxy resin.....	107
Fig 4.8: XRD of Ni powder (a) 5µm, (b) 10 µm, (c) 15 µm.....	108
Fig 4.9: Graphite sheet.....	108
Fig 4.10: Susceptor powder.....	109
Fig 4.11: Setup for microwave welding.....	114
Fig 4.12: Parameters affecting the microwave welding.....	115
Fig 4.13: Flow chart of microwave welding.....	117
Fig 4.14: Step wise procedure of microwave welding.....	119
Fig 4.15: Welded pieces of SS304 as per DOE.....	122

Fig 4.16: Macrostructure of welding zone.....	123
Fig 4.17: a) Showing mounting press, b) polishing machine, c) optical microscope	124
Fig 4. 18: Drawing for tensile testing as per ASTM.....	125
Fig 4.19: showing, a) setup for microwave hybrid heating, b) setup inside microwave, c) welded piece cutting as per ASTM, d)joint piece for tensile testing.....	126
Fig 5.1: Specimen for tensile testing.....	131
Fig 5.2: Specimen after tensile testing.....	131
Fig5.3: showing tensile value for a) Normal plot of residuals, b) predicted v/s actual	134
Fig 5.4: Welding time effect on tensile strength.....	138
Fig 5.5: Powder size effects on tensile strength.....	139
Fig 5.6: Slurry weight effects on tensile strength.....	139
Fig 5.7: (a), (b), (c) Interaction effects of input parameters on tensile strength.....	140
Fig 5.8: (a), (b), (c) Showing contour effect of input parameters for tensile strength.....	141
Fig 5.9: (a), (b), (c) showing 3D effect of input parameters for tensile strength.....	142
Fig 5.10: Showing microhardness value for, a) Normal plot of residuals, b) predicted v/s actual.....	145
Fig 5.11: Welding time effect on micro hardness value.....	147
Fig 5.12: Powder size effect on micro hardness value.....	148
Fig 5.13: Slurry weight effect on micro hardness value.....	148
Fig 5.14: (a), (b), (c) Interaction effects of input parameters on microhardness.....	149

Fig 5.15: (a), (b), (c) Showing contour effect of input parameters on microhardness.....	149
Fig 5.16: (a), (b), (c) Showing 3D effect of input parameters on microhardness.....	150
Fig 5.17: showing a) normal plot of residuals, b) predicted v/s actual values, c) residuals v/ predicted values, d) residuals v/s run.....	154
Fig 5.18: Showing a) welding time effects, b) slurry weight effects and c) powder size effects on surface temperature.....	156
Fig 5.19: Showing interaction effects of a) welding time & slurry weight, b) welding time & powder size and c) powder size & slurry weight, on surface temperature....	156
Fig 5.20: (a), (b), (c) Showing contour effects on surface temperature.....	158
Fig 5.21: (a), (b), (c) Showing 3D effect of input parameters on surface temperature.....	158
Fig 5.22: (a), (b), (c) Showing xrd pattern of 5 μ , 10 μ and 15 μ respectively.....	159
Fig 5.23: (a), (b) and (c) Showing xrd pattern of joint area for maximum, medium and minimum value of outcomes respectively.....	160
Fig 5.24: Shows microstructural images of a) base metal, b) at 100x, c) at 200x for minimum value of outcomes.....	162
Fig 5.25: Shows microstructural images of a) base metal, b) at 100x, c) at 200x for medium value of outcomes.....	162
Fig 5.26: Shows microstructural images of a) base metal, b) at 100x, c) at 200x for maximum value of outcomes.....	162
Fig 5.27: Shows FESEM images of joint area a) at X20, b) at 150X, c) at 5000X for minimum value of outcomes.....	164
Fig 5.28: Shows FESEM images of joint area a) at X20, b)at 150X, c)at 5000X, for medium value of outcomes.....	165

Fig 5.29: Shows FESEM images of joint area a) at X20, b) at 150X, c) at 5000X for maximum value of outcomes.....165

Fig 5.30: Shows FESEM images of fractured joint.....167

Fig 5.31: Shows EDS analysis for maximum value of outcomes at different portions.....168

Fig 5.32: Shows EDS analysis for middle value of outcomes at different portions.....169

Fig 5.33: Shows EDS analysis for minimum value of outcomes at different portions.....169

LIST OF TABLES

Table 3.1 Microwave oven.....	88
Table 3.2 Specification of Tensile Testing Machine.....	89
Table 3.3 Specification of Microhardness testing machine (Struers Duramin-40).....	91
Table 3.4 Specifications of Optical Microscope.....	93
Table 3.5 Specification of FESEM machine.....	96
Table 3.6 Specification of XRD machine.....	98
Table 4.1 Chemical compositions (wt%) of substrate materials by spectroscopy....	103
Table 4.2 Mechanical properties of substrate material.....	104
Table 4.3 Ni powder mixed with resin in percentage.....	107
Table 4.4 Process parameter with levels.....	112
Table 4.5 Details of Unit and Processing Parameter.....	115
Table 4.6 Central Composite Design matrix for butt joint.....	119
Table 4.7 Experimental input values as per CCFCD with welded pieces.....	120
Table 5.1 Experimental results for tensile strength.....	132
Table 5.2 ANOVA table for full quadratic for tensile strength.....	135
Table 5.3 Experimental results for micro hardness.....	143
Table 5.4 ANOVA table for full quadratic for micro hardness.....	145
Table 5.5 Experimental results for surface temperature.....	151
Table 5.6 ANOVA table for full quadratic for Surface Temperature.....	153

NOMENCLATURE

ANOVA	Analysis of Variance
ASTM	American Society for Testing and Materials
CCDFC	Central Composite Design with Face Centered
DOE	Design of Experiments
DOF	Degree of Freedom
EDS	Energy Dispersive X ray Spectroscopy
EM	Electro Magnetic
FESEM	Field Emission Scanning Electron Microscopy
GHz	Giga Hertz
HAZ	Heat Affected Zone
MHz	Mega Hertz
MPa	Mega Pascal
MS	Mean Square
MW	Microwave
OM	Optical Microscope
RSM	Response Surface Methodology
SS304	Stainless Steel 304
SS	Sum of Squares
UTM	Ultimate Tensile Machine
XRD	X-Ray Diffraction

LIST OF SYMBOLS

<i>m</i>	Meter
<i>Mm</i>	Millimeter
λ	Wavelength
<i>H</i>	Magnetic Field
<i>C</i>	Specific Heat of Material
<i>Cm</i>	Centimeter
<i>E</i>	Electric Field
<i>Erms</i>	Root Mean Square of Electric Field
<i>f</i>	Frequency
<i>Hrms</i>	Root Mean Square of Magnetic Field
<i>m</i>	Mass of Material
<i>min</i>	Minutes
<i>nm</i>	Nanometer
<i>P</i>	Power Absorbed
<i>Po</i>	Incident Power
<i>t</i>	Time of Microwave Exposure
$\tan \delta$	Loss Tangent
<i>TC</i>	Time Taken in Conventional Heating
<i>TM</i>	Time Taken in Microwave Heating
<i>V</i>	Volume of Material
<i>W</i>	Watt
<i>wt:</i>	Weight
<i>A</i>	Attenuation Factor
Δ	Skin Depth
Δt	Temperature Difference
ϵ'	Dielectric Constant
ϵ''	Dielectric Loss Factor
μ	Electrical Resistivity
μ''	Magnetic Loss Factor
$\mu\text{m:}$	Micrometer
<i>Mo</i>	Magnetic Permeability
σ	Electrical Conductivity

CHAPTER 1: INTRODUCTION

1.1 Introduction

In the majority of manufacturing and assembly businesses worldwide, the permanent joining of materials is a crucial need. Welding, soldering, and brazing are some of the traditional permanent diffusion processes for combining materials, but each has its own benefits and drawbacks. The drawbacks of conventional techniques include longer processing periods, greater energy demands, expensive setups, restrictions on the types of materials that can be bonded and joint flaws. Additionally, issues with joint processing, environmental risks, and operator safety are of the utmost importance. One of the main concerns of technologists, researchers, and academicians is the effective processing of materials. There is a pressing need to reduce energy consumption in material processing, which has led to the development of more clean and green technologies. Due to rising energy usage and decreased efficiency, it has been observed that existing manufacturing and processing technologies are becoming obsolete.

Microwave material processing is developing as one of the most promising long-term industrial processes. Microwave radiation's unique properties, such as volumetric heating, low power consumption, environmental friendliness, high quality goods, and so on, are attracting a growing number of researchers to this subject. Material joining is a key manufacturing method that is frequently utilised in industries to manufacture complex products. The principles of microwave radiation and their uses in numerous fields of engineering and technology are covered in this chapter.

1.2 Metal Joining Process

The metal joining process is the methods used to metallurgical attach two or more pieces of metal together, either with or without the application of heat, pressure, or both. The traditional joining techniques include welding, brazing, soldering, adhesive bonding, and more. Materials are also joined using cutting-edge technologies, including laser welding, electron beam welding, ultrasonic welding, microwave joining, and others. On the other hand, compared to other conventional and unconventional techniques, microwave joining offers several unique features. The ability to microwave-heat specific regions is one of the most important characteristics for the joining process. Metal joining process depends on,

- Types of material to be joined.
- The metal's physical, chemical, and metallurgical characteristics.
- The joining process's economic and financial efficiency.
- The partnership will acquire certain properties.

1.2.1 Types of joining process

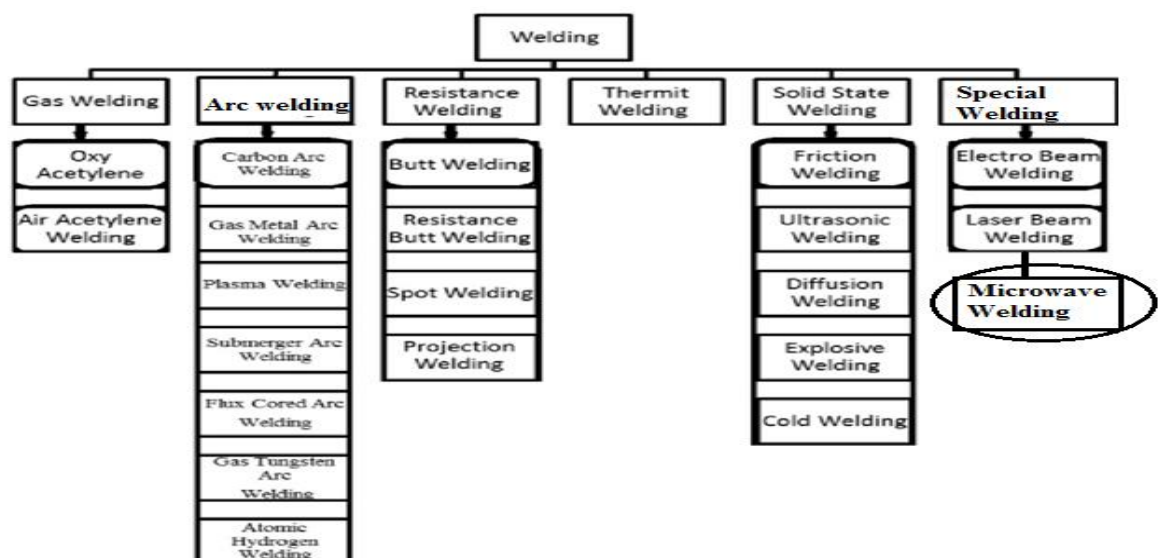


Fig. 1. 1: Types of joining process

Gas Welding

Fuel gases (gasoline) and oxygen are used in the metal joining process known as gas welding to weld and cut metal. Additionally, it is a method of combining metals when edge pieces of a metal that needed to be joined are heated at their interface by causing coalescence using one or more gas flames, such as acetylene and oxygen. Filler material can be applied to the joint during the welding process or not. These processes are also referred to as oxy-fuel, oxyacetylene, and oxy welding. French engineers Edmond Fouche and Charles Picard created it in 1903. Instead of using air, they raise the temperature of the flame using pure oxygen. The flame facilitates the melting of metals and alloys, such as steel.

Arc Welding

The most commonly used fusion method for joining metal parts is arc welding. An arc column is formed during this welding process between the cathode, which is the power source's negative pole, and the anode, which is the positive pole. When these two conductors of an electric circuit are brought together and then separated by a little distance, the current can continue to flow via a path of ionised particles known as plasma and create an electric arc. More ions can move from the anode to the cathode thanks to the low-resistance conductivity of this column of ionised gas. Heat is produced as the ions collide with the cathode. The metal that has to be joined or the filler metal, which is subsequently used as a welding metal joining material, are both melted using this heat. The electrode is either consumable or non-consumable depending on the welding needs. Between 6000 and 7000 degrees Celsius are present at the arc's centre.

Resistance Welding

One of the first electric welding techniques still in use today in the industry is resistance welding. Heat, pressure, and time are combined to create the weld. Resistance welding gets its name from the fact that the localised heating in the component is brought on by the material being welded's resistance to current flow. The pieces to be welded are held in close proximity before, during, and after the welding current time cycle by the pressure applied by the tongs and electrode tips through which the current passes.

Thermit Welding

Thermite welding (TW) is a method for joining metals together by applying the heat produced by an exothermic process. The name comes from the term "thermite," which is a general term for reactions involving metal oxides and reducing agents. Thermite is produced by combining metal reducing agents, which have low temperatures of production when reduced, with metal oxides, which have high temperatures of formation when oxidized. The additional heat produced during the creation of the reaction product serves as the energy source for the weld.

Solid State Welding

A series of welding techniques known as "solid state welding" don't need brazing filler metal and instead generate coalescence at temperatures that are effectively below the melting points of the base materials being connected. One may or may not apply pressure. This collection of welding techniques, which are also mistakenly referred to as solid state bonding techniques, consists of cold welding, diffusion, explosion, forge welding, friction welding, hot pressure welding, roll welding, and

ultrasonic welding. Time, temperature, and pressure can be used alone or in combination to generate coalescence of the base metal without significantly melting the base metal in any of these processes.

Special Welding

Research was done on improved welding methods to better understand the advantages of materials processing technologies in the demanding world of engineering. The primary goals were to lessen energy usage, produce high-quality goods, speed up production, and eliminate environmental contamination, which is still an issue with traditional welding techniques. Since 1970, laser welding and cladding procedures have become one of the cutting-edge methods for treating materials. These procedures represent the greatest ways now available for processing materials in terms of claddings, joining, welding, precision production, etc. These procedures have achieved considerable breakthroughs.

The primary disadvantages to laser material processing are the high initial cost of the machinery, greater maintenance costs, safety concerns, and decreased rate of performance. The occurrence of high thermal stresses brought on by rapid heating in limited places can cause thermal cracking and the change in shape of microstructures. Further, plasma was used in the coating, melting, and casting of materials, but, as before, cost is the key to long-term sustainability.

The development of sustainable, green, and energy-efficient processing techniques is the main emphasis at the moment. Therefore, it is crucial for researchers to look for alternate processing methods and procedures that might potentially compensate for or lessen the shortcomings of current ones. The suggested methods are anticipated to

create better-quality goods at a reasonable processing cost while reducing CO₂ and other undesirable emissions and using less energy. Many benefits are possible with microwave heating technologies that are not possible with traditional heating methods.

1.3 Introduction of Microwave

The EM spectrum includes microwaves, which have frequencies between 300 MHz and 300 GHz and wavelengths between 1 m and 1 mm. The term "microwave" was first used by A.G. Clavier in a study published in 1931 by the International Telephone and Telegraph to describe the transmission of an 18 cm wavelength radio connection from Dover, UK, to Calais, France in a study published in 1931 by the International Telephone and Telegraph. The electromagnetic theory of Maxwell must be examined in order to comprehend microwaves. A material's complicated permittivity and permeability are what define its electromagnetic characteristics.

The heating effect in microwave heating has been attributed to the material's interaction with the electric field; the magnetic field is typically disregarded. According to [Sobol and Tomiyasu, 2002], heating results from the material's charges being polarised by the electric field but being unable to keep up with the electric field's fast changes. In a different publication written by Clavier in 1933, wavelengths of roughly 0.5 m were referred to as microwaves.

The Ultra High Frequency (UHF) band, which has frequencies between 300 MHz and 3 GHz; the Super High Frequency (SHF), which has frequencies between 3 and 30 GHz; and the Extremely High Frequency (EHF), which has frequencies between 30 and 300 GHz, are additional classifications for microwaves [Gupta and Wong, 2007].

A mathematical foundation for comprehending the combined effects of electricity and magnetism was provided by Maxwell's electromagnetic theory [Osepchuk, 1984].

1.3.1 Development of Microwaves

Faraday made the discovery of electromagnetic induction in 1831. In his mid-20s, Maxwell started experimenting with Faraday's notion of the lines of force, and in 1864, he put out the electromagnetic theory [Sobol and Tomiyasu 2002]. Invisible electromagnetic waves with a wavelength greater than that of light were predicted to exist by Maxwell's electromagnetic field theory, and Heinrich Hertz made the first direct observation of their existence in the late 1880s. He used equipment that comprised of a spark-gap generator that stimulated a dipole and a parabolic cylinder antenna operating at a microwave frequency of around 450MHz to show the reflection of radio waves from objects [Skolnik, 2002].

Hertz's experiment was expanded upon by the Indian scientist Jagdish Chandra Bose in the 1890s, using more advanced equipment at higher frequencies between 60 and 120 GHz. Investigations into microwaves between 1900 and the 1930s resulted in the creation of the fundamental radar ideas. The high-power cavity magnetron and the urgent need to enhance radar detection of enemy aircraft and submarines brought about the fast development of microwave technology during World War II. Microwaves were widely employed in World War II for electronic warfare, radar detection, and telecommunications systems. While testing the MW generator, Percy Spencer accidentally discovered the heating capabilities of microwaves when a candy bar in his pocket started to melt. In 1945, he applied for a patent on microwave-assisted food heating. Initially, low-temperature applications such as food heating,

resin is cure, wood drying, and material drying were the main emphasis of microwave heating [Appleton et al., 2005 and chanda et al., 2009].

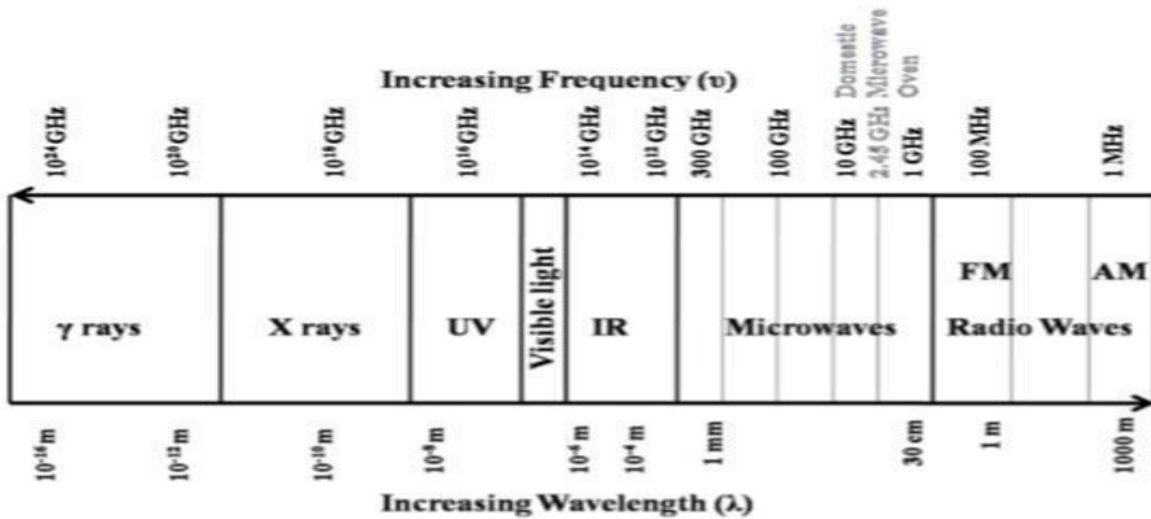


Fig 1.2: Classification of electromagnetic waves

Rapid developments in microwave radar research and development as well as related technologies that arose during the conflict are well-documented in the M.I.T Radiation Laboratory Series [MIT, 1999]. The majority of residential microwave ovens operate at a frequency of 2.45 GHz in several nations. Higher frequency microwave and millimetre wave furnaces, on the other hand, have been developed for a variety of materials processing furnaces range in frequency from 1 to 30 GHz. The frequency of the residential microwave oven in India operates at 2.45 GHz, as illustrated in Fig. 1.2, which depicts the electromagnetic radiation spectrum.

1.3.2 Mechanisms of Heating by Microwaves

The source, transmission lines, and applicator are the three essential components of microwave heating devices [Thostenson and Chou, 1999]. The electromagnetic radiation is produced by the microwave source (vacuum tubes, magnetrons, klystrons, etc.), and it is transmitted by transmission lines to the heating region of the applicator.

Microwaves are either directly absorbed or reflected by materials stored in the cavity, depending on the load (materials to be heated).

Power, frequency, efficiency, gain, bandwidth, phase, size, weight, and cost are just a few of the variables that influence which types of microwave generators should be used. Due to its great efficiency, small size, and low cost, the magnetron is the most widely used microwave generator. Radar systems and microwave ovens both often use it. A magnetron runs normally at a frequency of 2.45 GHz and transforms electrical energy into microwave radiation. [Granastein et al, 1999 and Ishii, 1995].

Researchers from Penn State University [Cheng et al, 2002] built on the preliminary work of [Cherradi et al, 1994], which showed that the magnetic field does contribute to the heating of dielectric materials (at high temperatures), semiconductors, and metals. They did this by demonstrating the radical heating behaviour of various materials in separate electric (E) and magnetic (H) microwave fields using a single-mode cavity. By applying the proper boundary conditions to the Maxwell equations (equation 1.1) [Thostenson and Chou, 1999] indicated below, the theoretical analysis of microwave heating may be examined and governed:

$$\nabla \times = , \nabla \cdot = 0 \quad (1.1)$$

$$\nabla \times = + , \nabla \cdot \quad (1.2)$$

With the necessary boundary conditions for the distribution behaviour of the electric field and magnetic field inside the microwave applicator, the Maxwell equations may be analytically or numerically solved. This distribution data determines where to position the load within the applicator for effective heating. Depending on the

intensity of the electrical or magnetic fields, appropriate locations can be found depending on the kind of applicator, such as single mode or multi-mode.

The basic characteristics of the dielectric constant and dielectric loss factor may be used to assess a material's initial heating behaviour, but other factors that affect how the absorbed MW energy is transformed into heat energy are also significant. Different heat-generating processes are involved depending on the kind of material, such as magnetic or non-magnetic. [Thostenson and Chou, 1999].

Internal electric fields are created when microwaves enter and propagate through dielectric materials. The local charge (bound charge and free charge) is moved by this produced electric field in both translational and rotational movements and results in polarization [Thostenson and Chou, 1999; Roy et al., 1999].

Heat is produced as a result of the internal, elastic, and frictional forces that oppose this motion. Since the process spreads across the volume of the materials, the internal heat that is produced is volumetric in nature. Dielectric properties (ϵ , ϵ'' and $\tan \delta$) play an important role in microwave interaction (penetration and propagation) within materials. Dipolar loss and conduction loss are the main phenomena in the processing of non-magnetic materials like aluminium, copper, ceramics, water, etc.

The phenomena of hysteresis losses, eddy current losses, and residual losses are significant in the case of magnetic materials such as Fe, Ni, steel powder, W, etc. Both the magnetic and electric fields interact as the materials are processed using microwave radiation. While the electric field's function is to provide free electron motion, the magnetic field's heating of magnetic materials during microwave

processing involves the phenomena of "electron spin," "domain wall movement "and" domain orientation" within the material.

Any magnetic metallic substance generates heat overall through a variety of losses, including magnetic and conduction losses brought on by electric fields (hysteresis loss, eddy current loss, domain wall resonance, and electron spin resonance). The entire energy that is turned into heat within a material is represented by the absorbed microwave power, which is the dissipated power caused by the magnetic and electric fields of microwave radiation. Finding the percentage of losses caused by electric and magnetic fields that contribute to total material heating is exceedingly challenging.

Another factor, namely power dissipation, is employed as the benchmark for efficient microwave heating in order to get around this issue. Furthermore, the depth to which microwave radiation is absorbed determines how much power is dissipated in any given material. The kind of material and its related qualities affect how microwaves penetrate that substance. The term "penetration depth" (i.e., the distance from the material's surface at which the incident microwave incident power drops to 1/e [36.8 percent] of the surface value) is used to describe the penetration of microwaves for non-metallic materials and is mathematically expressed in equation (1.3) [Mishra and Sharma, 2016].

$$Dp = 1/\sqrt{(0.5\mu_0\mu'\epsilon_0\epsilon'\left\{\sqrt{\left(1 + \left(\frac{\epsilon'_{eff}}{\epsilon'}\right)^2} - 1\right\})}$$

(1.3) While microwave penetration is negligible in metallic-based materials under normal conditions, the equivalent depth is known as "Skin Depth." Equation (1.4) mathematically expresses the skin depth (δ), which has the fewest factors and is quite straight forward [Mishra and Sharma, 2016].

$$D_s(\delta) = \frac{1}{\sqrt{\pi f \mu \sigma}} = 0.029 (\rho \lambda_0)^{0.5} \quad (1.4)$$

In this equation, δ stands for the thickness of the skin, σ for electrical conductivity, f for microwave frequency (GHz), μ for electrical resistivity, and λ_0 for incoming wavelength.

This demonstrates how the electromagnetic properties and thickness (volume characteristics) of the materials bombarded affect the power absorbed during microwave radiation. Below represent the expected power absorbed per unit volume (W m^{-3}) for thin sections of materials.

$$P = 2\pi^{1/2} \epsilon_0 \epsilon'' E_{rms}^2 + 2\pi f \mu_0 \mu'' H_{rms}^2 \quad (1.5)$$

Where, P is the power absorbed (W m^{-3}), μ_0 is magnetic permeability of air (H m^{-1}), μ'' (magnetic loss factor) is the imaginary component of the magnetic permeability (H m^{-1}). E_{rms} is the root mean square of the electric field (V m^{-1}) and H_{rms} is the root mean square of the magnetic field (A m^{-1}).

The $2\pi f \mu_0 \mu'' H_{rms}^2$, phrase in the case of non-magnetic materials can be disregarded because it is negligible. The power absorbed for thick portions can be calculated using equation 1.5 of Lambert's Law [Mishra and Sharma, 2016].

$$P_x = P_0 e^{(-2ax)} \quad (1.6)$$

Where P_0 , is the incident power (W) at the surface of material, x is the distance (m) at which power is to be determined and is called the attenuation factor (dB m^{-1}). But, the material properties get altered as the temperature changes and in such cases; it becomes highly cumbersome to estimate the power absorption. To estimate the power

absorption up to some extent, an energy balance equation as expressed in equation 1.6 [Mishra and Sharma, 2016] can be used.

$$\sum mC\Delta t = 2\pi f \varepsilon_0 \varepsilon'' E_{rms}^2 Vt \quad (1.7)$$

Where, m is the mass of material (kg), C is the specific heat ($\text{J kg}^{-1}\text{K}^{-1}$) of material, Δt is the temperature difference ($^{\circ}\text{C}$), V is the volume of the material (m^3) and t is the time of microwave exposure (s). The penetration and propagation of incident microwave can significantly be enhanced by altering the dielectric properties (ε'' and $\tan \delta$) of materials which are temperature dependent.

1.3.3 Microwave – Material Interactions

Materials may reflect, transmit, or absorb the electromagnetic wave's electric field component. Instead, the electromagnetic wave's magnetic field component interacts with magnetic materials. This restricts the range of materials that may be directly treated by microwave radiation [Clark and Sutton, 1999]. This is because various materials have varying electrical, dielectric, and magnetic characteristics, and microwave absorption behaviour varies as a result. Researchers have recently focused their attention on a number of processes, including microwave cladding [Zafar and Sharma, 2014], microwave joining of bulk metals [Bansal et al, 2013; Srinath et al, 2011c and Salot et al, 2017]. These initiatives spur scholars to carry out more studies in this intriguing sector, which is rife with unknowns. The following categories can be used to group microwave interactions with materials:

1. **Opaque materials-** Metals and other conducting materials with free electrons are examples of opaque materials because they reflect electromagnetic waves and prevent them from passing through. Lower microwave penetration depths, which are further attributed to lower skin depths associated with such materials, are the principal cause

of MW reflection. However, under rare circumstances, surface heating may occur as a result of some microwave radiation penetration, although the majority of the radiations are reflected. Bulk metals are one of the best examples of such opaque, reflecting materials.

2. **Transparent materials-** Transparent substances are several materials that easily allow the passage of microwaves without creating any alterations to the E or H field. As a result, there is no contact between the materials and the microwaves, and no microwave energy is absorbed. Such materials are referred to as transparent materials with low dielectric loss or insulating materials because they reflect and absorb electromagnetic waves insignificantly while permitting microwaves to flow through readily and with minimal attenuation. This could be a result of the materials' high skin depths and low loss tangents. Quartz, teflon, thin plastic sheets, glass, ceramics, and air are a few common examples of materials that are transparent to microwaves.

3. **Absorbing materials-**Materials with conductor to insulator qualities make up the category of absorbing materials. They are frequently referred to as "high dielectric loss materials" or "loss dielectrics." These substances easily absorb electromagnetic energy and transform it into heat. The skin depths of the materials also have a significant impact on how well microwaves are absorbed. Effective heating by microwave absorption is possible if the material size and skin depth are similar. Such substances may efficiently transform microwaves received into heat at lower frequencies and temperatures. Water, silicon carbide, ceramics, carbon fibres, graphite, charcoal, etc. are typical examples of these materials.

4. **Magnetic materials-**As a result of their interaction with the electromagnetic wave's magnetic component, magnetic materials like ferrites heat up.

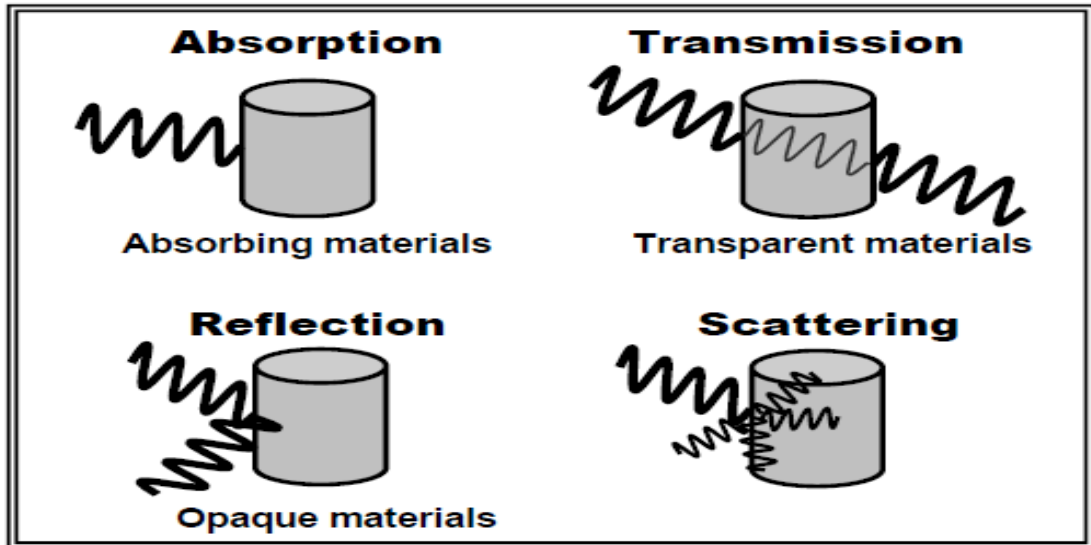


Fig.1.3: Interaction of electromagnetic field with materials

The interaction between the microwaves' electric and magnetic field components and the materials during microwave processing of materials can result in heating as a result of dielectric and magnetic losses. The redistribution of charges or polarisation caused by an alternating external electric field is the cause of dielectric losses, which have been widely researched. Electronic, orientation (or dipolar), atomic (or ionic), and interfacial dielectric polarisation losses are among them (Maxwell-Wagner).

Heating is dependent on conduction losses in materials with strong conductivity, such as metals. Hysteresis, eddy current, domain walls, and electron spin resonance are examples of magnetic losses in magnetic materials that lead to heating. However, there are drawbacks with the current classical electrodynamics approach that relies on electric (E) and magnetic field (H) strengths to explain electromagnetic interactions, leading researchers to re-evaluate Maxwell's equations in order to use gauge potentials—as Maxwell himself first suggested—and quantum physics to do so [Gronwald and Nitsch, 2001].

1.4 Application of Microwaves

In addition to radar and communication, microwave technology has been broadened to a wide range of uses since its fast development during World War II [Gupta and Wong, 2007].

- Communication, radar detection, microwave heating, and navigation
- Electronic Medical Warfare
- Industrial Scientific
- Power transfer and weather regulation

1.4.1 Communications

Because of their high frequency, short wavelength, and capacity to transmit signals and information with the least amount of loss through the earth's atmosphere, microwaves are widely used in satellite communication. Microwaves have a high frequency, which increases their bandwidth capacity and allows for the transmission of more data within them.

1.4.2 Radio Detection and Ranging (Radar)

Using equipment that works at microwave frequencies, radar is a technique for figuring out a target's existence, position, velocity, and other details. Radar transmits a microwave signal, which is returned to it by the target or object. To ascertain the targets or object's velocity, range, azimuth, elevation, and form, the broadcast signal and the reflected signal are compared. The Global Positioning System (GPS), which was first created for military purposes, is a well-known illustration of the use of radar in navigation [Skolnik, 2002].

1.4.3 Electronic Warfare

Through the control and manipulation of electromagnetic radiation, electronic warfare tactics are used to lessen the efficacy of an enemy's radar and electronic equipment and to increase the survivability of one's own forces. It may be divided into three categories: electronic attack, electronic defence, and electronic assistance. Radar is used by electronic support to gather data and offer surveillance, detection, identification, and warning for precise assessment. An electronic attack involves the use of electromagnetic radiation to interfere with the opponent's radar and other electromagnetic energy-using equipment as well as to kill or disable hostile soldiers. The goal of electronic defence is to thwart enemy electronic support and attack [Scott, 1993].

1.4.4 Medical Applications

Due to their capacity to produce strong heat and serve as a power source in medical apparatus for radiological treatments, microwaves are used in a variety of medical applications. In radiation treatment, a medical linear accelerator uses microwaves as a power source to accelerate electrons to high energy before directing the electrons to smash into a metal target [Scott, 1993].

1.4.5 Scientific Applications

Measurement of microwave radiation from astronomical objects, chemical and biological research, linear accelerators, and nuclear research are examples of scientific uses. In order to comprehend the creation and composition of stars and galaxies, astronomers use radio astronomy to study the microwave radiation emitted by these objects in space. Antennae are used by astronomers to collect electromagnetic

radiation emissions from celestial objects and turn them into images. Chemical synthesis and reactions have been considerably accelerated and improved by the use of microwaves. Widespread use of microwave-accelerated organic synthesis is being seen in chemical, biological, and pharmacological research. Microwave absorption spectroscopy, nuclear magnetic resonance spectroscopy, and electron spin resonance spectroscopy are three more chemical uses for microwaves [Ishii, 1995].

1.4.6 Industrial and Commercial Applications

Microwaves are used to create plasma for reactive ion etching and plasma accelerated chemical vapour deposition in semiconductor manufacturing methods, which is one of their industrial uses [Stein, 1994]. Because they produce ultraviolet light more effectively than traditional UV sources while emitting less infrared radiation and heat, microwave discharge lamps are used for curing [Osepchuk, 2002]. The use of microwaves in the security industry is a significant commercial application. Currently, microwaves are used in perimeter security and intrusion detection at critical infrastructure sites including airports, prisons, military bases, nuclear power plants, and significant commercial and government buildings. Recent terrorist threats have increased concerns and regulations around transportation security, which has sparked research into microwave security devices.

The traditional metal detectors used at airports to screen travellers are restricted to just detecting metal things. Because they employ ionising radiation, other security technologies, including X-ray imaging used to check bags, are inappropriate for screening individuals. Microwaves are now being used in new detecting technology to find and locate suspicious things (both metallic and non-metallic) that are covered in clothes. The use of microwaves for identification and tracking may be the most

widespread commercial use. In the 1960s, radio technology and radar were combined to create radio frequency identification (RFID), which was originally used to track nuclear and other dangerous items [Srivastava, 2005].

1.4.7 Potential Applications

Due to their special characteristics, microwaves have a wide range of possible uses. There have been reports on the possible use of microwaves in waste cleanup, regeneration, and recovery [Stein, 1994; Clark and Sutton, 1996]. Mineral processing is a further possible use for microwaves [Patnaik and Rao, 2004]. According to research, microwaves can improve the extraction of gold, iron, zinc, and titanium while desulfurizing coal to enable cleaner burning. The use of microwaves for power transmission and solar-powered satellites is one potential use for the technology that has attracted a lot of interest [Osepchuk, 2002; Matsumoto, 2002].

1.4.8 Microwave Heating/Processing of Materials

Because they can heat things, microwaves are used. The residential microwave oven, which is used to heat and cook food, is where microwave heating is most frequently employed. In the business world, microwave heating has been used for vulcanizing rubber, tempering frozen foods, manufacturing potato chips, and frying bacon. Numerous studies have documented the use of microwaves in the processing of both organic and inorganic materials, including polymers, ceramics, and minerals [Osepchuk, 2002; Stein, 1994; Clark and Sutton, 1996; Ishii, 1995].

1.5 Characteristics of Microwave Heating

A substance must be able to directly absorb electromagnetic energy in order to be heated by microwaves. It is a cutting-edge and distinctive approach that can process a wide range of already used materials as well as new materials that cannot be handled

using traditional methods. Another benefit of microwave heating is that it can enhance the characteristics of materials that have already undergone conventional processing. There are a number of distinctive qualities that microwave heating has over traditional heating. [Stein, 1994; Clark and Sutton, 1997; Thostenson and Chou, 1999; Bykov et al, 2001] list the following as the major attributes of microwave heating:

1. Penetrating radiation;
2. Rapid heating;
3. Controllable field distributions;
4. Material selection heating;
- and 5. Self-limitation.

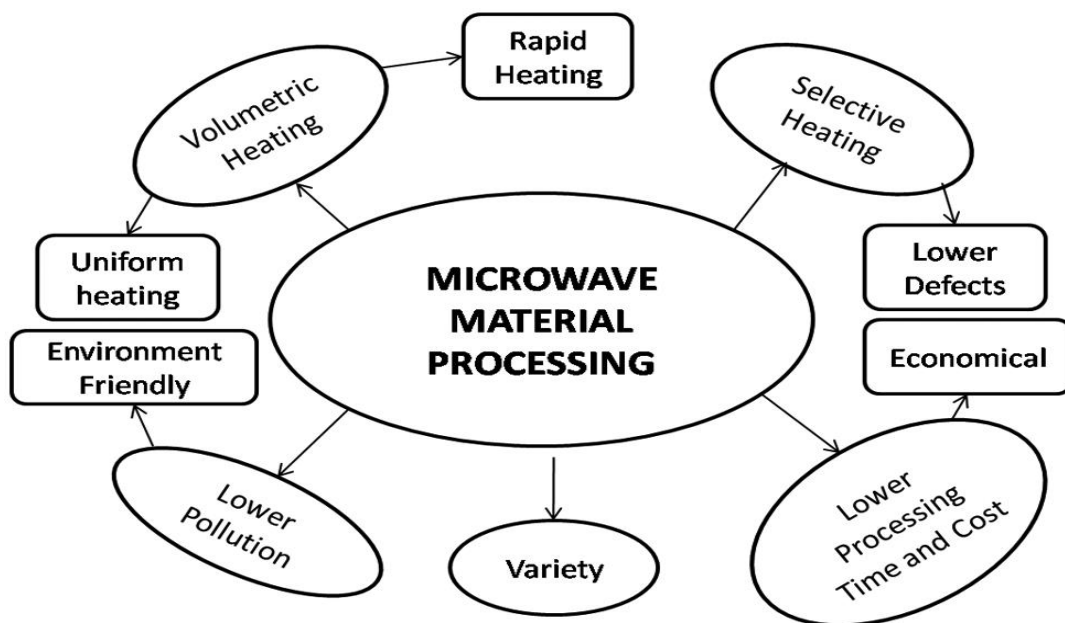


Fig.1.4: Characteristics of Microwaves Heating

1.5.1 Penetrating Radiation

The heating of materials using a microwave oven differs significantly from traditional resistance heating. The way heat is transmitted to the substance is the main distinction between conventional and microwave heating. In typical thermal processing, heat created by external sources, such as a resistive heating element, is transported to the material from the outside to the inside by conduction, convection, and radiation. In

microwave heating, heat may be created from inside the material itself as a result of the material's direct absorption of microwave energy and does not depend on the transmission of heat from the surfaces. This is possible due to the penetrating capability of microwaves.

The microwave's ability to penetrate deeply varies substantially depending on the material's dielectric and magnetic characteristics; microwave frequency and power; temperature; conductivity; size; and densification. The energy source and the substance don't even need to touch. The temperature at the core is often greater than the temperature at the surface because the surface loses heat to the environment while heat is created from inside the volume of the material and radiates outward. When compared to traditional thermal processing, this results in the material's temperature profile being inverted.

Microwaves' capacity to enter materials and heat them from the inside allows for quick and volumetric heating without overheating the surfaces [Bykov et al, 2001]. Depending on the kind of material and skin depths involved, MW can be reflected, transmitted, and/or absorbed. The materials will absorb microwave radiation, which will permeate within and turn into heat inside, raising the temperature of the materials. The heating process is impacted by the heat loss from the surface to the surroundings, and the interior regions reach greater temperatures, as illustrated in Fig. 1.5.

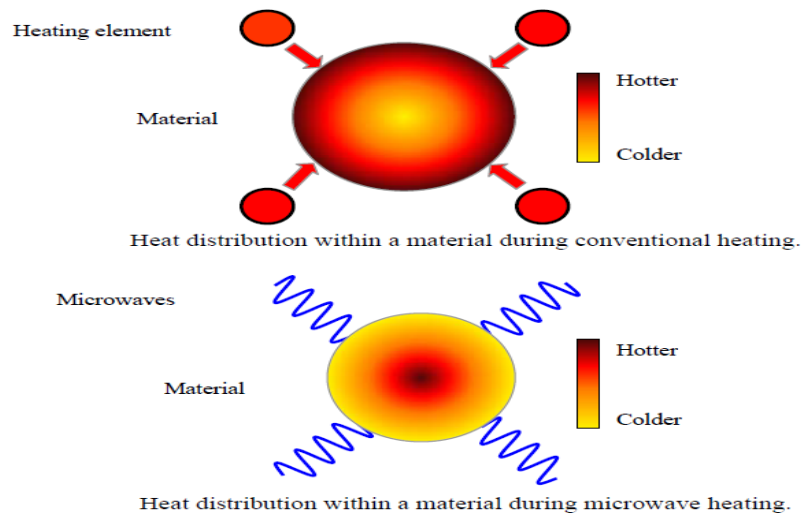


Fig.1.5: Heat distribution during Conventional and Microwave heating

1.5.2 Rapid Heating

Due to their quick heating rates as compared to traditional heating techniques, microwave heating may be finished in a fraction of the time. Numerous studies have demonstrated that microwave processing dramatically shortens the processing time while maintaining or even improving the characteristics of materials handled traditionally. Additionally advantageous is rapid heating's ability to minimise undesired intermediate thermally activated processes [Bykov et al, 2001].

1.5.3 Controllable Field Distributions

The electromagnetic field distributions inside the cavity can be changed depending on the microwave applicator utilised. It is impossible to separate the magnetic and electric fields in a multimode cavity because the cavity is stimulated in several modes. Since only one mode is generated in single-mode applicators, the electric and magnetic fields may be separated with the right tuning, enabling researchers to examine the effects of E and H fields on various types of materials individually.

1.5.4 Selective Heating of Materials

Materials may be selectively heated using microwaves, which is not feasible with traditional heating. Heating can be targeted to particular areas within a single-phase or multiphase component, depending on the material's properties (such as dielectric properties, size, and molecular structure), ability to couple with microwave fields, and other factors. Materials that don't work well with microwaves can nevertheless be processed with the help of selective heating [Loupy, 2004].

1.5.5 Self-limiting Characteristic

Some materials have a tendency to absorb less microwave energy when heated over a given temperature or when a phase shift or reaction takes place. As microwave radiation is absorbed less efficiently, heating slows and eventually reaches its self-imposed limit. Self-limiting heating can also be managed by carefully determining the material's kind, quantity, and design [Zeng et al, 2003].

1.6 Microwave Heating Types

Pure microwave heating and hybrid microwave heating are the two categories under which microwave heating can be classified.

Pure microwave heating involves directly exposing objects to microwave radiation by placing them inside a microwave cavity. The substance heats up as a result of absorbing microwave radiation. Materials that may readily couple to microwaves are often subjected to pure microwave heating. Examples of typical materials include food, water, certain pottery, etc. Even though heating can happen quickly, the homogeneity of direct heating of materials is a key problem. Higher processing

durations generate more heat inside the core, which can cause hot spots that significantly harm the materials. When exposing materials (such as SiO₂, ZrO₂, alumina, etc.) directly to microwaves, author [Ryynanen, 1995] have documented a number of problems, including thermal instability and non-uniform heating and cracking.

A method of indirect heating known as "microwave hybrid heating" has been developed to combine microwave and conventional heating for the thermal treatment of materials that absorb microwaves ineffectively, such as metals and ceramics, until they reach a temperature where they will do so. It includes heating the material with two different sources of energy, including thermal energy from an outside source and microwave energy.

A separate conventional heat source, microwave susceptor materials, which combine with microwaves at ambient temperature and quickly heat up, can supply the additional thermal energy. Conventional methods of heat transfer are used to transmit the generated/developed heat to the metallic or non-coupled materials. This raises the temperature of materials that aren't very good at absorbing microwaves, allowing them to pair with them at a higher temperature. According to studies, hybrid heating tends to deliver more uniform heating by lowering the temperature gradient existing in the materials and preventing the production of hotspots [Stein, 1994; Clark, 1997; Thostenson and Chou, 1999; Bykov et al, 2001 and Wong and Gupta, 2005].

1.6.1 Microwave Assisted Processing of Materials

In the realm of materials processing, microwaves have recently been combined with other technologies, allowing the benefits of microwave heating to be combined for

increased efficiency and improved material quality. The microwave assisted plasma approach for producing carbon fibres has been the subject of much research. At the moment, microwave assisted technologies are employed in many industrial applications. This permits the integrity of other processes with an effective microwave heating process that aids in cost reduction and allows for the coupling of the beneficial aspects of both procedures. The relevance of microwaves in several industrial applications has increased as a result of research on microwave plasma assisted CVD, which has been used in the processing of various materials.

1.6.2 Selective Heating

This sort of heating is a component of the direct microwave heating technique, in which the load is placed within the microwave applicator and heated at a chosen spot. The ideal use of selective heating is in the joining of materials, where the joint areas are exposed to microwave radiation while shielding materials keep other sections from exposure. Figure 1.6 depicts the schematic for selective heating (d). It has been utilised for localised doping and heating of materials and is very successful when heating needs to be done in specific regions [Lin et al., 2011].

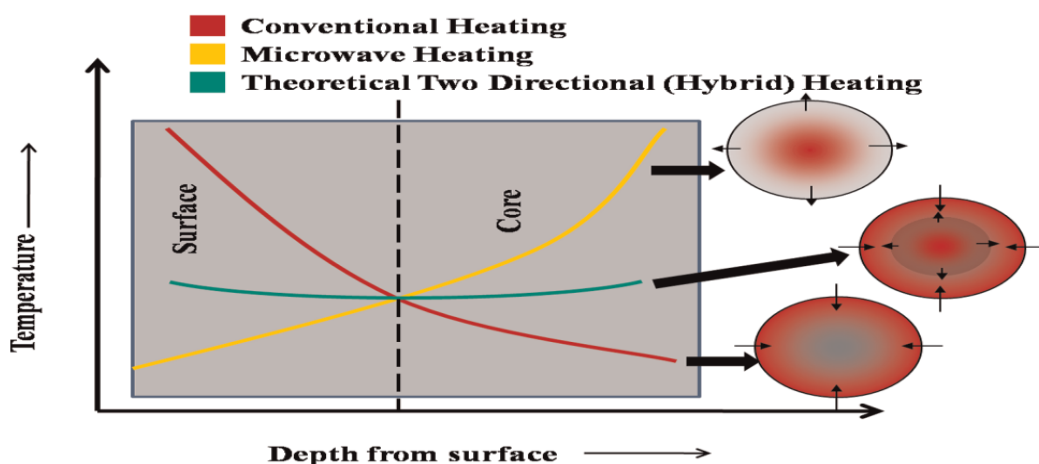


Fig.1.6: Temperature distribution in conventional, microwave, and microwave hybrid heating

When materials are heated conventionally, heat transmission occurs inside the material with little variation in temperature. This may result in poor surface microstructure as well as surface overheating or burning [Sharma and Krishnamurthy, 2002]. As seen in Figure 1.6, microwave heating has an inverted profile compared to traditional heating, meaning that it begins by heating the material from within and then transmits heat outward. According to [Yadoji et al, 2003], microwave heating mode can result in the core's poor microstructure, which can result in thermal runaways, core cracking, and core burning.

Researchers employed a method known as two-directional heating, to compensate for the difference in temperature gradients between the surface and the core. The fundamental idea behind MHH is to simultaneously work on the phenomena of traditional heating and microwave heating so that materials may be heated both internally and externally.

The figure illustrates several heating events and roughly flattens the specimen's internal temperature profile using MHH. The MHH results in quick heating, minimised temperature gradients. Flattening the temperature profile can result in improved microstructures both at the core and on the surface by reducing differential heating. Metallic powders may be coupled with microwaves at high temperatures thanks to the initial heating of the powders by conventional methods during MHH, which promotes more even heating and faster heating rates. Future advancements in microwave radiation-based materials processing will depend on MHH.

1.7 Development of Microwave Heating

More than 70 years after Maxwell developed the electromagnetic theory in 1864, microwave heating was invented in the 1940s. The idea of using microwaves for

therapeutic purposes was first put forth in 1938-1939 by Hollman from Germany and Hemingway and Stenstrom from the USA because microwaves can be more precisely focused than high frequency diathermy to produce heating of deep tissues without excessive heating of the skin [Sobol and Tomiyasu, 2002; Guy, 1984]. After World War II, industrial uses for microwave heating emerged from radio frequency heating [Osepchuk 1984]. In a 1943 Scientific American article, the intriguing features of this kind of heating action were outlined.

New uses were developed as the food sector came to understand the microwave's potential and adaptability. Microwaves were first used in the food industry. The main use of microwave heating nowadays is in the preparation of food. Other industries benefited greatly from the numerous applications of microwave heating. In the end, microwaves were employed to cure adhesives and dry materials, including cork, ceramics, paper, leather, tobacco, and textiles. Currently, only a few businesses are using microwave heating on a large scale. These include vulcanization of rubber, analytical chemistry, and food processing [Stein, 1994; Clark, 1997]. Although microwaves are frequently used to treat food, only a few other materials have been subjected to this technology.

However, as indicated by the rising body of research on the processing of various materials using microwaves, microwave processing has recently received more attention. Numerous materials, including ceramics, polymers, metals, semiconductors, rubber, glass, minerals, biomaterials, chemicals, powders, and wastes, have been heated using microwave technology. Applications include waste remediation and recycling, as well as drying, sintering, melting, brazing, joining, infiltration, diffusion, and chemical synthesis [Manoj and Wong, 2007].

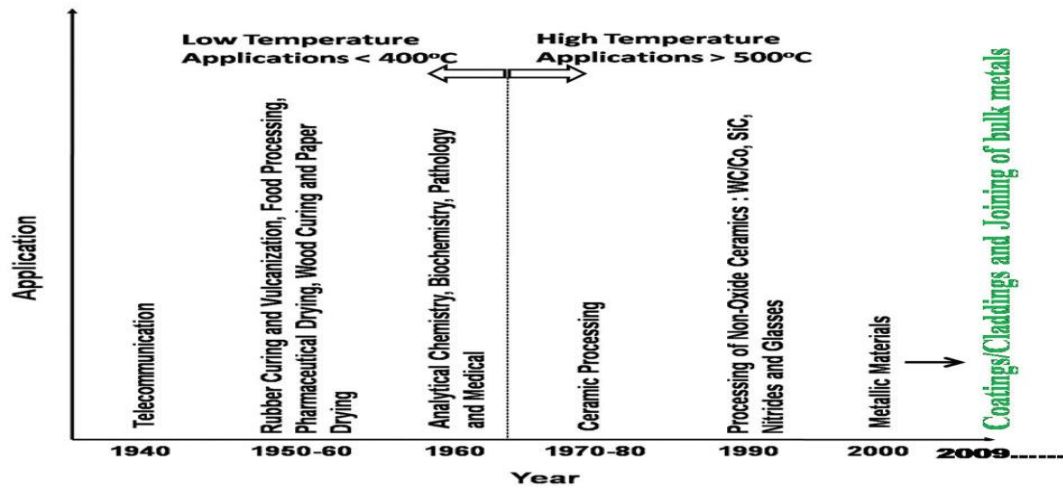


Fig.1.7: Developments in the field of microwave materials processing in chronological order

Microwaves were initially successfully used in communication networks. Later, studies and innovations on the heating effects of microwaves resulted in numerous successful applications, such as food processing, wood drying, waste management, improved chemical reactions, vulcanization of rubber, processing of ceramics and metallic materials, steel making, and energy recovery [Appleton et al., 2005; Bruce et al., 2010; Fang et al., 1997; K Ishizaki et al., 2006; Saitou, 2006].

The first effective use of microwave material processing was the sintering of various ceramic materials. The successful sintering was attributed to the ceramic powders' improved microwave absorption at room temperature. As a result, research into various ceramics and their composition was sped up in this area and is still ongoing. However, processing bulk metallic materials at ambient temperature was a severe task for researchers since metals reflect microwaves and lead to the production of plasma.

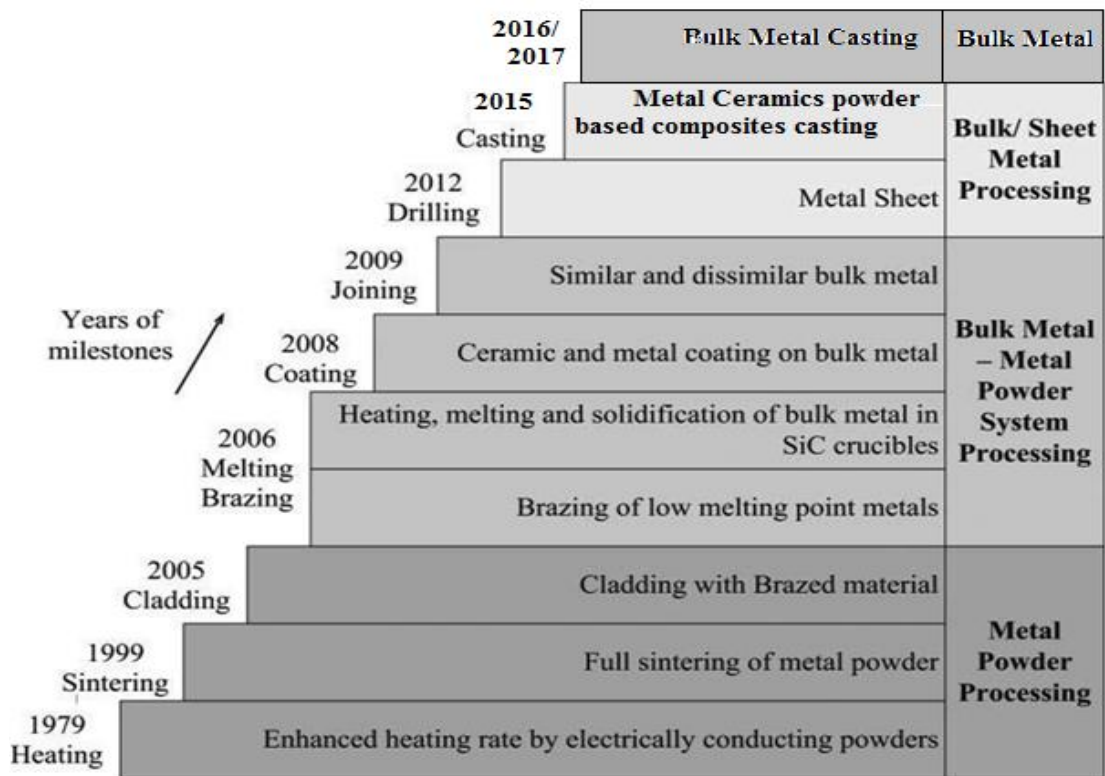


Fig.1.8: Chronological developments in microwave processing of metallic materials

Figure 1.8 displays the year-by-year changes in the field of treating bulk metallic materials using microwave radiation. [Roy et al., 1999] conducted the first research on the successful sintering of metallic materials, demonstrating that metallic materials in the form of tiny powders may combine with microwaves. This excellent study inspired researchers [Sethi et al., 2003; Gupta and Wong, 2005 and Horikoshi et al., 2013] to concentrate on the processing of metallic powders using microwaves. Subsequently, researchers have reported good sintering results.

[Sharma et al., 2009] successfully tried the task of connecting bulk metallic materials using a household microwave oven in order to treat metallic materials in bulk for higher temperature applications. Additionally [Gupta and Sharma, 2010], made use of claddings of metallic materials on metallic substrates to exploit the use of a home

microwave oven in high-temperature applications. According to reports, partial melting of metal powders was seen during the microwave joining [Srinath et al., 2011] and cladding processes [Gupta and Sharma, 2014; Zafar et al, 2013, 2014] processes, which ultimately resulted in the metallurgical bonding. The partial melting of nickel particles demonstrates that microwaves may be used to reach melting temperatures. Researchers are currently moving toward the melting and casting business thanks to the successful advancements in the sintering of metallic-based powders, which lit the fuse for the processing of metal-based materials using microwaves.

The development of metallic powder-based welding using the microwave heating process was spurred by this, leading to the improvement of welding parameters. No research on the optimization of metal processing by microwave melting has been identified in the current literature review. Therefore, it is worthwhile to try to create and improve the process parameters of a new technique for using microwave energy to weld together powders with metallic bases. The created procedure would produce small-scale welding and be effective and environmentally beneficial.

1.8 Overview of the Thesis

Chapter 1 covered the need for joining processes, an introduction to the various metal joining processes used in industry, an electromagnetic spectrum overview of microwaves, a timeline of their development, an explanation of how they interact with materials and how this differs from conventional welding, temperature gradients in conventional heating, microwave heating, and microwave hybrid heating, and finally a discussion of the processing of metal year wise.

Chapter 2 reviewed the literature related to the topic of microwave heating, and it is discussed how various types of materials have been connected by utilising these procedures, along with any remaining research gaps. This includes a discussion of the study's research goals and an experimentation flow diagram.

Chapter 3 gives the details of machines used for experiment and for testing purpose elaborate fully with its diagram and technical specification.

Chapter 4 finds information about the established setup for butt joining of austenitic stainless steel 304 utilising a hybrid microwave heating technology, as well as microwave heating mechanisms, procedures, and experiments. The full discussion of the microwave welding operating concept was discussed. This section elaborates on the parameters and steps of the experimental method. The tensile test, micro-hardness, XRD, microstructure, and SEM information have been described.

Chapter 5 provided the details of the findings and a discussion of the experiment. A base plate made of stainless steel 304 is employed as the surface for the experiment. It is thoroughly described how process variables affect tensile strength and micro-hardness. Images of the microstructure and sem were used to understand surface morphology. Utilizing the RSM approach of experiment design with CCD with face-centered is included in this chapter.

Chapter 6 includes the conclusion drawn from this research work, significant contributions and future scope of the research study.

1.9 Summary

The research on microwave processing of materials shows that this kind of production is not only environmentally friendly but also cost-effective and capable of greater

heating rates. These qualities of microwave processing have drawn scientists to the joining of bulk metals, which is made possible by the MHH approach. As metal reflects microwaves at ambient temperature, joining metal with microwave heating is a somewhat complicated procedure. To get over the aforementioned issue, hybrid heating was adopted as explained through introduction. Types of metal joining were discussed. Introduction to microwaves along with the microwave generation was also covered. The effects of magnetic and electric fields of microwave on metal were discussed. Discussed as well are microwaves and material interactions. This section also elaborates on the properties of microwave technology and its applications in several fields. With the aid of the figure, the development of microwave heating across the time frame was reviewed. Also included is a summary of the thesis.

CHAPTER 2: LITERATURE REVIEW

2.1 Introduction

In order to increase production efficiency and product quality, multiple methods were hybridised. However, many processes have certain built-in limits, either because they were made for particular materials or because they had a hefty initial investment. However, microwave heating has become a viable option for treating a range of materials. This chapter elaborates on the literature based on various materials processing pathways using microwave technology. The many metal processing techniques, such as cladding, joining, sintering, melting the material, etc., are described in literature.

2.2 Thermal Application of Microwaves

2.2.1 Food Processing

Since food contains moisture that easily couples with microwaves to facilitate heating, food preparation is one of the most popular and effective uses of microwaves. The main uses of microwaves for food include cooking, drying, sterilising, thawing, tempering, blanching, baking, and extraction.

[Tong et al., 1993; Ovadia et al., 1995] Bacon frying, food baking, and the heating of baked goods are a few examples of successful microwave cooking uses. The loaf's inside was heated more uniformly thanks to the microwave baking procedure, which also helped the crust form well.

[Heddleson and Doores, 1994] looked into the factors affecting temperature and bacterial inactivation in meals heated with microwaves, and they found that the microorganisms were only inactivated by the thermal impacts of the microwaves.

[Ryynanen, 1995] Many factors, including the dielectric characteristics, size, shape, and arrangement of the food ingredients, influence how well food is heated by microwaves. Permittivity is the most important of these. The design of the microwave heating apparatus and the choice of suitable packing materials both depend on an understanding of the dielectric characteristics. According to permittivity measurements, the composition of the food material, the temperature, and the frequency all affect the dielectric characteristics (ϵ' and ϵ'') of the material.

[Tajchakavit et al, 1997] To render the unwanted enzyme pectin methylesterase inactive in orange juice, microwaves were utilised as an alternative to pasteurisation. It was discovered that microwave heating was non-thermally contributing and substantially quicker than traditional thermal heating.

[Tajchakavit et al, 1998] Under continuous flow microwave heating, certain spoilage bacteria in apple juice may be eliminated more quickly than under normal heating settings. In 2000, Nelson et al. studies on microwave heating of macaroni and cheese food items revealed that, at high microwave frequencies, the dielectric constant decreased with temperature (5 to 30 °C) (915 and 1800 MHz).

[Zhang et al., 2001] It was later discovered that the best heating can be achieved by selecting the right combinations of parameters such as geometry (shape and size) and dielectric qualities during microwave-aided sterilisation of solid meals (composition).

[Zhang et al., 2006] investigated a variety of microwave-assisted drying techniques for fruits and vegetables. They claimed that using the microwave with other drying techniques shortens the drying time and enhances the quality of the finished product.

[Varela et al., 2008] using a susceptor packet when heating food samples in a microwave might increase their crispness.

[Sosa et al., 2010] reported on the dielectric characteristics of various food items at different frequencies. microwave heating can be used to enhance food quality depending on the values of the loss factor and dielectric constant.

[Ben-Lalli et al., 2011] Studies on the effects of heat treatment on dried fruits like dates have shown that microwave heating preserves food quality better than rigorous traditional heating.

2.2.2 Ceramic Processing

[National Research Council, 1994], SiC interacts with microwaves better at room temperature than ZrO₂ when both materials are simultaneously exposed to microwaves because of its significant dielectric loss capabilities. Up to 500°C, nothing changes, but after a critical point is reached, ZrO₂'s dielectric loss dramatically climbs with temperature. ZrO₂ absorbs the bulk of the microwave radiation because of its higher loss factor than SiC at a certain temperature and self-limiting absorption.

[Thostenson and Chou, 1999] Microwaves have been extensively employed in the ceramic processing industry, second only to food processing. Microwave heating has become more popular during the past 20 years because ceramic procedures often demand high temperatures.

[Ramesh et al., 1999] It was discovered that microwave sintering takes place at lower temperatures than traditional sintering.

[Upadhyaya et al., 2001 and Brosnan et al., 2003] various ceramics, including alumina, zirconia (3Y-TZP), and Ni-Zn ferrites, were microwave sintering successfully with improved mechanical properties.

[Gupta and Wong, 2007] therefore, microwave heating may be used to quickly heat ceramic materials with significant dielectric loss, such as SiC, CuO, and Fe₃O₄. Other ceramic materials, such as Al₂O₃, ZrO₂, Si₃N₄, and AlN, do not pair with the 2.45 GHz microwave at room temperature. Therefore, weakly absorbing ceramic materials were initially heated using a hybrid heating approach to a critical temperature above which they could easily pair with microwaves.

[Almeida et al., 2007] Microwave processing benefits include producing high-quality products in addition to rapid heating and quick melting. Microwaves were able to produce greater melt homogeneity and lower power consumption thanks to convection that was brought on by the greater heat gradients.

[Menezes et al., 2003 and Menezes et al., 2008] performed hybrid rapid sintering on porcelain bodies and alumina zirconia nano composites. They discovered that the primary component in attaining hybrid microwave rapid sintering—in which sintering cycles of 35 minutes were used for alumina-zirconia samples and heating cycles of less than 60 minutes were used for the porcelain bodies—was the regulation of the heating cycle.

[Das et al, 2008] In comparison to traditional processing, microwave processing of a hard glass-ceramic (MgO-Al₂O₃-TiO₂ system) coating on a nickel-based super alloy substrate resulted in a coating with a reduced surface roughness value and greater hardness (6GPa). [Chanda et al., 2009] A 3 kW microwave system running at a

frequency of 2.45 GHz was used to microwave sinter calcium phosphate ceramics (hydroxyapatite and tricalcium phosphate). For all compositions, it was discovered that the samples sintered in the microwave at 1250°C for 30 minutes exhibited high density and homogenous microstructure.

[Wang et al., 2008] Due to its capacity to melt glasses in a brief amount of time and due to its capacity to achieve high heating rates, found applications in glass processing, [Duval et al., 1997] glass ceramics, and [Kharissova et al., 2010 and Hemono et al., 2010] glass reinforced with metals. Additionally, microwaves were used to apply metal, carbon, metal-oxide, and organic paint coatings to glasses.

[Deng et al., 2010] showed how to produce activated carbon from cotton stalk using microwave radiation and various activators (KOH and K₂CO₃).

2.2.3 Polymer Processing

[Balanis, 1989] There are several uses for microwave heating for preparing polymers. The diffusion rates in the solid-state polycondensation of PET and Nylon were accelerated using microwave radiation.

[Mallon et al., 1998] The stimulation of tiny molecules' rotational states by microwaves, rather than the heating of polymers, was what caused the diffusion to be enhanced.

Microwave-assisted polymerizations have been the subject of much investigation.

[He et al., 2001] investigated the microwave-heated, potassium persulfate-initiated polymerization of n-butyl methacrylate in soapless emulsions. In comparison to

traditional polymerization, they discovered that microwave polymerization had a significantly greater rate and wider particle size dispersion.

[Zhu et al., 2003] Compared to traditional heating, microwave heating demonstrated a higher rate of polymerization.

[Sinnwell and Ritter, 2007; Wiesbrock et al., 2004] Microwaves are used in the step-growth polymerization of polyamides, polyimides, polyethers, and polyesters; the ring-opening polymerization of caprolactms and caprolactones; and the free radical polymerization of monomers like styrene or methyl methacrylate.

2.2.4 Microwave Processing of Composites

Many novel and cutting-edge materials, including metallic powders, were made more sinterable by microwave hybrid heating. Researchers in the field of processing composites and nano composites were influenced by this development [Bao et al., 2013; Bian et al., 2012; Tang et al., 2013; Lin and Xiong, 2012; Shannigrahi et al., 2012; Ravindran et al., 2013; Bao and Yi, 2014; Ravindran et al., 2013; Demirskyi et al., 2013].

The creation of amorphous particle reinforced light metallic composites employing microwave-assisted heating technology and a hot extrusion process was the subject of research conducted by [Jayalakshmi et al., 2014]. By using structural and mechanical analyses, the Mg-based composite with various volume fractions of Ni₆₀Nb₄₀ amorphous alloy particles was created. According to the structural study, the amorphous character of reinforcement was still present, and its distribution was based on the volume percentage. According to the claim, reinforcement-reinforcement interactions caused the clustering to begin at a greater volume proportion. Compared

to standard Mg-based alloys, composites also show improved mechanical characteristics.

The experimental study by [Rajkumar and Aravindan, 2013] was based on the tribological behaviour of copper-nanographite composites that had undergone microwave processing. Due to its exceptional qualities, nanographite was utilised as reinforcement in a copper matrix. It was determined that nanographite-reinforced composites outperformed graphite-reinforced composites in terms of wear resistance and friction. It was claimed that more nanographite surface area resulted in a thicker, more adherent tribo layer of graphite at the contact surface and decreased frictional force.

[Benavente et al., 2014] emphasised the rapid microwave sintering of alumina-zirconia nanocomposites and analysed the resulting composite's mechanical characteristics and microstructure. ZrO₂ reinforcement in different volume fractions was employed in an alumina matrix and treated at 2.45GHz between 1200 and 1400⁰C. At different volume fractions of reinforcements, it was reported that homogenous structures with improved densification, hardness, Young's modulus, and good fracture toughness were achieved. The increased characteristics of nano composites were brought about by higher densities and better homogenised microstructures achieved by microwave processing.

[Zheng et al., 2014] focused on the creation of microwave-sinterable metal matrix composites using an aluminium foundation. Using TEM, the microstructure and mechanical characteristics, as well as the bonding mechanism between the reinforced matrix and the microwave processing, were studied. The outcome showed that void-free interfaces and a diffusion layer were produced between the matrix and the

reinforced particles as a result of the liquid aluminium phase's presence around the reinforcement during microwave sintering, leading to better mechanical characteristics. Again, it has been established that all of these researchers were drawn to create composites employing microwave sintering procedures since they allow for economy as well as improved material quality.

2.2.5 Microwave Joining of Ceramic and Polymer Composites

The permanent joining of materials is a critical requirement in the majority of manufacturing and assembly businesses around the world. The joining of various materials using conventional techniques, such as traditional welding, energy welding processes using lasers and electron beams, friction stir welding, soldering, and brazing, has already been extensively studied [Ren and Liu, 2014; Hajiannia et al., 2013; Guo et al., 2014; Satyanarayana et al., 2005; Cao et al., 2014 and Lu et al., 2012]. Research in these areas is still ongoing. These procedures, however, each have advantages and restrictions of their own. The main drawbacks of traditional techniques include longer processing periods, more energy demands, more expensive setups, restrictions on the material that may be bonded, and inevitable joint imperfections.

Therefore, the solution is to create new, innovative methodologies and processing techniques that offer improved material qualities and much fewer faults, with economic benefits through expedited product development. According to research, microwave processing is not only an environmentally friendly manufacturing technique but also a cost-effective, high-volume production process. It serves as an alternative to the common heating methods used in enterprises.

The experimental study of [Yarlagadda and Soon.,1998] concentrated on the characterization of ceramic joints that were microwaved together. Flexural strength, grain size, composition, and porosity were all characteristics of the joints that were created. According to reports, a solid junction might be produced with strength of 60 to 95 percent of the foundation material's flexural strength.

The work done by [Yarlagadda and Chai, 1998] was based on the microwave welding of thermoplastics.

[Aravindan and Krishnamurthy, 1999] stated that by employing microwave hybrid heating at 2.54GHz frequency and 700W power rating, sintered alumina and 30% zirconia ceramic composite could be successfully joined. The results of the flexural strength of joints with interface powder were around 28 MPa.

The findings of the study [Ahmed and Siores, 2001] showed that the yield joint strength produced was greater than (107%) the base material. This piece was created by combining ceramics that were 48% alumina, 32% zirconia, and 20% silica.

2.2.6 Environmental Applications:

Growing industrialization has increased the need for waste treatment and necessitated the development of innovative waste and pollution-reduction technologies. [Menendez et al., 2002] For the treatment of sewage and industrial waste water, plastic wastes, organic wastes, nuclear wastes, hospital wastes, and radioactive wastes [Schulz et al., 1994; Tata and Beone 1995; Kawala and Atamanczuk, 1998; Cravotto et al., 2007], microwave radiation has been used.

2.3 Specimen Based Developments:

Microwave joining has been used to join many specimen types, from thin sheets to bulk metallic materials. When using an MHH-based join, the cross-dimensions section and shape are key factors. This is so that melting and connecting processes can take as long as necessary. Numerous academics have looked at the joining of cross-sections with rectangular and circular cross-sections of various diameters.

[Siores and Rego, 1995] used a magnetron with a 2 kW power rating to successfully combine thin metallic materials with rectangular cross sections that ranged in thickness from 0.1 mm to 0.3 mm. During the joining process, arcing was seen at the point where two specimens were pressed up against one another with a narrow space between the mating surfaces. Arcing leads to melting of the mating surfaces which were then forced against each other under externally applied pressure in order to create the joint.

One of the hardest materials to combine using traditional methods is copper. [Srinath et al., 2011] developed a novel method to connect copper in bulk form using microwave radiation. The tests were conducted on copper plates measuring 15 x 12 x 4 mm³ in length, breadth, and thickness, as well as coins measuring 18 mm in diameter and 12 mm in thickness. A uniform microstructure was produced, which may be attributed to the joint zone's volumetric heating. It was discovered that microwave irradiation altered the atomic structure of copper powder. The presence of oxides during joining increases the coupling of microwaves with metals. Microwaves interacted well with metallic powder particles of smaller sizes. Hardness and porosity values were found to be 78±7 Hv and 1.92% respectively. Joints had an average ultimate tensile strength of 164.4 MPa and an elongation of 29.21 percent. The

combined effect of ductile and brittle failures was discovered to be the mode of failure of the copper joint.

Using a microwave radiation approach, [Srinath et al., 2011] also succeeded in connecting austenitic stainless steel (SS-316). For joint development, specimens with dimensions of 25 mm, 12 mm, and 6 mm were collected. An almost complete metallurgical fusion was seen in the joint region. The development of grains at the interface was columnar, whereas grain growth in the joint's centre was equiaxed. Field-emission SEM, XRD, micro-hardness, and tensile strength measurements were used to characterise joints. The joint's core was determined to have an average micro-hardness of 290 ± 14 Hv.

By using microwave joining, [Srinath et al., 2011] connected heterogeneous specimens. They collected MS-SS316 samples that were 25 mm, 12 mm, and 6 mm in size. They applied a coating of nickel-based powder with a particle size of 40 μm in slurry form at the interface of the two substrates. It was possible to successfully connect two different metals by metallurgy. Mechanical parameters included a Vicker's micro-hardness of 133 Hv, an ultimate tensile strength of 346.6 MPa, and an elongation of 13.58 percent following the characterization of dissimilar joints. It was shown that fracture of dissimilar junctions under tensile stress was caused by both shearing of the brittle carbides and oxides and the plastic flow characteristic of a ductile matrix.

Because of their higher melting points than aluminium, specimens made of MS, SS, Inconel, and other metals are more challenging to prepare for a microwave joint. [Bansal et al., 2012] achieved effective microwave-based joining of MS plates. Trials were conducted on MS plates with the following dimensions: $30 \times 10 \times 5$ mm³, with a

0.3 mm gap between the two substrate interface surfaces. The micro-hardness of the joints, according to Vicker, was 420 ± 30 Hv, which was much greater than the base metal. 6% elongation and 250 MPa of average tensile strength were attained.

[Bansal et al., 2012] effectively joined Inconel 718 plates through the application of EM energy. Inconel 718 plate measurements of $15\times 10\times 4$ mm³ were the subject of experiments. Between the interface surfaces of the specimens, a 0.2 mm thick coating of nickel powder with an average particle size of 40 μ m was applied. Techniques like XRD, SEM, and EPMA were employed to characterise welded connections. They came to the conclusion that the MHH approach may be used successfully to melt the powder particles that make up interlayers, resulting in metallurgical bonding at fluid interfaces. According to UTM, the reported ultimate tensile strength of welded joints was 400 MPa with an elongation of around 6%. The ductile character of failure was shown by fractography of failed welded joints.

Mild steel (MS) plates of lengths of 15 mm and 10 mm were used by [Bansal et al., 2013] to create a butt joint with a rectangular cross-section of 10×4 mm². The distance between the two specimens was maintained at 0.4 mm. The Vickers' micro-hardness tester, scanning electron microscope, scanning electron probe microanalysis, and universal testing machine were all used to characterise joints (UTM). The production of substitution type solid solutions at the interface area was visible in the XRD spectrum of joints. SEM photos of joints indicated that all powder particles had completely melted. Diffusion bonding takes place between the substrates and the powder particles.

[Gupta et al., 2013] investigated the formation of microwave joints with stainless steel (SS) specimens measuring $50 \times 12 \times 3$ mm³. Joints were described using

microstructure, tensile strength, percent elongation, and micro-hardness. The characterization results revealed that an extremely fine microstructure was created. Final tensile strength, percent elongation, and hardness values were recorded as 340.16 MPa, 11.67%, and 130 Hv, respectively.

[Gupta and Kumar, 2014] performed SS-SS joint formation on a specimen with dimensions of 50 mm, 12 mm, and 4 mm. The findings of the characterization showed that the metal and tiny microstructure effectively fused, leaving a distinctly visible junction. Micro-hardness, tensile strength, and elongation values were measured and were 145.3 Hv, 323.16 MPa, and 11.30%, respectively.

[Bansal et al., 2014] characterised joints of bulk SS-316 with diameters of 25x15x4 mm³. It was deduced from the characterization that epitaxial growth was present close to the fusion zone and equiaxed microstructure was present in the joint zone. Cr carbide was poured into the grain boundaries and deposited there. Vicker's micro-hardness attained was substantially higher than that existing in the fusion zone due to the existence of hard carbides at grain boundaries. The joint's measured ultimate tensile strength was 425 MPa with a 9.44 percent elongation. Tensile testing showed that the existence of intermetallics, metallic carbides, and joints failing owing to ductile fracture in the material were the constraints for a greater rate of plastic deformation.

1018 MS joints were microwave-joined by [Dwivedi and Sharma, 2014]. To determine their impact on the intended output parameter (tensile strength) of the joint, three input factors (power, time, and temperature) were employed. The interface powder was properly fused with the base material as a consequence of the macrostructure and microstructure of the welded connections being within the

permitted range of process parameters. They came to the conclusion that tensile strength had an inverse relationship with rated power output while exhibiting a direct relationship with welding duration and temperature within a specific set of process parameters.

The researchers [Bansal et al., 2014] used several factors. Smaller specimens measuring $25 \times 10 \times 4 \text{ mm}^3$ and SS-316 powder with $50 \mu\text{m}$ sized particles served as the interface material. They employed 1200 W power level to complete the joining procedure as opposed to 900 W power level used before [Srinath et al., 2011]. In addition to XRD, field-emission SEM, micro-hardness testing, and tensile testing, they used an integrated non-contact infrared pyrometer to detect the temperature of the heating zone during the characterisation of welded joints. The ideal joining temperature was discovered to be 1360°C . The flexural strength of joints with different welding types was also tested. Following a microstructure analysis of the welded joints in the fusion zone, a dendrite type microstructure was discovered. Magnitude of 380 Hv of micro-hardness was found in the core of welded zone which was significantly higher than base material. Average ultimate tensile strength and flexural strength of welded joints were obtained as 420 MPa with an elongation of 6.67 % and 787.5 MPa with an elongation of 5.14 % respectively.

The research previously mentioned solely relates to connecting specimens with rectangular cross sections. However, [Saxena et al., 2014] also looked into circular cross-sections for connecting bulk copper pipes with an outer diameter of 10 mm and a wall thickness of 1.6 mm. They also investigated the impact of other process variables on joint formation, including duration, the position of the work piece in the applicator cavity, specimen length, slurry thickness, and susceptor material type. The

investigation was useful in determining the workpiece's ideal location, which was found to be 16 mm tall at the base plate's centre for optimising the intensity of incoming microwave radiation. The length of the specimen was seen to be limited to 10 mm since there was no melting above that and an average length of 8 mm was taken during experiments.

[Singh et al., 2015] performed bulk joining of an aluminium alloy. Plate-like specimens with dimensions of 35 x 12 x 5 mm³ were utilised. To characterise the joints, microstructure analysis, elemental analysis, a micro-hardness survey, and X-ray diffraction (XRD) were performed. A 600-second microwave heating exposure duration produced a successful joint fabrication. The joint's hardness was measured at 72.4±10 Hv.

[Bansal et al., 2015] also successfully joined Inconel 718 and SS-316L using MHH. In that work, plates made of SS-316L and Inconel-718 with dimensions of 25 mm, 10 mm, and 4 mm were employed. The plates were maintained in a butt arrangement with a 0.5 mm gap. The average micro-hardness, ultimate tensile strength, and elongation were identified to be 230.5 Hv, 517.5 MPa, and 18.18%, respectively.

[Badiger et al., 2015] looked at Inconel-625's microwave joining capabilities for parts measuring 51 mm, 12 mm, and 6 mm. It was discovered that the micro-hardness observed at the joint interface was greater than that of the joint zone. The joint zone's average micro-hardness, as measured, was 350±10 HV. The joints' tensile strength was 326 MPa with a 9.04 percent elongation.

[Bansal et al., 2015] discovered structure and property correlations for Inconel-718 microwave-based junctions using alloy plates with 30x4 mm³ dimensions. They came

to the conclusion that by precipitating strengthening phases in the matrix during the post-weld heat treatment process, the mechanical characteristics of materials may be improved. As an alternative to completely heat-treated conditions (solution treated and aged), they suggested post-weld ageing treatment.

[Rana and Sandhu, (2015)] constructed EN-31 microwave welded joints measuring 125 mm by 22 mm by 0.6 mm with an interface material width of 0.5 mm for the purpose of examining the microstructure and micro-hardness. Microwave joining, oxyacetylene gas welding, and tungsten inert gas (TIG) welding were all compared. Weld bead width, porosity, and joint hardness were used as performance benchmarks for comparison. In comparison to oxy-acetylene and TIG welding, the width of the weld bead was less when using microwave welding. In microwave-based joints, the value of vocalization of carbon and ferrous particles was also lower, which further decreased the likelihood of porosity. The microwave joining technology produced the hardest joint possible.

A comparative investigation of the microwave joints of SS304 specimens with various interface materials was carried out by [Bagha et al., 2016]. In order to compare the two interface powders, they were both nickel-based: one was EWAC (Tungsten carbide bearing alloy) powder, while the other was 99.9 percent pure nickel powder. It was discovered that the 99.9% pure Nickel powder-based joint's hardness (42.67 HRC) was greater than the EWAC Nickel powder-based joint's (30 HRC).

The impacts of the interface material's interface powder size on the selective hybrid carbon microwave joining of SS304 specimens were examined by [Bagha et al., 2017]. They obtained experimental workpieces with dimensions of 40 mm in length, 5 mm in thickness, and 3 mm in breadth, all in accordance with the ASTM designation

E8/E8-09 standard. After welding joints were tested, the findings of the hardness test showed linear increments from the heat affected zone to the bead centre. Nickel powder with smaller grain size can produce harder welding beads with higher tensile strength. However, the joint's ductility is reduced as a result.

2.4 Susceptors Based Developments:

MHH may be performed in two different ways: by combining microwaves with a separate heat source, such as an electric furnace, or by employing an external susceptor that effectively links with the microwaves. Susceptor is utilised as a microwave-absorbing substance in the latter approach. Heat is transferred to metallic material in a typical manner when microwaves strike a susceptor, causing it to become hotter beyond the melting point. Metal temperatures rose after acquiring heat until they reached a certain critical point (T_c). They begin direct coupling with microwaves once they have reached the crucial temperature.

As it prevents diffused metal from flowing beyond the joint region, the susceptor may be used to restrict the liquefied interlayer in addition to starting the coupling of microwaves with metals and alloys. When it comes to using microwave radiation to heat a particular zone without heating the entire material, the MHH approach appears to have significant promise. As a susceptor medium and to focus the microwaves for localised heating, charcoal powder is typically utilised. It is soft, readily accessible, and reasonably priced. Susceptor placement is crucial for achieving selective heating in the connecting zone. Placing a susceptor as close to the joint region as feasible is a good idea. Researchers have also looked into using susceptors besides charcoal, as discussed next.

When connecting copper pipes, [Saxena et al., 2014] conducted a comparative examination of three distinct susceptors, namely wooden charcoal, stone charcoal, and graphite powder. Even after 12 to 15 minutes, the melting point was not achieved; furthermore, red-hot conditions were not seen while using stone charcoal. The melting point of wooden charcoal was discovered after 10 to 12 minutes. In comparison to the other two susceptor media, the red-hot state and melting point conditions were promptly detected for graphite powder. The corresponding states were attained in around two to three minutes and six minutes, respectively. No quick burning, melting, or arching was seen during studies using graphite powder with an approximate weight of 5–6 gm and an exposure period of 420–540 sec. Therefore, it was discovered that graphite powder performed the best as a susceptor material among the three materials.

By raising their temperature to a critical level, silicon carbide (SiC) powder was employed by [Singh et al., 2015] to start the direct coupling of microwaves with metals. Additionally, it served to prevent direct microwave contact with metals and alloys.

SiC was employed as a susceptor in powder form by [Bansal et al., 2015]. In a different study, they employed a SiC substrate with dimensions of 25 x 25 x 10 mm³ as a susceptor [Bansal et al., 2014].

2.5 Interface Powders Based Developments

Materials can be heated and bonded directly if they have high absorption qualities and the capacity to transform microwave radiation into heat effectively. But when microwave connecting low dielectric loss elements, such as metals, it is necessary to employ an interface material. The majority of researchers employed nickel-based powder at the joint contact. As a bonding agent, interfacing slurry made of epoxy

resin (Bisphenol-A, Blumer 1450XX) and interfacing powder is utilised. Epoxy resin aids in tying the powdered interface components together, resulting in a smooth connection. Slurry thins out and forms a layer at the interface gap. The epoxy glue evaporates as the temperature of the joint zone rises, and molten interfacing powder particles fill the interfacing gap. Different interface materials were used during experiments by researchers.

In addition to pure nickel, interface powder has been used in several studies. In order to achieve the joining of copper in bulk form, [Srinath et al., 2011] employed a sandwich layer made of copper powder with a purity level of 99.5% and an estimated particle size of 5 μm . Some copper powder particles were converted into copper oxides, according to an XRD pattern. According to XRD data, a preferred orientation (1 1) was formed during microwave processing of copper powder after a transition from the dominant orientation (3 1 1).

To create MS-SS joints, [Gupta et al., 2013] conducted trials using a variety of interface powders, including cast iron, nickel sulphate, nickel carbonate, and zinc sulphate. However, in all such connections, inadequate interface powder coupling with base materials was the main cause of worry. However, the base material and EWAC-1002 ET with a particle size of 40 μm were effectively linked to create a good welded joint.

[Bansal et al., 2014] Compared with all bonding materials, nickel-based powder (EWAC) welds well and has a greater capacity to couple with stainless steel. Researchers concluded that a 95% nickel-based powder and 5% epoxy resin mixture could be used to successfully connect MS and SS and SS-SS.

[Bagha et al., 2017] conducted comparative tests to examine the effects of various sizes of pure nickel powder on joint characteristics. The relationship between homogeneity and nickel powder particle size was inverse. For the smallest powder particle size, the hardness and ultimate tensile strength were higher after characterization.

[Sexena et al., 2014] used copper powder with a purity level of 99.5 percent and a particle size of 5 μm as the interface layer to connect bulk copper pipes using MHH technology. During microwave irradiation, homogenous heating caused by metallic powder in the joint zone led to the fusing of powder particles and bulk metal interfaces.

In the interface layer of aluminium substrates, [Singh et al., 2015] employed aluminium powder with particle sizes ranging from 45 μm to less. A dense and similar junction was produced through metallurgical bonding using specimens ascribed to the melting of powder particles.

[Dwivedi et al., 2014] employed nickel-based EWAC-1002 ET powder with an average particle size of 50 μm as the interface layer between 1018 MS specimens. An appropriate fusion of nickel-based powder and base metal was accomplished within the specified range of process parameters. Through XRD examination, the existence of Fe_3C , FeNi , and Cr_{23}C_6 phases was established.

[Srinath et al., 2011] joined dissimilar metals (MS and SS-316) with particles as small as 40 μm using nickel-based powder as filler material. The sandwich layer's dielectric characteristics were drastically changed after the creation of different carbides, oxides, and intermetallics after the interaction of microwaves with metallic powder.

As a result, the sandwich layer's microwave connection was improved, which led to further localised melting and the creation of excellent joints.

[Bansal et al., 2014] employed SS-316 in powder form with a particle size of 50 μm as an interface material to link MS and SS-316. According to XRD studies, chromium has a great propensity to react with carbon at high temperatures to generate chromium carbide. The ambient heating environment during processing is credited with the formation of intermetallics such as NiFe_2O_4 .

[Bansal et al., 2014] employed an interlayer of SS-316 with particles that were around 50 μm in size between the SS-316 specimens. When the filler material used for joining is of the same composition as the parent material to be joined, microwave treated joints exhibit improved qualities.

In the joining process of Inconel 718 and SS-316 L utilising EM radiation, Inconel 718 in powder form with an average particle size of 30 μm was utilised as filler material [Bansal et al., 2015]. The oxide layer that formed on the flaking surface of Inconel-718 was caused by the presence of chromium (Cr) and aluminium (Al). The composition of the flux UV 420 TT was $\text{SiO}_2+\text{TiO}_2$ (15 weight percent), $\text{CaO}+\text{MgO}$ (35 weight percent), $\text{Al}_2\text{O}_3+\text{MnO}$ (21 weight percent), and CaF_2 (25 weight percent) was used to dissolve the oxide layer, which further helps in wetting the surfaces of candidate material.

When creating SS304-SS304 joints, [Bagha et al., 2016] employed EWAC Nickel-based powder. The performance of these joints was compared to joints made of 99.9% pure nickel powder. When compared to pure nickel powder-based joints, EWAC powder-based joints demonstrated greater weldability. When compared to pure

nickel-based joints, the surface polish of joints produced with EWAC powder was greater and the bead size was much smaller.

2.6 Experimental Set-up Based Developments:

900 W, 2.45 GHz household microwave applicators have been used for the majority of the work relating to microwave joining. However, several researchers have also made use of variously powered industrial microwave ovens. Refractory brick-based setups and insulating box-based setups are the two basic types into which experimental MHH setups may be divided.

A slot is supplied on the top face of a refractory brick in a set-up using refractory bricks (insulation, ceramic bricks). The interface material is inserted between the specimens and placed into this slot together with the specimens. A graphite layer is then placed over the joint area. At normal temperatures, metallic objects reflect microwave radiation. Therefore, an extra insulating block or element is also employed to cover the specimens that will be linked from above in order to prevent direct microwave contact with metal. The charcoal powder-containing susceptor material is maintained above the graphite sheet. The use of graphite sheets helps prevent the mingling of interface and susceptor materials. During the connecting process, it can also withstand high temperatures from burning susceptor material. If more graphite is needed, it can be applied to the joint zone's bottom face to further isolate it from the lower refractory brick. The entire set-up is then inserted into the microwave applicator's cavity. The location of the entire arrangement greatly affects how microwaves interact with it.

Microwaves may readily and uninterruptedly travel through a box constructed of low dielectric loss material, which is necessary for insulation box-based setups [Bansel et

al., 2015]. Additionally, the box functions as a thermal insulator, which stops heat from escaping into the environment. The specimens that need to be linked are typically arranged in a butt orientation, and the space between them is filled with an epoxy resin and interface powder slurry. After that, this assembly is set on a graphite plate and then placed within an insulating box. Instead of the small-sized graphite sheet used in brick-based setups, graphite plate is employed. The specimens are separated from one another by a graphite plate. Additionally, it can survive the intense heat produced during the joining process. Finally, the insulation box is kept inside the microwave oven and the joining process is started.

The experimental set-up for microwave joining of metals, ceramics, and polymers was established in 1995 [Siores and Rego, 1995]. Arcing was produced using a magnetron with a 2 kW power output, and this led to the localised melting of thin steel specimens. The main issue for joining process improvement was focusing microwave radiation at the desired location. They concentrated on peripheral amenities and microwave guide design when developing their prototype. Design elements that ensured minimal EM wave leakage were given careful consideration.

The experimental setup utilised for connecting austenitic stainless steel was addressed in 2010 [Srinath et al., 2011]. After prepping the samples, they set them on the turn table of the domestic microwave applicator's insulating material. They employed masking material to prevent the direct interaction of microwaves with the parent metal. Charcoal powder was applied on the whole masking surface as well as the area where the two materials meet. Later in 2011, they changed the setup by adding a solid graphite layer that served as a barrier between the contacting zone and the susceptible substance.

[Bagha et al., 2017]) modified the experimental setup used by [Gupta et al., 2013]. They suggested using a vertical cavity type feeder to heat target materials only when necessary. Utilizing a vertical type feeding system for processing metals improves weldability. Due to the selective and quick heating of target materials, the process time was also decreased.

2.7 Power Consumption in Microwave Processing of Materials

Microwave heating includes the materials directly absorbing radiation, which is subsequently transformed into heat energy and causes the materials to heat up in volume. According to the authors' research [Siores and Rego, 1995] microwave heating requires 10–100 times less energy and 10–200 times less processing time than traditional methods. Numerous losses, including the heating of furnaces, their walls, and heat transfer media, are eliminated by the direct transmission of energy. With them, greater temperatures may be reached faster and at higher rates of heat transfer than with traditional techniques. Researchers' experimental work [Upadhyaya et al., 2007; Giberson and Sanders, 2009; Komarneni, 1999; Bruce, 2010; Holcombe, 1991] shows that the amount of time and energy needed for processing different materials in the microwave is significantly less than conventional routes.

When sintering W-Cu alloys with microwaves, [Mondal et al., 2013] discovered that the processing times were shorter than when using a conventional furnace. This demonstrates a six-fold decrease in processing time ($T_c/T_m = 6$). The study done by [Panda et al., 2006] concentrated on the sintering time, densification, and microstructure of various steels and demonstrated about 90% time savings, which resulted in energy savings, as shown in fig. 2.1, which shows the time profile for both the methods for processing austenitic and ferritic stainless steels. Time was saved by a

factor of 10 ($T_c/T_m = 10$). The advantages of microwaves demonstrate the novelty of this material processing method.

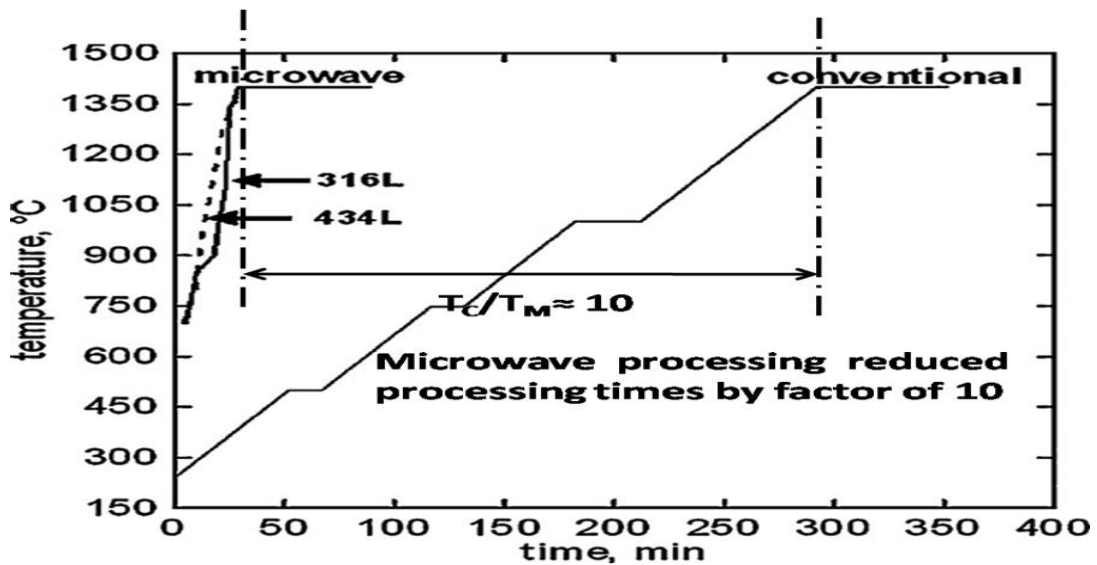


Fig. 2.1: Temperature versus time profiles for austenitic stainless steel grades 316L and 434L when heated using a microwave and traditional heating methods

[Panda et al 2006]

The comparison of power consumption and heating time for conventional and microwave sintering is depicted in Fig. 2.2, according to [Upadhyaya et al., 2007]. The results clearly showed a time and energy reduction of 7 and 4, respectively, and they supported microwave processing in terms of lower power usage and faster processing times.

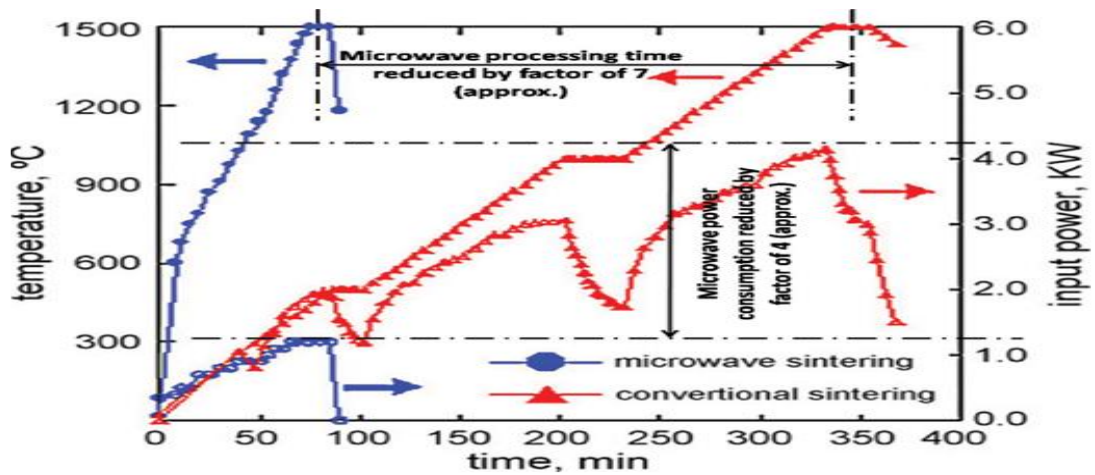


Fig. 2.2: Comparison of power consumption and heating time for conventional and microwave sintering [Upadhyaya et al., 2007]

2.8 Microwave Materials Sintering Processing

Sintering is a manufacturing technique used to manufacture a variety of materials, including metals, ceramics, polymers, composites, and others.

The main finding of researchers studying microwave processing of metallic materials up to 1995 was that it was impossible to sinter pure metal or alloy powders. [Roy et al., 1999] have also conducted research on the sintering of several metallic-based powders.

High temperatures, rapid heating rates, even temperature gradients, and even thermal distribution throughout the specimen is common conditions for the sintering process. Because the typical sintering technique cannot provide homogeneous heating or temperature gradients, the compact must be processed at high temperatures for a longer period of time. Compacts have become distorted and coarser due to sluggish heating rates and longer processing times.

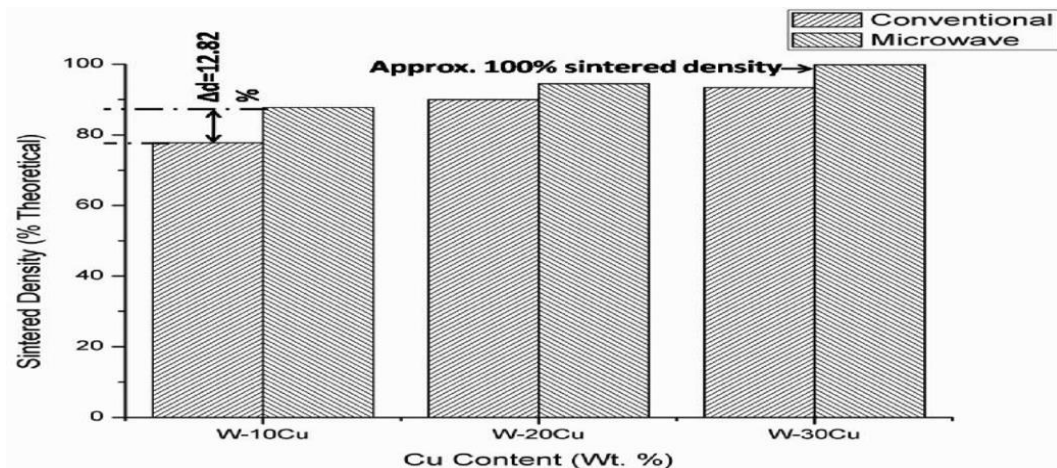


Fig. 2.3: Theoretical W-Cu composite sintered densities (in percent) after microwave and traditional sintering are compared [Mondal et al., 2013]

Due to the compacts' being submerged for a longer period of time at higher temperatures, the resulting microstructures are uneven, coarse, and contain a number of flaws, such as porosity and cracking. By using a process called microwave sintering, these issues can be reduced [Leonelli et al., 2008; Agrawal, 2006; Menezes et al, 2008; Huang et al, 2009; Wang et al., 2008; Upadhyaya et al., 2007; Giberson and Sanders, 2009; Komarneni et al, 1999; Bruce et al, 2010 and Holcombe and Dykes, 1991]. This process also produces relatively homogeneous microstructures with improved properties and at a shorter time scale. In microwave processing, better microstructures and improved characteristics are made possible by greater heating rates, uniform material heating (volumetric heating), and shorter times to reach higher temperatures.

Densification parameter- Dimensional measurements and the Archimedes density measuring method may both be used to determine the density of powder compaction. The compact sinter ability accounts for the impact of originally pressed density

fluctuations, which are described and may be stated in terms of a normalised, dimensionless densification parameter, or factor.

Densification Parameter = (sintered density - green density) / (theoretical density – green density)

According to [Mondal et al., 2013] theoretical sintered density findings, which are shown in Fig 2.3, microwave processing yields densities that are significantly greater than traditional processing. When compared to conventional processing, microwave processing increased the density of the W-10Cu composite by about 13%, yielding nearly full-density composites.

[Menezes and Kiminami, 2008] experimental study revealed that a hybrid microwave sintering procedure virtually completely densified Al₂O₃-ZrO₂ nanocomposites. Many authors [Menezes et al., 2008; Wong et al., 2007; Wang et al., 2008; Sharma et al., 2002; Brosnan et al., 2003; Fang et al., 2000] reported the complete densification of Alumina-alumina composites.

Uniform grain growth- The interaction between the processes of densification and grain coarsening determines the microstructures that are produced during the heating and processing of materials. By maximising a number of variables, including temperature, heating rates, heating periods, and temperature gradients, better microstructures can be achieved. As opposed to typical slow heating techniques, the quick heating used in microwave processing has several advantages, including higher sintered density and finer microstructures. In comparison to traditional processing methods, these finer microstructural changes, finer average grain size, better densification parameters, and reduced porosity defects provide materials with

improved mechanical qualities. Authors [Tao and Shi, 2012; Mondal et al., 2009; Padmavathi et al., 2012; Plucknett and Wilkinson, 1999; Mondal et al., 2009] described fine microstructure characterisation of microwave-treated materials. Figures 2.4–2.6 display the SEM images from [Mondal et al., 2009; Upadhyaya et al., 2009 and Panda et al., 2006].

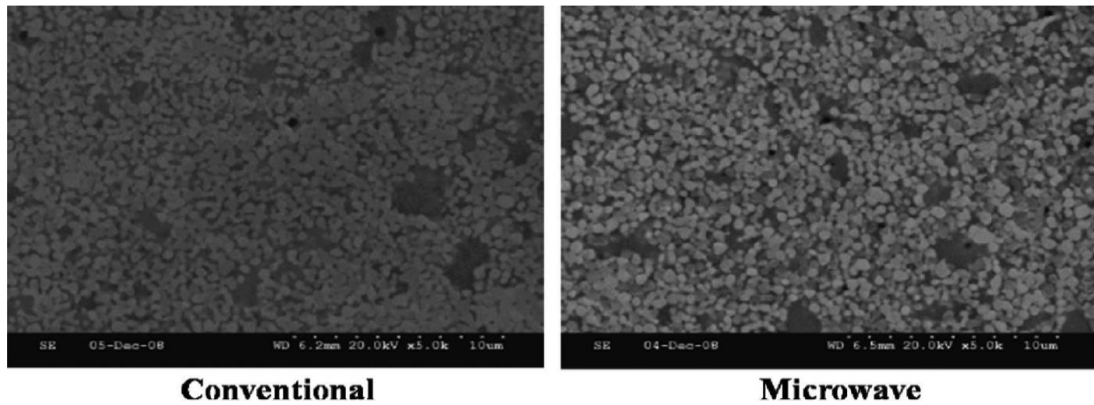


Fig. 2.4: SEM of W–Cu composite subjected to conventional and microwave heating [Mondal et al., 2009]

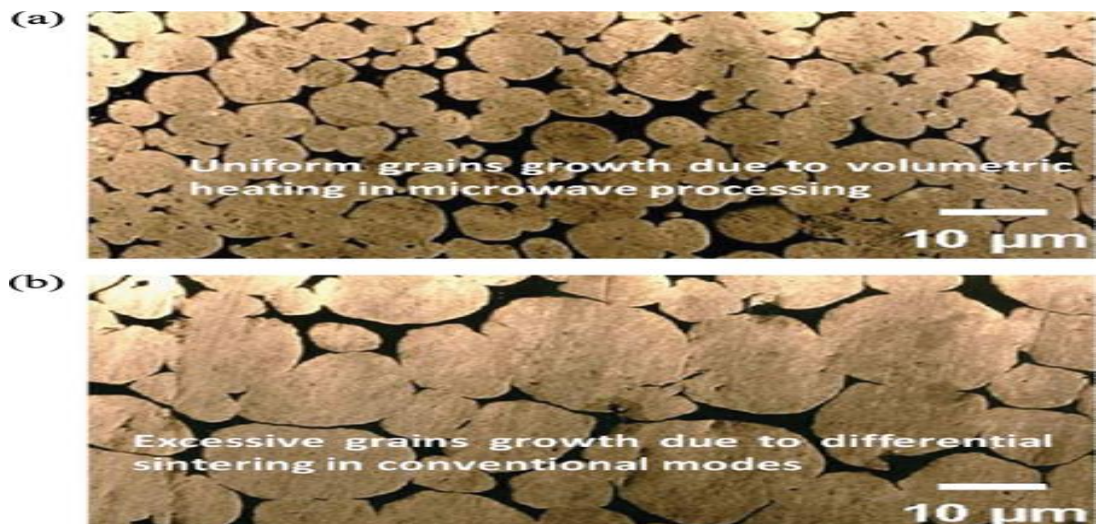


Fig. 2.5: SEM micrographs of (a) microwave and (b) conventional

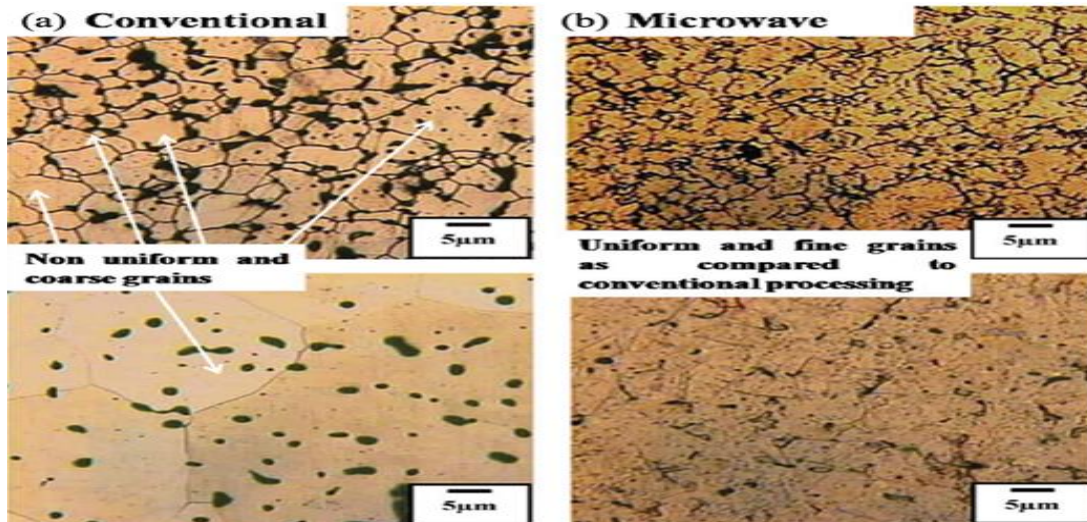


Fig. 2.6: 316L and 434L steel compacts' optical microstructure after being sintered for 1 hour at 1400⁰C in a conventional furnace and a microwave furnace, respectively, according to [Panda et al., 2006]

Better microstructures were reportedly formed as a result of homogeneous heating rates, shorter processing times, and temperature conditions present in microwave processing but lacking in traditional heating.

The most recent advancements in the field of employing microwaves to treat materials were evaluated by [Agrawal, 2013]. Complete evaluations of the sintering of certain significant ceramics, including ceramic metal composites based on Al₂O₃, ZrO₂, BaTiO₃, and WC-Co, have been published. Iron, steel, Cu, Al, Ni, Mo, Co, Ti, W, WC, Sn, and other metallic powders and their alloys were successfully sintered. This was reported. Additionally, the author gave an explanation of the steel-making process and demonstrated that microwave processing may be a brand-new, environmentally friendly method of producing steel. According to the report, pure microwave technology was used to make steel, resulting in a 50% reduction in CO₂ emissions compared to traditional methods. There have been reports of the use of

microwaves in oil shale extraction and tyre recycling. The conversion of the entire tyre into items like steel, solid carbon, and oil was explored.

In typical heating systems, where material was heated from the surface to the inside with larger temperature gradients, the issues of obtaining bad microstructures were also documented. The report goes on to describe how much energy is used during microwave sintering. The fact that microwaves transport energy directly into the materials, forgoing volumetric heating and preventing heating of other materials, accounts for the decreased power usage in microwave sintering. It was stated that the heating was volumetric and consistent, saving time and energy and improving the mechanical characteristics of the samples. The study also discusses the processing characteristics of different ceramics, metal matrix composites, and metallic powders.

2.9 Microwave Drilling

In microwave heating, processing of ceramics, polymers, composites, metallic powders, and environmental remediation, in-depth evaluations have been documented. In the current study, the advancements in the fields of iron and steel processing were covered. The microwave drilling setup was investigated and suggested for drilling in concrete, silicon, ceramics, rocks, glass, and other materials with a diameter range of 0.5 to 13 mm. Microwave drilling has been used effectively for ceramic materials that are difficult to drill using traditional techniques because they are hard and brittle.

According to the article, carbon fiber-reinforced plastic materials interact with microwave radiation quite strongly and have improved mechanical characteristics. Microwave heating applications in manufacturing and machining were still in the

early stages of consideration and held great promise for treating a range of materials. The safety issue while employing microwave technology was the source of the severe worry. According to a report, microwave energy poses a risk to the user owing to the human body's high rate of absorption, which heats up tissues.

2.10 Microwave-Processed Coatings/Claddings

In order to impart and enhance the desired qualities of the materials, there is a lot of research being done in the subject of surface engineering. Figure 2.7 illustrates the potential applications of surface engineering, which primarily include improvements to mechanical properties, surface conditions, thermal insulation, anti-wear qualities, corrosion and oxidation resistance, and metallurgical modifications. But the laser cladding equipment is pricey, and it results in several inevitable flaws, including excessive distortion, porosity, and cracking.

[Gupta and Sharma, 2011; Gupta et al., 2012 and Gupta and Sharma, 2012] Microwaves application in the field of cladding was explored by using domestic microwave applicator.

[Gupta et al., 2012] utilised for creating ceramic claddings on metallic substrates. Higher speed and reduced power usage were cited as key characteristics of this technique. Microwave cladding processing results in decreased flaws like porosity and enhanced mechanical characteristics.

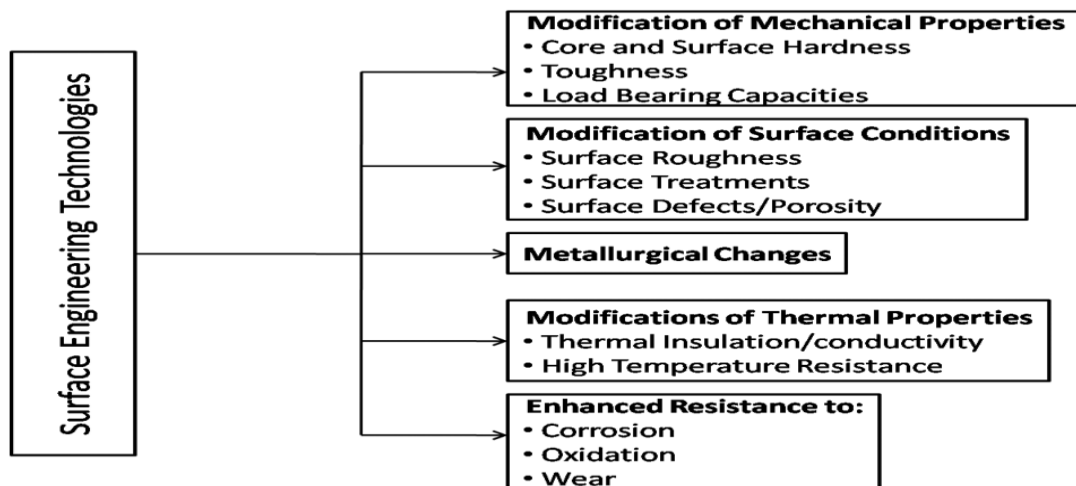


Fig. 2.7: Potential areas of surface engineering technologies

[Adachi and Udeda, 2013; Gnyusovand Tarasov., 2014; Lai et al., 1993] As a result, numerous surface modification processes, including carburizing, cyaniding, nitriding, coating/cladding, etc., are used in practise to somewhat mitigate the aforementioned issue. The current techniques, however, provide difficulties in terms of manufacturing prices, processing times, capital expenditures, improvements in surface qualities, flaws in treated components, environmentally friendly processing, etc.

The impact of annealing on the mechanical and microstructural characteristics of titanium coated with a combination of nickel and aluminium was examined by [Cammarota et al., 2009]. In order to create a coating on titanium, 2.45GHz microwaves were utilised to initiate a self-propagating high-temperature synthesis in a combination of Ni and Al powder. The energy of microwave radiation and the exothermic nature of the process allowed temperatures to increase to the NiAl melting point. The molten NiAl interacted with the titanium layer underneath it to create a ternary eutectic of Ni-Al-Ti at the contact. It was demonstrated that the reinforcement phase is formed by the interlocking network that makes up the intermediate layer that was created by the interface. Compared to the original NiAl coating, the produced

layer was harder and tougher. By quickly annealing the intermediate layer at temperatures above the eutectic temperature, the thickness of the layer was further changed. It was determined that the intermediate layer's hardness and fracture toughness were significantly greater than those of titanium and NiAl coating alone due to the strong constraining effects of the interlocking microstructure created during microwave processing.

[Gupta and Sharma, 2010] An Indian patent application was submitted for a technique of metallic cladding on a metallic substrate employing microwave radiation. It was asserted that treating cladding using microwave radiation is a time and energy-efficient, cost-effective procedure. It has been discovered that clad heated by microwaves has fewer imperfections such as solidification fractures and porosity, which may help to improve its mechanical qualities. In this section, researchers that study microwave-based surface coatings and treatments present some of their most significant reviews. In general, low-temperature uses of the household microwave oven, notably for warming food, are recognised. The usage of the microwave oven, however, was expanded by the researchers to include high-temperature applications for a variety of uses.

The focus of [Boromei et al., 2010] was on the high-temperature oxidation resistance of aluminide coatings made using a microwave-assisted self-propagating high-temperature synthesis technique. Using microwave radiation, the mixes of Al and Ni powders were employed to create intermetallic coatings on titanium substrates. The major objective of this study was to evaluate the performance of titanium at high temperatures with a Ti-Ni-Al layer produced using microwaves. According to experimental results, ternary layers exhibit oxidation resistance that is equivalent to

NiAl up to 7500°C, but at 900°C NiAl exhibited greater oxidation resistance due to the low Al concentration in ternary compounds caused by microwave processing, which prevents the development of scale. The outcomes of the isothermal oxidation test, which was carried out in dry air flowing at 750 and 900°C for 5 hours.

[Lin et al., 2011] focused their experimental work on using a microwave plasma system to process nitride layers on a biomedical stainless steel substrate. In an AST-MW1200W plasma reactor, microwave plasma was used to create the nitride layers. Using a continuous power of 700W at a frequency of 2.45GHz, microwave plasma was created. High microhardness and enhanced antibacterial activities were identified in the created coating layers.

The experimental study conducted by [Gupta and Sharma, 2011] was primarily concerned with SS-316 and the evaluation of the sliding wear performance of clad created using a unique hybrid microwave method. The material was then microwave-irradiated to create a wear-resistant cladding made of tungsten, and the material was then evaluated using XRD, FESEM, and Vickers microhardness. Using a pin-on-disk sliding device against an EN-31 hard facing surface, the tribological characteristics were examined. Due to the uniformly distributed hard carbide phase, the produced clad exhibited notable wear resistance. The microwave-developed clad's microhardness research found that it was in the 1064–99 Hv range and that its porosity was around 0.89 percent. According to wear testing, microwave clad demonstrated an 84-times greater resistance to wear than SS-316 steel, which corresponds to a sliding speed of 0.5 m/s.

The sliding wear performance of WC10Co2Ni composite cladding created by microwave processing was studied by [Gupta and Sharma, 2011]. A pin on disc

sliding was used to examine the tribological parameters of the cladding against an EN-31 (HRC-70) material. The cladding was created from austenitic stainless steel (SS-316). Because there was a consistent distribution of the hard carbide phase, the clad that were formed demonstrated notable wear resistance. The microhardness of microwave-developed clad was 1064-99 Hv, with a much lower porosity of 0.89 percent. Wear testing revealed that microwave clads outperformed SS-316 steel by 84 times, corresponding to a sliding speed of 0.5 m/s. Furthermore, the scientists claimed that variations in speed have only a minor impact on the wear resistance of microwave clad (within 16%). Lower material loss was achieved during sliding due to the formation of an unstable oxide layer (tribofilm), although at faster sliding speeds, this layer quickly became smeared. The major causes of clad wear were fatigue-induced debonding, micro crack formation, micro cutting (shear), and spalling. These microwave processing or microwave-assisted procedures may be used to generate various claddings, coatings, and films on a range of substrates, including metals and ceramics, with the goal of accelerating the production of tough and wear-resistant surfaces.

[Gupta et al., 2012] used a microwave radiation hybrid approach to create a EWAC 20 percent Cr23C6 cladding on an austenitic stainless steel SS316 substrate. Vicker's microhardness measurements, energy dispersive X-ray spectroscopy, FE-SEM, and other pertinent methods were used to characterise the produced claddings. The XRD pattern revealed the presence of nickel silicide, nickel iron, and chromium carbide phases, which helped to increase the microhardness of the clads. There were no discernible interfacial fractures in the 1 mm thick clads. Clads have a microstructure that resembles cells in many ways. When compared to the substrate material, the

produced clads are more microhard. It was determined that these claddings would work well in situations requiring wear resistance.

On an austenitic stainless steel SS-316 substrate, [Sharma and Gupta, 2012] constructed a carbide-reinforced (tungsten carbide-based) metal matrix composite cladding.

By partially diluting the clad material, the produced clad demonstrated the presence of a strong metallurgical connection with the substrate. It was discovered that many novel phases were present, including WC, W₂C, NiSi, NiW, and Co₃W₃C. The three-point bend test was used to investigate the peel-off strength of the clads and revealed two separate load transitions for the matrix and reinforced phases. The clad failed at the upper transition stress, and the SS-316 substrate took on additional strain. The created clad's excellent stiffness and adhesion properties prevented cracks from forming because of the soft Ni-based matrix's ductile nature.

The microstructure and flexural strength of metal-ceramic composite cladding created by microwave irradiation were studied by [Sharma and Gupta, 2012]. The hardness at the interface is around double that of the substrate, according to the Vicker's microhardness profile created from the samples along a composite clad cross section. The load-bearing behaviour of the substrate and generated clad is demonstrated by the load versus displacement graphs obtained for the composite cladding during the three-point bending test. The clad failed at the upper transition load, and the SS-316 substrate took on additional strain; nonetheless, there was no evidence of clad peeling. According to reports, the developed clad's soft Ni-based matrix prevented cracks from forming.

[Mallia and Dearnley, 2013] Surface deterioration of engineering components is a concern in many engineering sectors, mostly because of wear and corrosion during service, which can lead to catastrophic component failure. The system may temporarily break down as a result of the catastrophic collapse, which might place an unwelcome financial load on the engineering sector.

The study by [Zhou et al., 2013] described a unique microwave-assisted technique for quickly and uniformly depositing an ultra-thin, crack-resistant apatite coating on titanium implants. The process for creating a coating consists of microwave irradiation in addition to a traditional biometric coating. The production of Ca-P nuclei was expedited by microwave radiation, which also completely coated the implant's surface with depositing material. The hydrophilicity, physical characteristics, and growth potential of microwave-assisted coatings were investigated, and these results indicated more promise in biological applications.

[Mazur et al., 2014] conducted research on indium-tin oxide coatings. Reactive magnetron sputtering with microwave assistance was utilised to produce these coatings on microscope slides and silicon substrates. AFM analysis of the coating surfaces showed that they were homogenous and extremely smooth, while XRD measurements showed that they were amorphous. When steel wool scratch tests were conducted, the mechanical characteristics of the deposited coatings based on the nano indentation approach showed good hardness and few scratches.

The experimental study by [Zafar et al., 2013] created a metallic coating of Inconel 718 powder on austenitic stainless steel using MHH method. According to the paper, 1 mm thick cladding was fabricated and examined using appropriate characterization methods including XRD, FESEM, and EDS. The microstructure analysis showed that

the cladding and substrate materials, which were mixed together during microwave heating, had undergone some partial dilution. It was determined that the cladding was devoid of porosity and interfacial fractures.

A review of the welding method for placing wear-resistant overlays on various materials was offered by [Mendez et al, 2014]. But among the frequently used industrial anti-wear solutions, laser cladding has been acknowledged as one of the most well-liked surface approaches [Nowotny et al., 2014 and Weng et al., 2014]. The drawbacks of laser claddings include greater setup costs in the beginning and inevitable flaws, including excessive distortion, porosity, and cracking that arise during processing.

[Sun and Bell, 2014] Many engineering components experience catastrophic failure as a result of the frequent surface degradation processes of wear, corrosion, and oxidation, which begin at the component's surface. Wear, corrosion, and oxidation cause the various components in gas turbine plants and hydropower plants to fail more frequently. Therefore, it is crucial to stop these components from failing frequently. To increase the service life of the components, functional surfaces must be modified, which may be done by employing a variety of accessible surface modification techniques. These different methods of surface alteration include coating/cladding, coating/nitriding, carburizing, and cyaniding.

2.11 Microwave Melting of Metals

The topic of microwave-assisted metal melting has a promising future despite the paucity of literature and research in this area. The sintering of metallic powders utilising hybrid heating methods is the major area of research interest. [Agrawal,

2013] wrote another review study that concentrated on the sintering of different metallic powders and applications for the processing of metals.

[Chandrasekaran et al., 2011] only provided experimental findings for the melting of tin, lead, copper, and aluminium metals with microwave processing. It was found that microwave processing was twice as quick as traditional processing, while microwave melting required less energy. It is claimed that using a microwave to melt metals is a more effective and secure method than using other methods. Further experimental data were modelled using a lumped parameter model, and predicted results were consistent with actual results at the same temperatures and processing conditions, indicating a 2.5-fold reduction in microwave melting time. Due to the favourable properties of energy and time savings, the casting industry will be the focus of future research in the field of microwave metal melting.

2.12 Microwave Joining of Bulk Materials

For industrial sectors, it's crucial to combine two metallic or non-metallic substrates that are identical or dissimilar with the least number of flaws possible. These innovations are still in the early stages and will take some time, updated technological knowledge, and improved research to be used as production methods in many sectors. These qualities have made researchers interested in connecting bulk metals, which is made possible by the use of microwave hybrid heating methods. Many researchers have lately become interested in this topic because of the use of microwaves to link bulk metallic materials [Sharma et al., 2009; Srinath et al., 2011; Bansal et al., 2013 and Bansal et al., 2014).

[Siores and Rego, 1995] successfully completed the work on connecting thin steel sheets of thickness 0.1-0.3mm using a 2kW multimode magnetron.

[Agrawal, 2006] reported on studies on utilising braze powders to combine steel and cast iron parts.

[Srinath et al., 2011] successfully fused base metals in a home microwave to combine bulk metallic chunks. This section expands on the developments in microwave-assisted metal joining.

[Srinath et al., 2011] studied a new method of microwave irradiation in a multimode applicator at 2.45GHz and a power of 900 W, by introducing a sandwiched layer of copper powder for metallurgical joining of high thermal conductivity materials (copper). Microstructure analysis, elemental analysis, phase analysis, microhardness survey, porosity measurement, and tensile strength testing were used to characterise the joints.

[Srinath et al., 2011] conducted an experimental study on the merging of dissimilar joints utilising microwave hybrid processing. Using a multimode applicator, stainless steel (SS-316) and mild steel (MS) were effectively microwave joined in bulk at 2.45GHz and 900 W.

The theoretical features of welding metallic materials in microwave cavities were the main focus of the research conducted by [Das et al., 2012]. The authors provided an explanation of the connection between the spatial oscillatory distributions of powdered particles and their electromagnetic field penetration. They created all the theoretical models that explain how volumetric heating works and how the whole weld zone operate as a heat source when exposed to microwave radiation.

The experimental investigations of single mode and multivariable frequency mode microwave processing and their applications in many domains were emphasised in the

work done by [Chandrasekaran et al., 2012]. Additionally, they went through the applicability of Lambert's law and Maxwell's electromagnetic field equations in the modelling of microwave heating systems. The creation of hot spots or thermal runaways was found to be the main issue with microwave heating in single mode microwave processing after the thermal and thermal impacts were researched. The use of microwaves with varying frequencies is supposed to lessen hot spots. The authors concentrated on hybrid heating systems as a way to treat materials that are difficult to combine with microwaves.

The emphasis of [Gupta and Kumar, 2014] research piece was the utilisation of microwave radiation to connect stainless steel. The Ni-based powder (EWAC 1002ET) has been used as a sandwich layer in the connecting of stainless steel, and the MHH idea has been used to make joints in a home microwave oven. Although the authors claimed that the joint was immune from cracking, microstructural analyses revealed a minor degree of porosity. According to reports, the joint tensile strength dramatically rose as nickel content and exposure duration increased.

This study also inspired [Bansal et al., 2014] to link bulk stainless steels utilising the MHH technique. It was claimed that the interfacial powder employed during the MHH process had the same base metal composition as the liquid metal, which caused the nucleation of new grains without changing the crystallographic orientations of the original grains. More mechanical testing was done on the joint. Microhardness measurements showed that the average hardness at grain borders was more than 650 HV, but the hardness was discovered to be 275 HV inside the grains.

[Singh and Sharma, 2019] utilising microwave with a fixed frequency of 2.45 GHz and a 900W rated output via the hybrid heating technique. A 1mm-thick clad

developed in 15 minutes, according to the 900 W power trials, which were conducted. SEM, XRD, and Vicker's microhardness measurements of the finished clad demonstrated a consistent and crack-free clad as a result of volumetric microwave heating. XRD may be used to detect the emergence of hard carbides such as W_2C and $Cr_{23}C_6$, which contribute to improving the coating's hardness. Vicker's microhardness was determined to be $761 \pm 1.5Hv$.

[Gautam and Vipin, 2018, 2021] examined a study that introduced microwave heating, its properties, the influence of process parameters on welding, and the work done in the field of microwave joining of similar and different materials in the previous ten years by many researchers.

[Bagha et al., 2017] looked at how pure nickel powder (99.9%) affected the selective hybrid microwave joining of SS304. The physical and mechanical characteristics were described using SEM, EDS, micro hardness, and tensile tests. As seen by SEM, nickel powder has an excellent melting ability, depending on the powder size. In comparison to the other nickel powder sizes, the lower micron sizes demonstrated better homogeneity. According to EDS, the constructed joint contains Cr, Ni, and carbon infused from the graphite sheet. According to tests on hardness, the hardness diminishes as the size of the powder increases. According to Micro-UTM, the smallest particle size has the maximum tensile strength.

[Soni et al., 2018] focused on the benefits of using nano-sized filler powder in the SS316-SS316 MHH connection.

[Bagha et al., 2019] improved the microwave joining method for SS304-SS304 without filler material. The desirability function attained its maximum value when the

cavity's diameter and height were adjusted to 15 mm and 31.1 mm, respectively (0.5907). The results of the SEM and EDS tests showed that the substrates completely melted and bonded, producing a homogenous joint. EDS identified the presence of C, Cr, and Fe. The joint's microhardness was found to be 260 HV and its HAZ to be 200 HV. The micro-tensile results for the joints were 271 MPa with 2.34 percent elongation.

A microwave beam was employed by [Pal et al., 2020] to enhance SS304/SS316 connectors. Three different sizes of nickel powder (Y1, Y2, and Y3) were combined in a 75:25 ratio with a very viscous epoxy resin (blumer 1450-XX) to create the filler material (by weight). characterizations using mechanical, SEM, and EDS methods were used. While EDS contains iron, chromium, carbon, silicon, manganese, nickel, oxygen, and sulphur in the joint region, SEM demonstrated uniformly scattered grain structure limitations. The joint attained its maximum micro-tensile strength (483 MPa) and micro-hardness (496 HV) at 70 nm, SS304, and 360 seconds.

The practicality of combining duplex stainless steel SS205 specimens with a cross-section of 3.5 mm x 5 mm and a susceptor of charcoal powder was examined by [Kumar and Sehgal, 2020]. Vickers micro-hardness testing was utilised to evaluate linked specimens as they were subjected to a 15-second, 5 kg strain. A Vickers micro-hardness test on the linked area revealed a 62.7 percent increase in hardness when compared to the base metal.

The impact of process variables on Inconel-625 joining with microwave hybrid heating was examined by [Sharma et al, 2020]. The size of the vertical coal feeder, the thickness of the separator, the thickness of the insulation brick, and the contact between the ceramics and the insulator brick were all studied as input factors

throughout the research. According to the study's findings, the joint zone has melted properly, there are no flaws, and the susceptor powder hasn't spread throughout the specimen.

[Kumar et al., 2020] constructed butt joints in stainless steel SS304 and SS316 specimens using a microwave hybrid heating method. Stainless steel 316 is used as the filler material. The results show that increasing the joint's hardness results in the generation of a homogenous joint. In SEM images, a junction that has formed without cracks is visible.

[Gautam and Vipin, 2021; Gautam et al, 2022] reviewed the research based on microwave hybrid heating and also reviewed the parameter and process flow chart of hybrid heating.

[Sourav et al, 2021] In this study, mild steel has been microwave-welded at various exposure times while the mechanical properties at the weld zone are analysed. In this investigation, commercial mild steel specimens measuring (20x20x2) mm are employed. Microwave frequency, interface material, power rating, susceptor, separator, and exposure time are process variables utilised in microwave welding. Tests on the welded piece's microstructure, porosity, and hardness were conducted to assess its mechanical properties. According to the findings, reliable welding takes place between 630 and 840 seconds, below which the weld is only partially complete and beyond which the specimen deforms. The obvious austenitic structure grains were disclosed by the weld region's microstructure. There were no apparent porosity defects in the weld zone. In comparison to the base metal's hardness, which is 49–50 HRB, the hardness at the weld joint and on the HAZ is each 58–59 HRB and 51–52 HRB, respectively.

[Gautam and Vipin, 2022] looked into the microhardness and tensile strength of stainless steel 304 plates joined by microwave heating radiation. Nickel powder in three distinct sizes—5 μm , 10 μm , and 15 μm —was employed as an interface material. Welding duration, change in slurry by weight, and varied sizes of nickel powder as slurry were selected as the main factors. To investigate the mechanical strength of the joint, tensile strength and micro hardness were used. In order to maximise the outcomes, experiments were designed using the centre composite design (CCD). The findings demonstrated that tensile strength and micro hardness decreased as nickel powder particle size increased, but tensile strength and hardness increased as welding duration increased. The mechanical characteristics of the joint are positively impacted by the weight of the slurry. The influence of welding duration stood out the most from the outcome, followed by powder particle size and slurry material weight. The ideal values for welding duration, particle size, and slurry weight as input factors were discovered to be 13 min, 5 μm , and 3 g.

[Gautam and Vipin, 2022] This entire study demonstrates the viability of fabricating type 304 stainless steel using microwave radiation and a novel process that incorporates a susceptor. The junction was joined using a multimode home IFB microwave oven operating at 2.45GHz and 900W. Using ambient conditions and a mixture of fine powder based on nickel-cobalt and glue, clean surfaces were joined together, and samples were subjected to microwave radiation to create the junction. Tensile tests, X-ray diffraction (XRD) for intermetallic compounds, microstructural analysis, and field emission scanning electron microscopy (FE-SEM), a micro hardness test, a porosity test, and surface temperature measurements were all used to analyse the weld joints. The tensile strength was 390 Mpa, or around 70% of the base metal. The weld metal area and base metal both had average measured microhardness

readings of 65–66 HRB and 71–72 HRB, respectively. The weld zone region's surface temperature was determined to be 926°C.

According to the conclusions drawn from academicians' and researchers' studies on the joining of bulk metallic materials, microwave-processed joints had fewer defects, higher mechanical qualities, and were created at lower power ratings. Although the research on material joining is still in its early stages, the authors' findings indicate that this unique technique will soon be applied to material joining in several promising ways.

2.13 Some Industrial Applications of Microwaves

Microwaves are finding more and more uses in the processing of materials, industrial research, and technological advancements. The usage of microwaves in industrial settings is the main topic of this section, which establishes them as a strong contender in the field of industrial technology.

[Sosnik et al., 2011] went into great length about the many uses of microwave radiation in the synthesis of various polymeric materials. The production of biomaterials using unprocessed synthetic and semi-synthetic polymers was thought to benefit greatly from the use of the microwave. Microwave irradiations, according to the authors, are one of the most adaptable and promising methods for creating biomaterials, and they will be critical to the growth of the pharmaceutical and biotechnology industries.

The focus of the study by [Yang et al., 2013] was on the application of MW non-destructive testing to assess the porosity of the top coating (TC) of plasma-sprayed thermal barrier coatings. One of the primary reasons for the failure of thermal barrier

coatings is the porosity of TC. The relationship between phase difference and frequency at various TC thicknesses was estimated using Computer Simulation Technology by Microwave Studio (CSTMWS simulation software) for microwave non-destructive testing. The findings showed that the sensitive frequency of MW varied with TC thickness, yet it was determined that TC porosity could be evaluated using non-destructive MW assessment by selecting the proper frequency in accordance with TC thickness.

The study conducted by [Saber et al., 2013] concentrated on the use of microwaves in pipeline biofilm monitoring and assessment. Poor heat transfer efficiency in heat exchanger systems, higher frictional drag as a result of decreased diameter, and accelerated bio corrosion in pipelines are just a few issues that bio films may cause. These issues prompted the creation of a microwave approach that utilised in-home transducers for microwave transmission and reception for online monitoring. This technology is advantageous for online monitoring of pipelines for deposited films because the change in dielectric characteristics caused by the deposition of bio films creates highly sensitive alterations to the signals.

According to studies by [Zanotto et al., 2013], the approach of cleaning multi walled carbon nano tubes before polymerization using microwave radiation was quicker and cleaner. The short MWNT that had undergone MW treatment had the best contact and dispersion with the poly (methyl methacrylate) matrix. According to the paper, the MW treated MWNT significantly influenced the composite's thermal characteristics. The commercial manufacturing of MWNT can use this microwave-based purifying procedure.

[Chen et al.,2014] focused on the microwave sintering and characterization of composites made of polypropylene (PP), multi-walled carbon nanotubes, and hydroxyapatite (HA). The study concentrated on employing microwave sintering to create biomaterials for bone tissue engineering. As a susceptor material, multi-walled carbon nanotubes (1%) were introduced together with varying concentrations of HA. Within one minute, the sintering process was finished, and when the HA concentration rose, the sintering time decreased even further. The homogenous distribution of HA was verified by back-scattered SEM and XRD. It has been determined that standard polymer processing methods may be replaced by microwave sintering.

Effective heating of the limonite material was the subject of the research published by [Srikant et al., 2013]. Limonite mineral heating effects using MW and traditional muffle furnaces were investigated. According to the findings, MW treatment of limonite has a number of benefits over traditional heating, including time savings, quick heating, increased process efficiency, and environmental compatibility. According to the findings, metallic iron with an iron content of 0.30 percent began to develop after 1 minute of MW heating and a distinct metallic phase with an iron content of 35 percent began to form after 10 minutes.

[Benedetto and Calvi, 2013] conducted a pilot study on the MW heating of asphalt. The manufacture and recycling of materials for road paving were the main subjects of the study. To verify that the findings of the numerical models were accurate, tests were carried out for conventional and MW heating of asphalt on a smaller scale in a lab. In contrast to conventional methods, the microwave heating impact dried the material from within and was more rapid. Microwaves were used to obtain whole dry

samples in 200 percent less time. The study offered encouraging results, and the authors recommended using microwave processing technology for different applications in construction and road engineering, including the manufacturing of asphalt.

2.14 Future Perspective of Microwave Materials Processing

In the realm of materials processing, microwave materials processing has recently attained widespread recognition. Ceramics, semimetals, metallic powders, bulk metals, and polymers have all been processed using microwave technology with success. Because microwave radiation has so many benefits over other types of radiation when processing materials, researchers have been looking at sintering, coatings, claddings, surface treatments, joining, heat treatment, heating optimization, and other related topics [Bykov et al.,2014; Bobicki et al., 2014].

As far as the author is aware, there isn't much literature on the following subjects: casting various metallic powders, MMC claddings on different metallic substrates, hard surface coatings for better tribological properties, nonmetallic coatings on metallic substrates to prevent oxidation and rust, joining various bulk materials and post-treating welded joints for enhanced properties, and sintering of complex shapes using microwave radiation are all examples of techniques that use this technique [Thuault et al., 2014]. These uses and the potential for research in the aforementioned fields assist in expanding the field of microwave material processing and aid industrial industries in achieving their objectives. Control over complicated shapes has not yet been shown, though.

2.15 Research Gap

From the literature review, following are the research gaps:

- The area of process parameter optimization and its implications on joint characterizations has not been studied.
- Even while some writers have taken into account different work-piece materials (substrates), powder sizes at the micron and nanoscale, etc., not all welding factors and their interactions have been thoroughly examined.
- The link between the mechanical characteristics and the aforementioned elements needed to be established, and multi-objective optimization needed to be used to maximise the mechanical properties.
- No progress has been made in detecting surface temperature of weld zone.

2.16 Motivation

- For advanced technical applications and industrial uses, new developments in welding techniques are currently replacing traditional welding techniques.
- The suppression of defects such as porosity, cracking, microstructure dislocations, etc. with microwave heating enables the improvement of characteristics.
- The microwave heating process has a high level of efficiency since it uses less energy and time to process materials and because there is no environmental contamination produced throughout the process.
- All of these properties are built into microwave heating and have allowed for frequent advancements in this area.

2.17 Research Objectives

Researchers are always trying to come up with materials processing techniques that use less energy, take less time, and are less harmful to the environment. Any country's industrial industry may be sustained with the use of such advanced technology. The

advancements in microwave material processing have produced outstanding outcomes in terms of processing that is economical. Microwave radiation is currently a well-established method in the industry for welding materials. When used as a heating source, microwaves can replace current and conventional sources while also overcoming the drawbacks of these methods.

Research gaps are found through the literature review. As a result, the following goals are created:

- To join commercial available stainless steel 304L through microwave heating
- Micro structural Characterization of joints sample through microwave processing (Scanning Microscopy, Energy Dispersive Spectroscopy, X-Ray Diffraction).
- Study the Mechanical Properties of joints (Vickers micro hardness and Tensile Testing).

2.18 Scope of the Work

The major scope of the present work is;

- Researching the ability of microwave heating to join and develop joints.
- Investigate the method for joining stainless steel 304 and metal nickel powders in a microwave oven.
- Collaborative development in a variety of process conditions.
- Microwave joint metallurgical characterization in terms of phase analysis, structural growth, crack evaluation, etc. X-ray diffraction (XRD), field emission scanning electron microscopy (FE-SEM), and energy dispersive spectroscopy are the methods employed for this characterization (EDS).

- Mechanical characterization of joint utilising Vicker's microhardness tester to measure microhardness and tensile tester to measure tensile strength.
- Joint-section surface temperature observations using an infrared gun.
- Using a joint section fracture surface, to study mode of failure.

2.19 Flow Chart of the Present Work

The flow chart in Fig 2.16 depicts the intended plan for the current task. A flow chart provides a condensed version of the full work that outlines the current task's step-by-step technique or procedure.

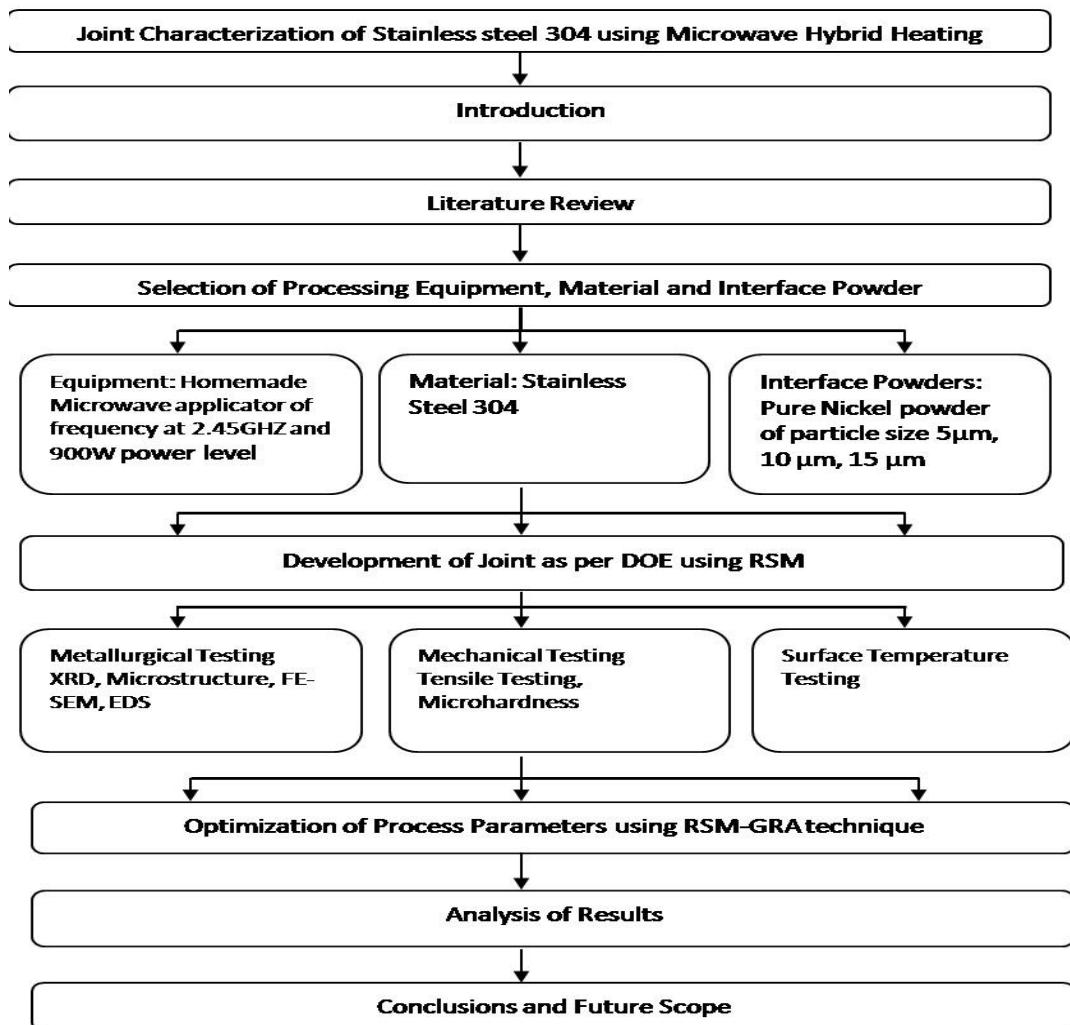


Fig. 2.9: Flow chart of Present Work

2.20 Summary

Stainless steel is a type of sophisticated material that is frequently used in structural, automotive, and aerospace applications. However, treating such materials necessitates high temperatures, which is challenging. Such materials require longer processing times and increased energy usage during conventional sintering. Although microwave sintering is a useful processing method, it is highly challenging to regulate the diffusion rate and remove flaws such as porosities. Due to the established uniformity, welding of materials can also increase their strength. But, melting and casting of such materials via the normal approach is an expensive way to go.

According to a thorough analysis of the pertinent literature on microwave processing of metallic materials that has been presented, microwave processing of metallic materials has been used in the past ten years to heat and sinter metallic particles as well as connect bulk metallic materials. However, it was noted that there is little literature on the improvement of metallic-based materials utilising microwave as a heating source. The research gaps that were found in the literature on microwave processing of metallic materials have therefore been investigated. The present study's goals and parameters have been established. A flow chart has been used to explain the specific research approach used in this paper.

CHAPTER 3: EXPERIMENTAL SETUP

The features of the machinery employed have been illustrated in this chapter.

3.1 Microwave Oven

A IFB microwave oven with frequency 2.45 GHZ and power output at 900W was used for experimentation work which is shown in fig 3.1 with its specification depicted in table 3.1, is an electric oven that uses electromagnetic radiation with a microwave frequency range to heat objects. As a result, the object is heated via a process known as dielectric heating, which causes the polar molecules there to spin and create heat energy. The contemporary microwave oven was invented after World War II by American inventor Percy Spencer using radar technologies created during the conflict. It was initially offered under the name "Radarange" in 1946. Between 1964 and 1966, Sharp Corporation unveiled the first microwave oven featuring a turntable. Microwave ovens are used for heating in several industrial operations, in addition to preparing meals.



Fig.3.1: Microwave oven

Table 3.1 Microwave oven	
Model	IFB 30SC4 30L
Capacity	30 litres
Dimensions	54x44x30cm
Power Source	230/50 V/HZ
Power consumption	1400W
Power at output	900W
Frequency	2.45GHZ

3.2 Tensile Testing

It was employed to assess the material under investigation's tensile qualities. Table 3.2 is a list of this machine's specifications. Figure 3.2 shows the machine configuration. The material specimen should be prepared in accordance with ASTM standards prior to testing. Before the test, the machine should be outfitted with the appropriate grippers depending on the style of the tensile specimen's ends. Because the machine's two grippers/jaws are properly aligned, adequate safeguards should be taken. The tensile test is a destructive test where the test substance is split in two parts.

The recommendation of a material for use in engineering applications is based on its mechanical characteristics, such as tensile strength, percentage elongation, etc. Tensile testing produces these results. The tensile strength of a material is governed by various attributes; some of the prominent attributes are listed below.

- **Molecular structure:** Because intermolecular forces are directly influenced by molecular structure, even minor changes in molecular configuration can affect tensile strength.

- Temperature: As the temperature rises, metal gains tensile strength up to a point where its properties begin to deteriorate.
- Composition: Variable compositions result in different molecular structural arrangements and levels of molecule binding, which affect the material's ultimate tensile strength (UTS).

Only by conducting tests on the material can the tensile strength of the material be determined. The Universal Testing Machine (UTM), which is seen in Fig. 3.2 and technical specification depicted in table 3.2, is used to test a material's tensile strength (UT-02-0100). The specimen for the same was made in accordance with the ASTM-E8 standard, and wire EDM machine was used to cut the sample. The sample's dimensions for tensile testing were prepared to resemble a dog bone. The processed sample tensile tests are conducted at room temperature with a constant cross-head speed of 1 mm/min.



Fig.3.2 : Tensile machine

Table 3.2 Specification of Tensile Testing Machine		
Capacity	KN	100
Clearance between columns	Mm	400

Maximum crosshead travel	mm	1000
Testing speed range	mm/min	0.001-500
Maximum speed at capacity	mm/min	250
Jog speed	mm/min	0.001-500
Return speed	mm/min	0.001-500
Dimensions (H x W x D)	mm	2000 x 1650 x 450
Weight	Kg	140

3.3 Microhardness

Microhardness testing is a method used to assess the material's hardness or resistance to penetration. When measuring tiny areas in a welded sample or when test samples need to be extremely small or thin, microhardness is examined. The microhardness analysis is performed using a Struers Duramin-40, as shown in Fig. 3.3 and its technical specification shown in table 3.3. During the microhardness test, a Vickers diamond indenter is driven into the material's surface using a penetrator and a low weight (300 gram). When a load is applied to a material, it penetrates an indentation and permanently deforms the material's surface into the indenter's shape. The test is carried out in a controlled environment by keeping track of the pressure on a square-shaped diamond indenter for a certain amount of time (20 seconds of dwell time). The Vickers hardness value is determined by measuring the diagonal that results from the indentation on the material's surface and using a formula to compute it.



Fig.3.3: Microhardness machine

Table 3.3 Specification of Microhardness testing machine (Struers Duramin-40)	
Model	Duramin-40 M1
Loads and Applications	
Load Range (Main Loads)	10 gf – 10 kgf
Vickers Capability	Yes
Knoop Capabiblity	Yes
Brinell Capability	Yes
Stages and Turrets	
XY-stage	Manual
XY-stage or anvil size (mm)	90 x 90
XY-stage stroke, max (mm)	25 x 25
Vertical capacity	172
Throat depth (mm)	170
Motorized Z-axis	Yes
Motorized turret	Yes

Turret positions	6
Anti-collision protection	Yes
Machine weight	101 kg
Camera and Optics	
Evaluation camera resolution	18 MP
Auto illumination	Yes
Stage illumination	Yes
Laser or LED guider	Yes
Interfaces and Connectivity	
Operation	Embedded Windows 10 PC with 15 inch touch screen.
Communication Ports	HDMI, VGA, RJ45, WLAN, USB, RS232
Wifi	Yes
Bluetooth	Optional

3.4 Optical microscopy

With the optical microscope shown in fig. 3.4, an Olympus GX41, the microstructure was assessed. Table 3.4 is a list of the microscope's specifications. The optical microscope is a type of microscope that magnifies images of small objects using a collection of lenses and visible light. An optical microscope's image may be captured by common light-sensitive cameras to make a micrograph. Photographic film was originally used to capture images, but modern improvements in complementary metal-oxide semiconductor (CMOS) and charge-coupled device (CCD) cameras allow for the capture of digital images as well. There are now fully digital microscopes

available that analyse samples using CCD cameras and show the resulting images on computer screens without the need for eyepieces [Roberts and Williams, 1999].



Fig.3.4: Optical microscope

The optical microscope utilised in this investigation has a setting that allows the specimen to only be held inverted. The microscope has three objective lenses with magnifications of 100 X, 200 X, and 500 X, as well as a rotating objective turret. The opposing turret was equipped with the objective lenses. To position the lens underneath the specimen, spin the objective turret. For separate coarse and fine settings, focus knobs might be employed. A light source was provided, and a different knob could be used to change the brightness. With the use of an eyepiece, the specimen's enlarged picture could be seen. The enlarged pictures could be seen and saved on a computer that was linked to the microscope.

Table 3.4 Specifications of Optical Microscope		
Optical System		UIS2 Optical System (Infinity-corrected)
Microscope Frame	Observation Method	BF/KPO*
	Reflected/Transmitted	Reflected
	Illuminator	-

	Illumination System	Reflected light	30W Halogen or Fiber Light Guide(Light source:100 W)
		Transmitted light	-
	Focus	Motorized/Manual	Manual Revolving Nosepiece Up/Down Movement (Stage Stationary Type)
		Stroke	9 mm
		Resolution/Fine adjustment sensitivity	Fine Stroke per Rotation 0.2 mm
	Revolving Nosepiece	Motorized type	-
	Manual type	Quadruple for BF	
Stage	Stroke		120(X)x78(Y) mm
Observation Tube	Standard Field (Field number 18)	Inverted Image	Tilting Binocular Observation Tube
	Standard Field (Field number 20)	Inverted Image	Binocular/Trinocular/Tilting Binocular Observation Tube
	Wide Field (Field number 22)	Inverted Image	Binocular/Trinocular/Tilting Binocular Observation Tube
		Erect Image	-
Dimensions			236(W) x 624(D) x 407(H) mm

Weight	10 kg (in Standard Combination)
--------	---------------------------------

3.5 FE-SEM

As seen in Fig. 3.5, field emission scanning electron microscopy (FESEM) is carried out with the aid of an electro-optical column. Table 3.5 lists its technical specifications. It is best to use an electron beam or electron probe that is as tiny as possible to explore the picture; normally, this size is kept at or below 10 nm. The resolution of the picture produced by the FESEM method is directly influenced by the diameter of the electron probe. Raster scanning refers to the method used to cover the whole specimen with the electron probe. Accelerated electrons are sent to the sample during scanning, and when they come into contact with it, they scatter. When electrons interact, the scattering phenomena are found to be both elastic and inelastic.



Fig.3.5: Field emission scanning electron microscope

Table 3.5 Specification of FESEM machine	
Electron optics	High-resolution FESEM column optimized for high brightness/high current
Ion optics	Magnum ion column with Ga liquid metal ion source with a lifetime of 1500 hours
Electron beam resolution	- 1.2 nm @ 30 kV @ high vacuum mode - 1.5 nm @ 30 kV @ ESEM mode - 1.5 nm @ 3 kV @ low vacuum mode
Ion beam resolution	10 nm @ 30 kV @ 1pA
Accelerating voltage	200V to 30 kV for electron beam imaging and 5 to 30kV for ion beam imaging
Detectors	Everhardt-Thornley SED, Low-vacuum SED, Gaseous SED, IR-CCD, EDS detector and Gaseous BSED
Specimen stage	4-axis motorized eucentric goniometer stage X = 50 mm, Y = 50 mm, T = -15 +75°(manual), Z = 50 mm (25 mm motorized), rotation = 360° continuous

The picture that results from the scanning might have varying brightness due to the bombardment of electrons. The varying brightness is caused by secondary electrons and backscattered electrons, which may be distinguished by their kinetic energy, with the latter having more energy. Images produced with the secondary electron simply depict topographical contrast; they do not reveal any information about the underlying structure. On the other hand, since the information is produced by signals originating from half the penetration depth, backscattered electron pictures have depth and provide details about the specimen's topography. On the basis of the specimen's

chemical makeup, they are known to display contrast in the photographs [Egerton, 2005].

3.6 XRD

A robust non-destructive method for characterising crystalline materials is X-ray diffraction. It offers details on crystal phases, preferred orientations for the crystals (texture), and other structural data including the average grain size, crystalline strain, and crystal flaws. The XRD spectrum is produced using the Bruker D8 advanced equipment, as seen in Fig. 3.6 and its technical specification is presented in Table 3.6. All of the generated X-ray diffraction measurements were performed using Cu K radiations at room temperature in the XPert PRO PAN analytical diffractometer. In the current study, the XRD scan rate in the 10 to 70° scan range was maintained at 1° min⁻¹.



Fig.3.6: XRD Machine

Table 3.6 Specification of XRD machine	
X-ray	
Source	2.2 kW Cu anode long fine focus ceramic X-ray tube
Running Condition	40 kV and 40 mA
X-ray Beam Shaping Optics	
Beam [Cu-K α 1]	Collimated, compressed and frequency filtered by a Gobel mirror and V-Groove
Collimated beam dimensions	0.3 mm by 11 mm
Göbel mirror	60 mm multilayer X-ray mirror on a high precision parabolic surface
Goniometer	
Maximum and minimum measurement circle diameter	250 mm & 100 mm
Smallest angular step size	0.0001°
Reproducibility	+/- 0.0001°
Maximum rotational speed	1500 °/min
Angular range (Theta)	-5° to 40°
Angular range (2Theta)	-10° to 60°
Reflectometry Sample Stage	
Samples size	200 mm in diameter and 50 mm thick
Detector	
Maximum count rate	2 x 10 ⁶ s ⁻¹ (although it should not be

	exposed to in excess of $5 \times 10^5 \text{ s}^{-1}$ for periods longer than about 1 second)
Detector electronics count rate	$3 \times 10^7 \text{ s}^{-1}$

A monochromatic beam of X-rays dispersed at certain angles from each set of lattice planes in a sample causes constructive interference, which results in XRD peaks. The atomic locations inside the lattice planes determine the peak intensities. Now the determination the position of the diffraction peaks is done with the help of Bragg's law ($n\lambda=2 dhkl\sin\theta$). $dhkl$ is the distance between the crystal (parallel) planes of atom. θ is the angle between the beam which is incident and the normal to the lattice where reflection has taken place. λ is the wavelength and n is the order of reflection (an integer). Bragg's law helps in identification of the angle at which diffraction peaks are observed due to constructive interference formed by the scattered X-ray from the crystal planes of atoms. As a result, the XRD pattern represents a material's unique fingerprint for periodic atomic groupings. A wide range of crystalline samples may quickly be phase identified using an online search of a standard database for X-ray powder diffraction patterns [Vishwakarma and Uthaman, 2020].

3.7 Surface Temperature Measurement

An infrared temperature gun(thermometer) of Mextech brand with range in degree Celsius (50 to 2200) that doesn't need direct touching contact was used to measure the temperature in the weld joint region, shown in fig 3.7. An infrared thermometer is a sensor that measures temperature by detecting thermal radiation produced by a heated metal at a distance. The surface temperature of the joint region is always lower than the inner temperature of the joint region.



Fig.3.7: Infrared gun

3.8 Summary

In-depth discussions were held on the various machines used in the experiments. The use of tensile machine, microhardness machine, optical microscopy, field emission scanning electron machine and XRD depicted in detail to highlight the mechanical characterization and metallurgical characterisation of microstructure, phase analysis, and elemental composition with their specification. Finally, the joint surface temperature measured using an infrared radiation gun was detailed.

CHAPTER 4: METHODOLOGY

It can be difficult to create innovative, energy-efficient processes for processing a range of materials. Even more difficult, each process development necessitates the validation and optimization of the process parameters and their cause-effect matrix. Well-planned experiments and outcomes are required to demonstrate the process development's scientific validity. For the established process to work at its best and be widely accepted, it must also be possible to explore the process capabilities. The process's underlying theory of science must be established as a sound scientific idea. The selection of basic materials, input parameters and their appropriate sizes are all covered in this chapter of the thesis. The rigorous process parameter selection and optimization work that was done to create a process for joining stainless steel metals using a microwave hybrid heating route has been illustrated, along with the experimental technique and data gathering information.

4.1 Material Selection

One of the most crucial steps and labour-intensive tasks in every research project is the choosing of the materials. It is usually ideal to have materials that demonstrate high strength and desirable qualities while being simple to mould into the necessary forms. Any experiment begins with choosing the components that will be used for the workpiece, the interface, and any other test subjects. Because the quality of joints is determined by the composition of these materials, careful selection of these materials is crucial. Before beginning the microwave joining procedure, there are a total of 7 factors that need to be evaluated. It will be challenging to complete a successful microwave connection without understanding these characteristics. By [Salot et al., 2017], several of these factors were covered. Other variables that are obtained from

the heating mechanism exist in addition to these [Kumar et al, 2019]. The following subsections provide a brief discussion of each of these parameters.

4.1.1 Substrate / Base Material

The most popular kind of stainless steel is 304. The majority of the nickel (between 8% and 10.5%) and chromium (between 18% and 20%) elements make up the steel's main non-magnetic components. The formula was created in 1924 at Firth-Vickers by W. H. Hatfield, and it was sold under the brand name "Staybrite 18/8." It is austenitic stainless steel. It is less thermally and electrically conductive than carbon steel. It is magnetic despite being less magnetic than steel. It is often used because it is simple to mould into different shapes and has more corrosion resistance than regular steel. SAE International specifies it as one of its SAE steel grades.

304 stainless steel has excellent resistance to a wide range of ambient conditions and a number of corrosive agents. 304 stainless steel is utilised in a wide range of domestic and commercial applications, including cutlery, vehicle headers, screws, machinery parts, and equipment for handling and processing food. Architectural exterior embellishments like water and fire features are also made of 304 stainless steel. Additionally, it is a typical material for vaporizer coils [Handbook, 9014].

The chemical compositions of substrate materials as determined by chemical spectroscopy are displayed in Table 4.1 as weight percentages. The 304 strip base metal is seen in Fig 4.1. In Fig. 4.2, the microstructure of the substrate material is depicted, and the broad grain boundaries or elongated grains are clearly visible. As determined by ASTM testing, the mechanical characteristics of the substrate material

are displayed in Table 4.2. Fig 4.3 displays the stress v/s strain curve for the substrate materials.



Fig. 4.1: Base metal SS 304

Table 4. 1Chemical compositions (wt%) of substrate materials by spectroscopy						
Chromium (Cr) %	Nickel (Ni) %	Manganese (Mn) %	Silicon (Si) %	Carbon (C) %	Phosphorous (P) %	Iron (Fe)%
18.29	8.05	1.14	0.25	0.058	0.041	71.13

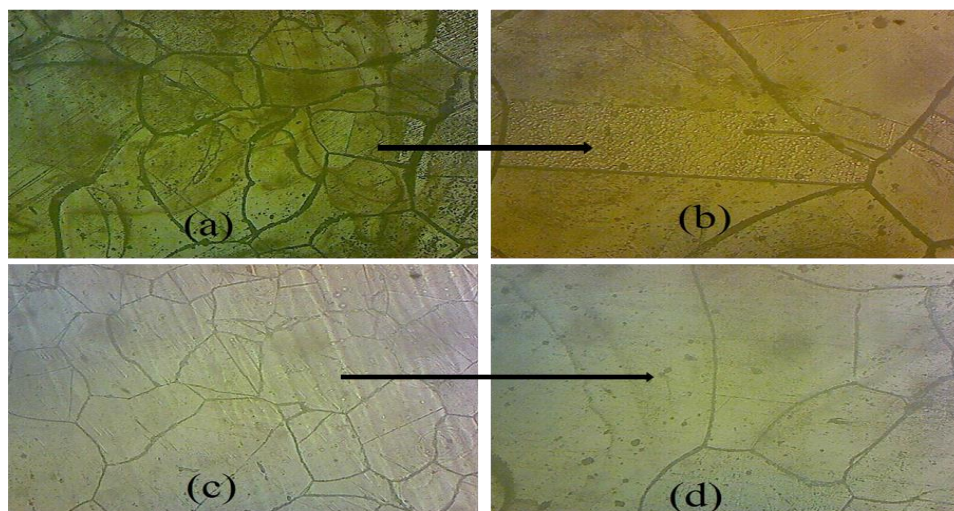


Fig. 4. 2: Microstructural images by optical microscope (a) & (c) Base Metal SS 304, (b) & (d) Magnified view of marked section

Table 4. 2 Mechanical properties of substrate material	
Property	Values
Ultimate Tensile Strength	706 MPa
Vickers Microhardness	208Hv

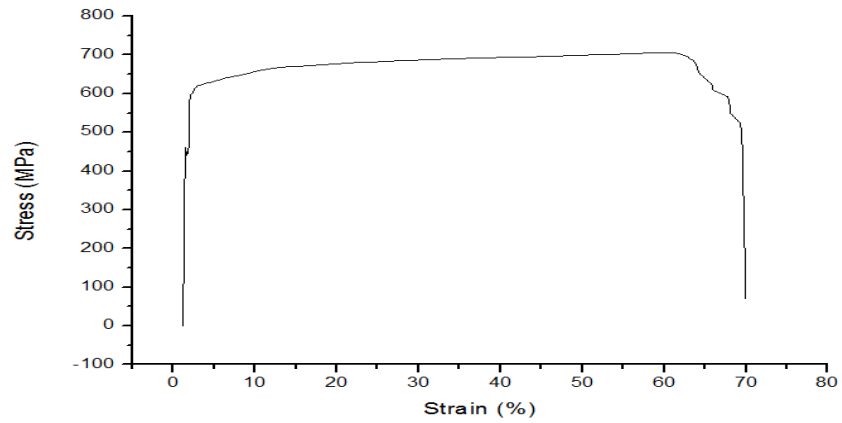


Fig.4.3: Stress strain curve of base metal

The parent materials, which constitute its constituent parts at various intensities as indicated in Fig 4.4, are shown by XRD plots and mostly comprise iron and nickel phases as well as chromium elements. Figure 4.5 displays FESEM images of the base metal that are evenly spaced grains in SS 304.

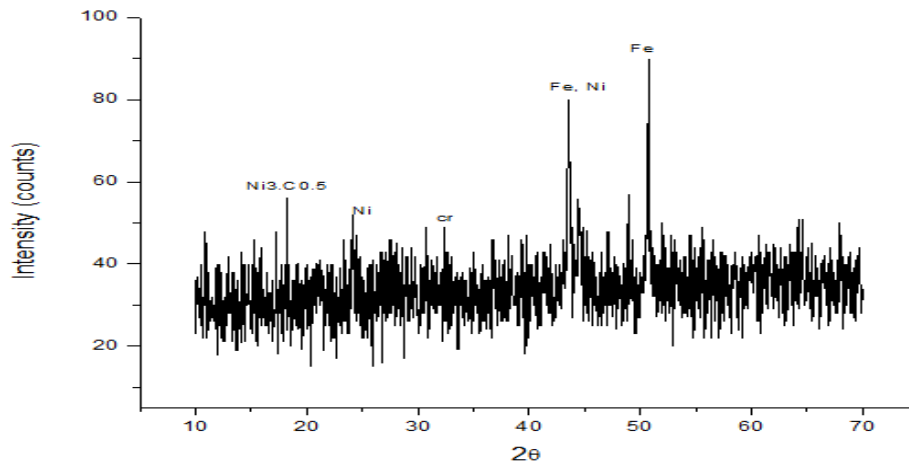


Fig. 4.4: XRD of base metal

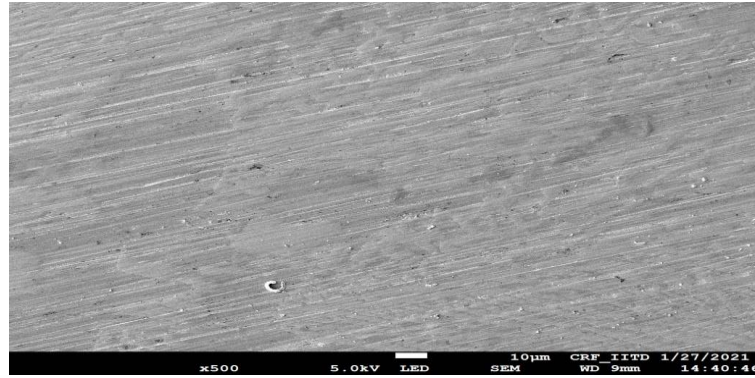


Fig.4.5: FE SEM of base metal

4.1.2 Refractory Brick

Refractory brick can be used as a fixture for a workpiece by cutting a horizontal slot into bricks that is the appropriate size of base metal and placing base material into this slot. Refractory bricks contain alumina in their composition. Refractory bricks made of alumina are better at absorbing heat and microwave radiation. The brick will absorb more heat when it has higher alumina content. However, it has been shown that bricks with higher alumina content fracture as a result of the brick absorbing excessive heat [Bagha et al, 2017]. The 25% pure alumina bricks work well for microwave processing because they remain profitable after several tests.



Fig.4.6: Refractory brick

4.1.3 Interfacing Material

Metallic powder and epoxy resin are combined in a certain proportion to create interface material. Epoxy resin is utilised as a binder and to produce the required form. At a temperature of around 100° C during microwave processing, the epoxy resin evaporates, leaving behind porosity and voids. The molten powder fills in these gaps. It is crucial to specify the precise ratio at which the epoxy resin and interface material are combined in order to achieve improved joint strength and a reduction in void development. Biphenyl A- Blumer 1450-XX acts as epoxy and pure nickel powder as the interface powder [Bagha et al, 2016].

Alloys based on nickel are often used in power generation, aviation, and maritime applications. Commercial applications of nickel and chromium-based coatings are made to a variety of engineering components to prolong service life and minimise the significant damage brought on by wear and corrosion phenomena. Nickel-based super alloys are frequently used in aerospace and turbine applications because of their exceptional qualities of high strength, toughness, and corrosion resistance at extreme temperatures. This powder is widely used for turbine repairs, high-strength structural welding, and turbine blade cladding.

According to [Gupta and Sharma, 2011], cladding EWAC powder produces stainless steel with a greater hardness than austenitic stainless steel (304±48 HV). The 500-gram packaging of the pure nickel powder, which is grey in colour and can be seen in Fig. 4.7a, is offered for sale in the market under the Larson & Toubro name in India (a-b). Fig 4.7b depicts the slurry after mixing the nickel powder with epoxy resin. Table 4.3 depicts the proportion of nickel and epoxy to form slurry. Figure 4.8 depicts the typical XRD spectrum of EWAC powder, which mostly exhibits nickel element

peaks with trace amounts of chromium, silicon, carbon, and iron. Observations of nickel peaks with diffraction angles (2θ) of 44.508° , 51.85° , 76.37° , and 92.95° . Some peaks of chromium (42.10° and 45.78°), silicon (48.93°) and iron (97.8°) were also observed.



Fig.4.7: a) Nickel powder, b) Nickel powder mixed with epoxy resin

Table 4. 3 Ni powder mixed with resin in percentage		
S.No	Ni based powder/ Resin in %	Response
1	70/30	No joint
2	75/25	weak joint
3	80/20	strong joint
4	85/15	strong joint
5	90/10	Strong joint
6	95/5	weak joint
7	100/0	No joint

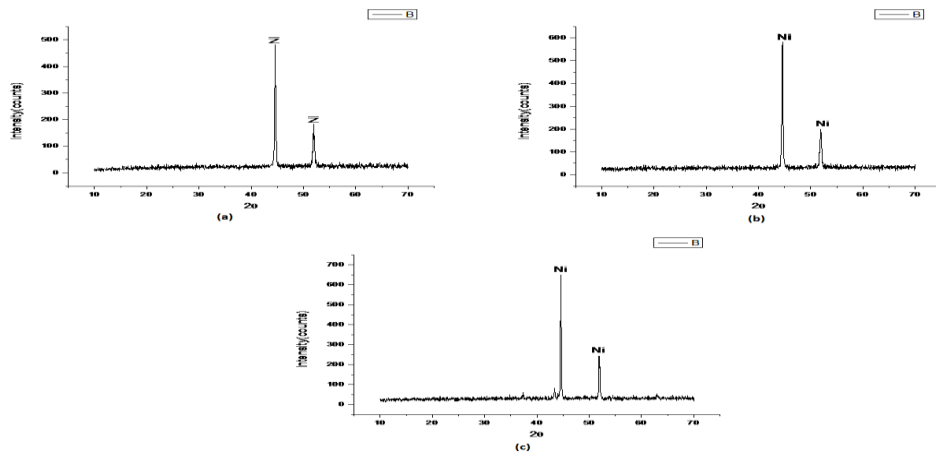


Fig.4.8: XRD of Ni powder (a) 5 μ m, (b) 10 μ m, (c) 15 μ m

4.1.4 Separator Sheet

A separator sheet's job is to prevent the mixing of base material with susceptor powder. By means of convective heat transmission, the separator sheet absorbs the heat that is emitted by the susceptor powder. The specimen is then exposed to the heat that was first absorbed, which finally causes the contact material to begin melting. The rate of heat transmission is significantly influenced by the thickness of the separator sheet; the higher the thickness, the slower the rate of heat transfers will be. Because of the shorter exposure time, improved joint strength, and rapid rate of heat transfer, about 1 mm is the suggested thickness. Graphite and silicon carbide sheets are the most commonly used separator sheets [Bagha et al, 2016] despite the fact that both separator sheets have almost the same effect on the exposure time.

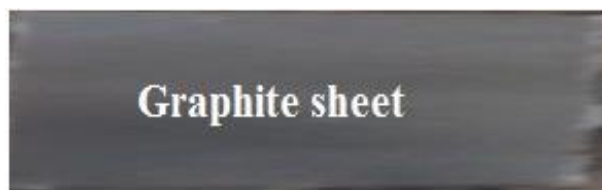


Fig.4.9: Graphite sheet

4.1.5 Susceptor Powder

The idea that metals cannot be treated using microwave radiation because they reflect the waves goes back in time. However, it was eventually discovered that metals only reflect microwave radiation at room temperature; as the temperature rises, the depth of the skin increases, and the metal begins to absorb the microwaves. Stone charcoal powder is used as susceptor powder to raise the specimen's starting temperature. The susceptor absorbs microwave radiation and has a larger dielectric loss, which heats the powder. Susceptor powder can be utilised in two different ways: either to mask the whole base metal or to target the interface material in a vertical hollow. These two techniques are referred to as microwave hybrid heating (MHH). Charcoal [Bagha et al, 2017] and silicon carbide powder are the most commonly utilised susceptor powders. The susceptor material accelerates the pace at which heat is transported with an increase in exposure power [Tamang and Aravindan, 2019].

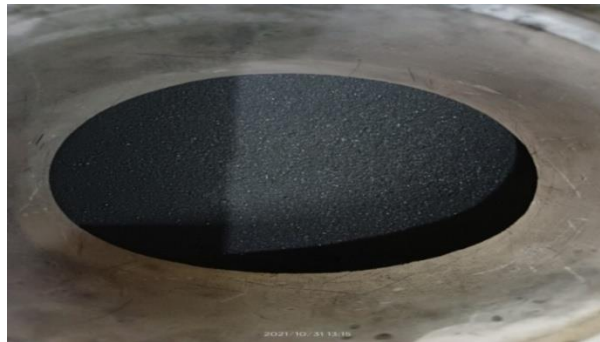


Fig.4.10: Susceptor powder

4.2 Process Parameter

The weld quality can be impacted by a number of microwave welding process factors. Numerous trials were conducted in order to choose the input process parameters (rated power output, welding time, slurry weight, nickel powder size and

temperature). Out of this, welding time, slurry weight and nickel powder size was chosen as process parameter.

Welding Time: Trials were done to select the welding time at which proper fusing of workpiece take place. After number of trial optimum time selected from 11 minute to 13 minute which gives the best result for stainless steel 304. As the welding time increased from the minimum to the maximum value, the mechanical properties (tensile strength and micro hardness) increased. The Ni-based powder needs some time to warm up once the heat is delivered from the charcoal susceptor. The mass and heat transport properties of the material determine how long the procedure will take. Therefore, for higher mechanical strength, a longer microwave welding period is always preferred [Dwivedi and Sharma, 2014]. The creation of high-quality joints, which led to the joints' high micro-tensile strength and micro hardness, was also improved by the diffusion of carbon from the graphite sheet [Pal et al, 2020].

Slurry weight: Nickel powder mixed with epoxy resin to make slurry. Different proportions was tried to make perfect slurry and after number of tried proportions 85:15 (85% nickel powder and 15% epoxy) and 90:10 (90% nickel powder and 10% epoxy) gives the best result in terms of mixing.

Powder size: Three different powder particle sizes (5 μ m, 10 μ m, 15 μ m) were selected as a process parameter. The base metal material and the filler powder particles were mixed uniformly to guarantee that a strong, void-free bead formed around the connecting area. Because smaller filler powder of size less than 100 μ m capable of fuse with substrate material and produces a strong joint, which have higher tensile strength and microhardness than larger filler powder joints. It was discovered that the

smallest powder size produced the highest micro-tensile strength and micro-hardness values [Pal et al, 2020].

4.2.1 Limits of the Process Parameter and Design Matrix

The top and lower limits of the process parameters were determined by doing a considerable number of preliminary trial runs while changing one of the parameters while keeping the others constant. During the testing periods, common flaws such as inappropriate penetration, fissures, a lack of fusion, and undercuts were seen. Each factor's practicable upper and lower bounds were set such that the processed composite should be devoid of any flaws.

To assess the model's importance for the experiment design in this study, a central composite face centred design (CCFCD) is employed (DOE). Using Design Expert (DE) software, CCD under RSM is carried out and helps to offer the best results with high precision from a small number of trials. An alpha value of 1 is preferred since it assures that the axial point will be located within the factorial portion region. It offers three unique levels for the variables that must be included in the experimental design matrix and is known as face-centered design (FCD). From equation 4.1, the total number of experiments created by CCD is determined.

$$N = k^2 + 2k + n \quad (4.1)$$

"N" indicates for the overall number of experiments, "k" speaks for the number of variables examined, and "n" stands for the number of repetitions. Since there are three elements (process parameters) in the butt microwave welding experiment, the minimum number of tests required by CCFCD is 20, including 5 repetitions. Each factor's upper and lower bounds were denoted by the codes +1 and -1, respectively.

In this study, enough sample trials were run to identify the parameter ranges that lead to successful, error-free welding. The specified process parameters and their levels are provided in Table 4.4.

Table 4. 4 Process parameter with levels				
S.No.	Input Parameters	Level 1	Level 2	Level 3
1	Welding time (Microwave) (minute)	11	12	13
2	Slurry weight (gram)	1	2	3
3	Powder size (μm)	5	10	15

4.2.2 Optimization of Process Parameters

To discover the ideal settings and validate the findings using simulation software, design of experiments (DOE), computational approaches, and optimization techniques are now extensively employed. The DOE is a method for examining the connections between variables that impact a process and figuring out how that process responds.

4.2.3 Response Surface Methodology

The main purpose of the response surface methodology (RSM) is to maximise the response by modelling and analysing how multiple independent factors affect a dependent variable. The importance of the model for the DOE is determined using the central composite design (CCD). RSM's CCD is completed using Design Expert (DOE). The goal of the response surface design study is to maximise the response, which is affected by independent factors such as x_1, x_2, \dots, x_n .

Three independent factors, such as welding time, slurry weight, and powder particle size, are selected for microwave butt joints. As a result, equation 4.2 gives the expression for the response function that represents the microwave butt joints.

$$Y = \varphi (A, B, C) \quad (4.2)$$

A, B, and C are the input variables, which are the welding time, slurry weight, and powder particle size, respectively, while Y indicates the responses and φ is the response function.

Equation 4.3, generic polynomial equation of second order is used to establish the link between responses and independent variables.

$$Y = b_0 + b_1x_1 + b_2x_2 + b_3x_3 + b_{12}x_1x_2 + b_{23}x_2x_3 + b_{31}x_3x_1 + b_{11}x_1^2 + b_{22}x_2^2 + b_{33}x_3^2 \quad (4.3)$$

b_0 is an intercept, while b_1 , b_2 , and b_3 are the coefficient values for linear effects, where Y stands for the responses. The coefficient values for interaction effects are b_{12} , b_{23} , and b_{31} . The coefficient values for quadratic effects are b_{11} , b_{22} , and b_{33} , and the coded levels for independent variables such as welding time (A), slurry weight (B), and powder size (C) are x_1 , x_2 , and x_3 .

4.3 Experimental Setup

Processing metal-based materials using microwave radiation is a difficult undertaking that calls for understanding of the materials' characteristics, heat transfer processes, and interactions with microwaves. Different materials react to microwave radiation in different ways. It is usually necessary to do some feasibility tests and then to optimise the process parameters before the needed metallic-based powder is joined and welded.

The literature on process parameter optimization using microwaves at 2.45 GHz is quite scarce, and it is exceedingly difficult to tune the parameters by repeated testing. The interactions between the microwaves and the targeted materials cause the warmth brought on by microwave radiation.

Metallic materials cannot be treated directly because, at 2.45 GHz and at normal temperature, metals will reflect microwaves back. These results in radiation reflecting off the surfaces, which becomes a serious problem when treating materials made of metallic elements. However, by adjusting temperature-dependent factors like resistivity (ρ) and magnetic permeability (μ), the skin depths (δ) associated with such materials may be changed and enhanced for a certain material at a specific frequency.

The skin depth of matrix material, such as EWAC, which contains 97 percent nickel, is $0.12\mu\text{ m}$, which is 330 times smaller than the average particle size of nickel particles, which is $40\mu\text{ m}$, according to [Gupta et al. (2011)]. Microwaves cannot be used to process powder directly because of the reduced skin depth of nickel particles, and if microwaves are used, the particles will reflect the radiation back to the source. Microwave hybrid heating is used to solve this issue. Figure 4.11 is a schematic illustration of microwave hybrid heating.

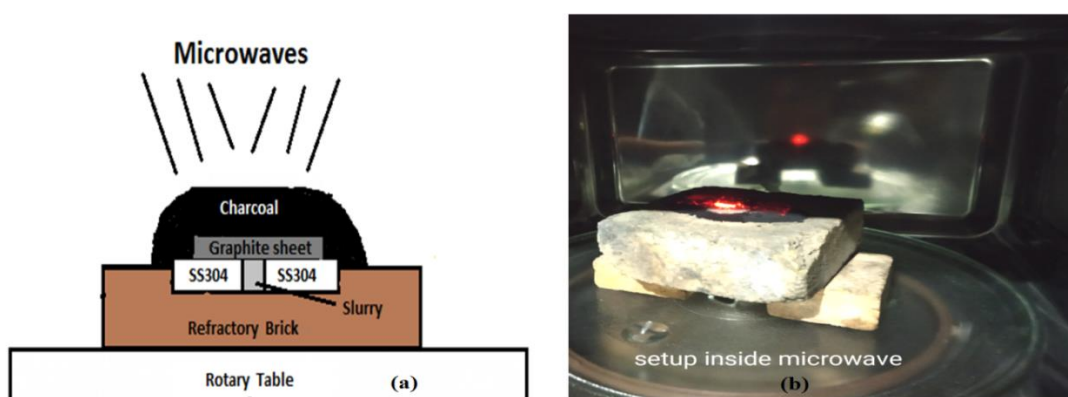


Fig.4.11: Setup for microwave welding

The characteristics of the chosen powders, the size of the powder particles, and processing variables like microwave power and exposure duration are the key determinants in the development of metal welding using microwave radiation. Fig. 4.12 displays the variables influencing the microwave welding process.

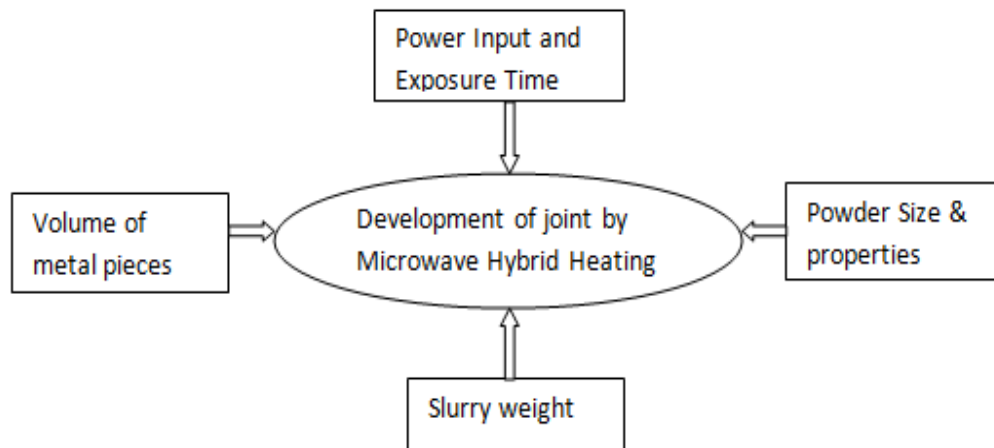


Fig.4.12: Parameters affecting the microwave welding

Some of the parameters, such as welding time, slurry weight, and powder particle size, are predefined and cannot be changed. The current work used a domestic microwave applicator with set power levels and frequency to conduct trial and final studies. Table 4.5 displays the specifics of the processing unit and its characteristics. The ideal processing parameter ranges, which are covered in the following sections, were determined by numerous initial tests.

Table 4. 5 Details of Unit and Processing Parameter	
Parameter	Specification
Microwave oven	IFB Multimode Microwave at 2.45GHz frequency (fixed)
Power Rating	900 W (fixed)

Interfacing Material	Nickel Powder with different particle size mixed with epoxy resin
Base Metal	Stainless steel 304
Dimension of Base metal	30x20x3 (all unit are in mm)
Susceptor	Fine stone charcoal powder
Separator	Graphite sheet of 1mm

4.3.1 Trial Runs

As for fixed specifications, a microwave IFB multimode oven with a frequency of 2.45GHz and a power output of 900W was chosen. The three process variables of welding time, powder size, and slurry weight were chosen as the process parameter. Trials were carried out to determine the ideal time at which metal edges fused to produce a weld after the welding time was chosen as the initial parameter. In order to create the slurry, we combined epoxy resin with nickel powder in three different diameters as the second parameter. In various ratios, various combinations of nickel powder and epoxy were explored. The nickel powder to resin ratios of 85:15 and 90:10 produced the best results. The slurry weight in gram was the third parameter. Through a series of tests, three slurry weight values were found to produce the best results.

Trial runs were first carried out to establish the input variable ranges. First, the welding time was adjusted in 30 second increments from 6 to 13 minutes. There was very fragile joining throughout the procedure, with a time variance of up to 9 minutes. A little joining occurs between 9 and 10 minutes. A sound weld connection is produced after 11 to 13 minutes of welding. Due to the specimen becoming

overheated, a deformed weld region was discovered after 13 minutes of process time. The same method is used to choose the other two input variables.

4.3.2 Final Experiment

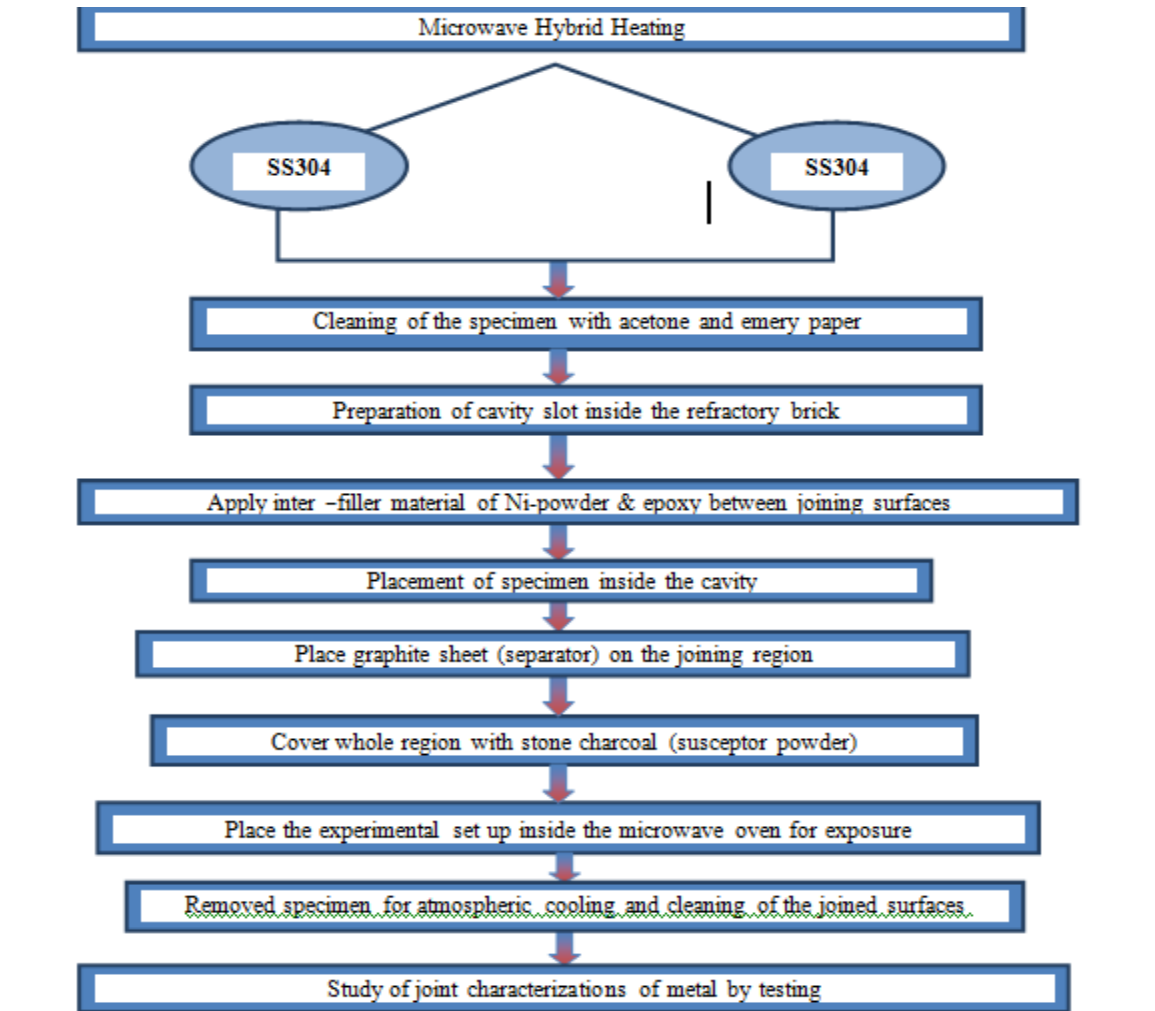


Fig. 4.13: Flow chart of microwave welding

In Fig. 4.13, a complete flow chart illustrating the step-by-step process of metal joining by microwave hybrid heating is shown. On the upper face of the insulating ceramic brick, a cavity slot is first created that is the same size and dimensions as the metal components. Various grades of emery paper were used to clean the facing sides of the metal parts. Surfaces were then cleaned ultrasonically for improved outcomes.

To prevent contamination, facing surfaces can be dipped into an acetone solution after cleaning. Then, cleaned specimens may be inserted into the brick's slot, and prepared, weighed slurry can be administered. Since metal at ambient temperature reflects microwaves, insulating brick avoids direct microwave contact with specimens.







A 1 mm graphite sheet was put over the specimen to avoid any mixing of the slurry with charcoal powder. The graphite sheet and specimen were covered all around with a fine stone charcoal powder. The entire mechanism is put inside the oven. The charcoal powder absorbed the microwave as soon as it was turned on for the set amount of time, and burning began within 40 seconds. Through the graphite sheet, the same heat was transmitted to the slurry material. At 100°C epoxy resin inside slurry evaporates, leaving nickel powder behind. Then heat transmits to facing surfaces and surface melting begin when the nickel powder melt as a result of the diffusion process that occurs between the nickel powder and metal surfaces, securing the joint. The entire arrangement was removed from the oven after the process time was completed, and the metal components were then subjected to ambient cooling [described by Fig. 3.14 (a-h)]. For improved outcomes, a joint area might be filed before testing. According to a design expert, a similar procedure was used for all values of the input variables.




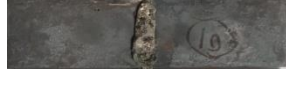

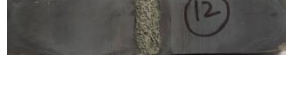
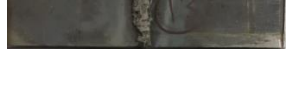
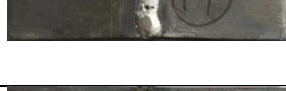
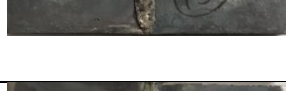
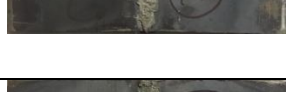
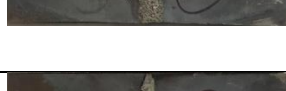

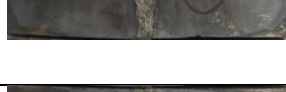



Fig.4.14: Step wise procedure of microwave welding

S.No.	Std	Process Parameters		
		Welding Time (minute)	Slurry weight (grams)	Powder size (μm)
1	20	0	0	0
2	11	0	-1	0
3	4	1	1	-1
4	10	1	0	0
5	13	0	0	-1
6	5	-1	-1	1
7	12	0	1	0
8	14	0	0	1
9	19	0	0	0
10	7	-1	1	1

11	16	0	0	0
12	18	0	0	0
13	1	-1	-1	-1
14	17	0	0	0
15	8	1	1	1
16	15	0	0	0
17	9	-1	0	0
18	2	1	-1	-1
19	3	-1	1	-1
20	6	1	-1	1

Table 4.7 Experimental input values as per CCFCD with welded pieces				
S.No	Welding Time (minute)	Slurry weight (grams)	Powder size (μm)	Welded piece
1	11	3	15	
2	12	2	10	
3	12	2	10	
4	13	3	5	
5	12	2	10	
6	11	1	5	

7	13	3	15	
8	13	1	5	
9	12	2	15	
10	12	2	10	
11	12	2	10	
12	12	2	5	
13	12	1	10	
14	13	1	15	
15	11	2	10	
16	13	2	10	
17	12	2	10	
18	11	1	15	
19	12	3	10	
20	11	3	5	

SS304 specimens were used in all of the tests to create joints using microwave radiation and a hybrid heating technique. The frequency of the microwave was fixed at 2.45GHz, and the power output was set at 900W. Table 4.6 displays the results of the determination of three process parameters at three different levels. The final joints were constructed in accordance with CCD, utilising the design matrix shown in Table 4.6 to centre the RSM face, and Table 4.7 displays the test results in accordance with DOE. According to the design expert, the same process was used for every input variable value. The developed joints are shown in Figure 4.15 in accordance with Table 4.7.



Fig. 4.15: Welded pieces of SS304 as per DOE

4.4 Sample Preparation for Testing

4.4.1 Macrostructure Characterization

For microstructural examination, samples measuring (30x20x3) mm were cut from the centre of the weld zone in a direction normal to the welding done using a microwave. The 15 x 15 mm square portion was removed from the weld region in order to prepare the specimens. The samples were ground in order to round the corners and level the uneven surfaces. The Bakelite mould was filled with the cut

samples. The specimens that had been placed in the mould were successively processed with sandpaper of progressively finer grit sizes on a spherical rotating machine. Then, using emery paper of grades (100, 320, 400, 600, 800, 1000, 1200, 1500, 1800, and 2000). The cross-sectional surface of the weld region was polished. Aluminium oxide and velvet paper were used to polish the surfaces in both rough and fine ways. Before the optical microscope's final examination, etching with the Keller agent was done. The weld area, which encompasses the weld region and the heat affected zone, is revealed by the macrostructure, as illustrated in Fig 4.16.

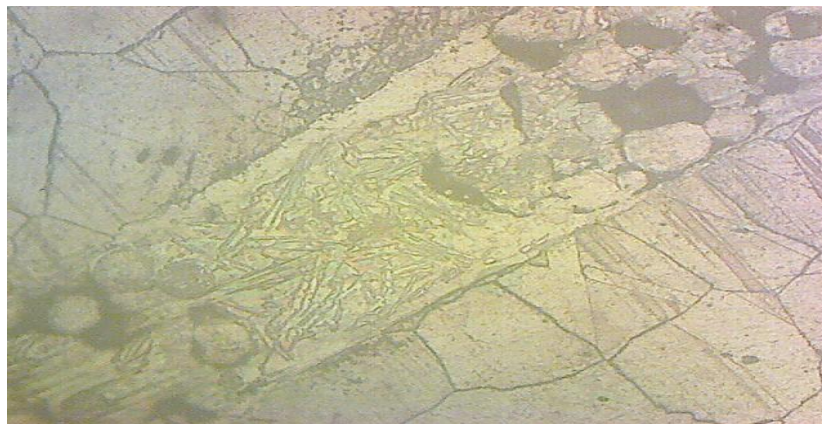


Fig.4.16: Macrostructure of welding zone

4.4.2 Microstructure Characterization

The characterization of the microstructure provides details on the grain size, grain boundaries, grain structure, etc. The primary tool for analysing the interior grain structure of the metal is an optical microscope. By removing the 15 x 15 mm square portion from the weld bead, samples were made. Using a hot mounting press set at 135°C for 20 minutes, the cross-sectional phase was mounted in bakelite powder (4.17a). These samples were then given 15-20 minutes to cool in the mounting press. Now, dry polishing of the weld bead's cross-sectional surface is done using various

grades of emery paper. Then, using alumina powder, velvet emery paper was utilised for wet polishing (fig 4.17b). The samples were etched, dried with a hot air blower, and examined under an optical microscope (fig 4.17c).



Fig.4.17: a) mounting press, b) polishing machine, c) optical microscope

4.4.3 Microhardness

Microhardness is a mechanical characteristic that indicates a material's hardness at the micron level. It resists being indented. The microhardness of the welded sample was assessed using the Vickers microhardness test. Previously a formula based on the size of the indentation is used to calculate the hardness after the indenter has been allowed to remain on the workpiece for a brief period of time, now software is used to evaluate the hardness value. Before the microhardness test, samples from the middle of the transverse section were cut, put on a mould, ground, and polished. In this work, specimen thickness in the middle of the transverse section was used to assess hardness values. At a 300 gram force and a 20-second indentation period, microhardness values were determined. The following procedures were used to prepare the surface for microhardness testing:

The hardness specimen was first dry polished using emery sheets of varying grades (180, 320, 400, 600, 800, 1000, 1200, 1500 and 2000). Next, wet polishing was done using velvet cloth and alumina powder of varying grades (I, II, and III).

4.4.4 Tensile Testing

Tensile testing is used to assess the material's strength prior to a basic lengthening procedure. The main functions of the testing apparatus are to generate the load v/s displacement and stress-strain curves. The mechanical characteristics of the material being examined are ascertained by the tensile test. Engineering applications might choose materials based on the results of tensile testing. To guarantee quality, tensile properties are frequently included in material specifications. As shown in Fig. 4.18, specimens were cut using a wire-EDM (Electrical Discharge Machine) in accordance with ASTM E8 (American society for testing and materials). In this project, a single sheet measuring 30 mm by 20 mm must be butt welded to another sheet of the same size and thickness. The final produced sample is 30 mm x 30 mm in dimension with a 20 mm cross-sectional side after welding. As a result, a sub-size tensile specimen (50 mm in length) is chosen over a full-size tensile specimen (100 mm)

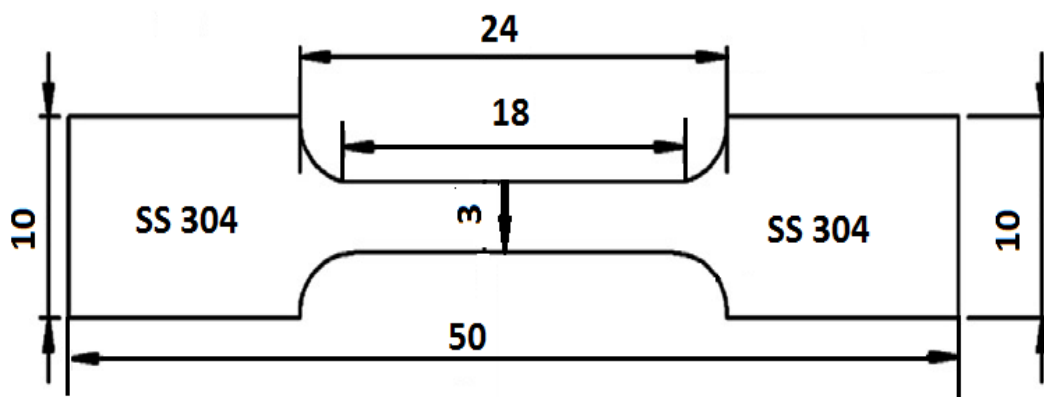


Fig.4.18: Drawing for tensile testing as per ASTM

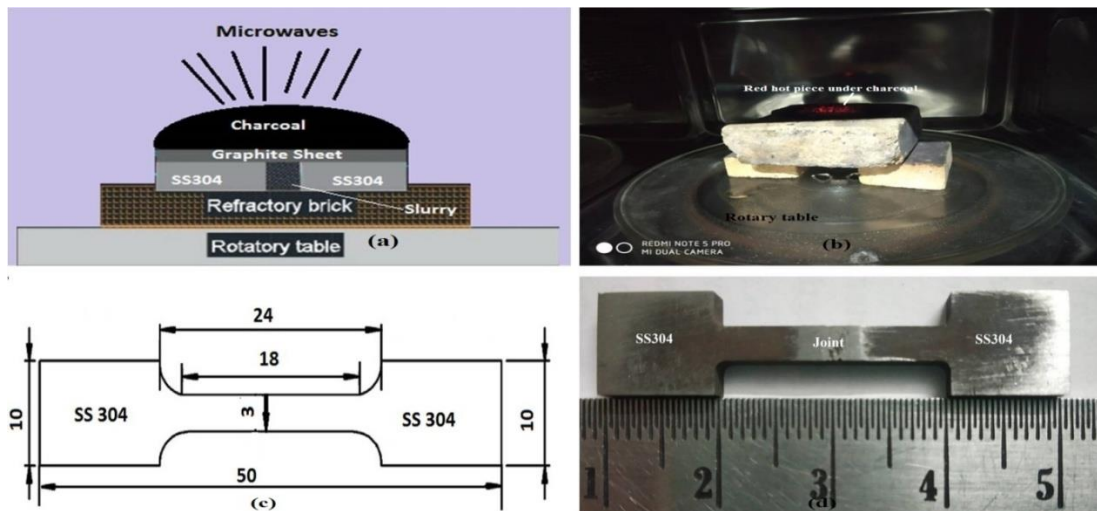


Fig. 4.19: showing, a) setup for microwave hybrid heating, b) setup inside microwave, c) welded piece cutting as per ASTM, d) joint piece for tensile testing

Figure 4.19 (a) depicts the setup for microwave hybrid heating. The configuration of the components within the microwave is shown in Figure 4.19 (b). The substrates were prepared in accordance with ASTM requirements and cut using wire EDM, as illustrated in Fig 4.19 (c). The item is shown in Figure 4.19 (d) after it has been welded and tested for tensile strength.

4.5 Summary

The materials for choosing a substrate metal were discussed in this chapter. Detailed descriptions of all necessary input and output parameters are provided. The substrate's mechanical characteristics were given. Levels and the choice of process parameters were explained. A detailed explanation of the RSM and for process parameter optimization is provided. The specimens that were created for the whole test complied with ASTM criteria. With the aid of an experimental setup and a step-by-step process flow chart, the idea of microwave hybrid heating was thoroughly presented. In-depth

descriptions of welded samples, samples for tensile testing, and samples following tensile testing were provided.

Step-by-step instructions were provided for sample preparation for several tests, including microhardness and tensile tests, macrostructure and microstructural characterization, and more. Mechanical characteristics techniques for tensile and micro-hardness were also covered. The use of Optical Microscopy (OM), Field Emission Scanning Electron Microscope (FESEM), X-ray Diffraction (XRD) and energy dispersive spectroscopy (EDS) to highlight the metallurgical characterisation of microstructure, phase analysis, and elemental composition.

CHAPTER 5: RESULTS & DISCUSSIONS

The detailed microstructural and mechanical characterization results are presented with illustrations. The effect of various reinforcements on the microstructure, XRD phases, EDS, microhardness, tensile strength and surface temperature of various microwave processed joint has been reported with proper discussion. Results are compared for the maximum, medium and minimum values of outcomes to evaluate the performance of different joints.

5.1 Introduction

In recent years, microwave joining has become one of the most advanced manufacturing processes for combining sophisticated materials that are comparable and distinct. Researchers discuss the heating of various metal oxide powders using microwave radiation for the first time [Walkiewicz et al, 1988]. Prior too recently, the use of microwave heating and sintering was restricted to the processing of a few oxide and non-oxide ceramics. However, this method is now being used to sinter metals and metallic powders for industrial uses. The advantages of using microwave material processing techniques include improved mechanical qualities, shorter processing times, economic efficiency, and clean & environmental friendly processing [Roy et al., 1999]. In addition, the researchers utilise microwave radiation in material processing due to the characteristic of volumetric heating. Sintering, cladding, brazing, joining, drilling, and casting are some of the uses for microwave processing [Clark and Sutton, 1996].

Later, the researchers created a hybrid heating method in which the metallic powder at the joint interface is selectively heated and fused with the help of a susceptor (material

that absorbs microwaves) to unite the specimens. The method is also frequently referred to as "hybrid heating." The factors that govern the most effective microwave processing of metallic materials must be understood and acknowledged. The joining process is complicated because microwaves are electromagnetic radiation (EM radiation), and it is significantly influenced by the dielectric and magnetic characteristics of the materials being treated. Researchers have already determined the numerous factors that influence microwave joining. According to [Kumar et al., 2019], the parameters include microwave input power, (ii) interface powder size, (iii) material dielectric and magnetic properties, (iv) separator size, (v) insulating medium, (vi) susceptor materials, (vii) spacing between two workpieces, and (viii) exposure period.

5.2 Optimization of Process Parameters

The most common methods used today to find the ideal parameters and verify the results using simulation tools in order to establish a mathematical connection include DOE, computational approaches, and optimization techniques. The significance of the model for DOE is determined using CCD (centre composite design). CCD under RSM is performed using Design Expert (DE) software. The majority of mathematical models and empirical relations on bead-on-plate have been produced for Metal Inert Gas (MIG) [Adak et al., 2015 and Lee and Rhee, 2000], Submerged Arc Welding (SMAW) [Gunaraj and Murugan, 2002; Chandel et al., 1997], and Tungsten Inert Gas (TIG) [Jou, 2003].

[Sharma et al., 2020] The effects of process variables are examined during the microwave hybrid heating and joining of Inconel-625. A microwave applicator is used to conduct experiments under various experimental circumstances. An analysis of the

effects of process parameter change on joint interface melting has been done. In this study, the impact of four input parameters—the size of the vertical charcoal feeder's drilled hole, the graphite sheet's thickness, the thickness of the insulation brick, and the surface contact between the insulation brick and refractory—on the melting region has been examined. Results of this work demonstrate the proper melting of the joint zone, the absence of flaws such as the development of craters, and the lack of any charcoal powder spreading over the specimen.

[Pal et al., 2020] Hybrid microwave heating technology to create SS304/SS316 joints that are optimised. By combining three distinct sizes of nickel powder, designated as Y1, Y2, and Y3, in a 75:25 ratio with very viscous epoxy resin (blumer 1450-XX), filler material was created (by weight). SEM and EDS were used for physical characterization, while micro-hardness and micro-tensile findings were used for mechanical characterization, respectively. As a consequence of homogeneous volumetric heating, the filler nickel powder's grain structure boundaries were totally melted and diffused with the SS304 specimen, as seen by the SEM results. The joint region included a number of different elements, including silicon, manganese, nickel, oxygen, and sulphur, according to the EDS data. Variation showed that the filler material size was the most important factor, followed by the specimen material and process time had the smallest impact. For 70 nm (Y1), SS304 (X1), and 360 seconds, the joint's microtensile strength (483 MPa) and microhardness (496 HV) were at their highest values (Z1). With a reduction in the size of the nickel powder (Y), both micro-hardness (P) and microtensile strength (Q) rose dramatically.

5.3 Experimental Results for Tensile Strength

According to ASTM (E8) standards, the bulk welding produced by microwave radiation was further machined to produce dumbbell-shaped standard tensile strength specimens [Srinath et al., 2011]. Figure 5.1 depicts test specimens for tensile strength. Uniaxial stress was applied throughout the tensile testing, and a strain rate of 8.3×10^{-3} mm/s was used. Fragmented specimens from the tensile tests are shown in fig. 5.2.



Fig.5.1: Specimen for tensile testing



Fig.5.2: Specimen after tensile testing

The CCFCD is used in experiments carried out in accordance with DOE in order to determine the ideal input process parameters. 20 experiments in all were performed on the welding procedure. Tensile strength, micro hardness, and surface temperature

are the process output characteristics, whereas welding time, slurry weight, and powder size are the input process factors. The experiment design matrix and associated tensile strength values are shown in Table 5.1.

Table 5. 1 Experimental Results for Tensile Strength					
Std	Run	Welding Time (minute)	Slurry weight (grams)	Powder size (μm)	Tensile Strength (MPa)
1	6	11	1	5	403
2	8	13	1	5	498
3	20	11	3	5	409
4	4	13	3	5	501
5	18	11	1	15	368
6	14	13	1	15	474
7	1	11	3	15	381
8	7	13	3	15	480
9	15	11	2	10	384
10	16	13	2	10	483
11	13	12	1	10	425
12	19	12	3	10	431
13	12	12	2	5	441
14	9	12	2	15	414
15	10	12	2	10	424
16	2	12	2	10	424
17	17	12	2	10	420
18	11	12	2	10	424

19	3	12	2	10	425
20	5	12	2	10	424

5.3.1 Mathematical Model of Tensile strength

Mathematical model for tensile strength was developed with the help of design expert software as shown in equation 5.1.

$$\text{Tensile strength} = + 423.90 + 49.10*A + 3.40*B - 13.50*C - 1.25*A*B + 2.25*A*C + 1.25*B * C + 9.00*A^2 + 3.50*B^2 + 3.00*C^2 \quad (5.1)$$

Mathematical model for tensile strength in terms of parameters as shown in equation 5.2.

$$\text{Tensile strength} = +1205.90000 - 168.90000*\text{Welding time} + 1.90000*\text{Slurry weight} - 11.00000*\text{Powder size} - 1.25000*\text{Welding time}*\text{Slurry weight} + 0.45000*\text{Welding time}*\text{Powder size} + 0.25000*\text{Slurry weight}*\text{Powder size} + 9.00000*\text{Welding time}^2 + 3.50000*\text{Slurry weigh} + 0.12000*\text{Powder size}^2 \quad (5.2)$$

5.3.2 Checking the Adequacy of the Model for Tensile Strength

Normal Probability: The plot shows if the residuals are distributed normally, in which case a straight line will connect the spots. Even with typical data, expect some dispersion. Look exclusively for distinct patterns, such as an "S-shaped" curve, which suggests that a response modification could lead to a better analysis.

Residuals vs. Predicted: This is a plot of the residuals against the projected response values, which are predicted to increase.

Run vs. Residuals: This is a visualisation of the experimental run order against the residuals. It searches for hidden factors that could have affected the experiment's response. A random dispersion should be seen on the plot. Trends suggest the presence of a time-related variable in the background. Blocking and randomization prevent trends from destroying the analysis.

Actual vs Predicted: A graph comparing the actual and predicted response levels. It aids in the discovery of a value or set of values that the model is unable to anticipate.

Tensile strength response predictions and actual responses are shown in Fig. 5.3, and they almost exactly match, proving the model's significance. The model's acceptability may be determined using the normal plot of the residual analysis. It displays the values' shifted from the typical straight line. Values should be close to the straight line to improve the model. A graph between the anticipated and residual values was also created to examine the model's suitability. From the graph, it can be deduced that the error distribution is normal and that all values are in order and sit roughly around the centre line. A graph between the residual and the input parameter can be used to examine the fluctuation of a single input parameter. From the graph, it can be concluded that variations are within the range.

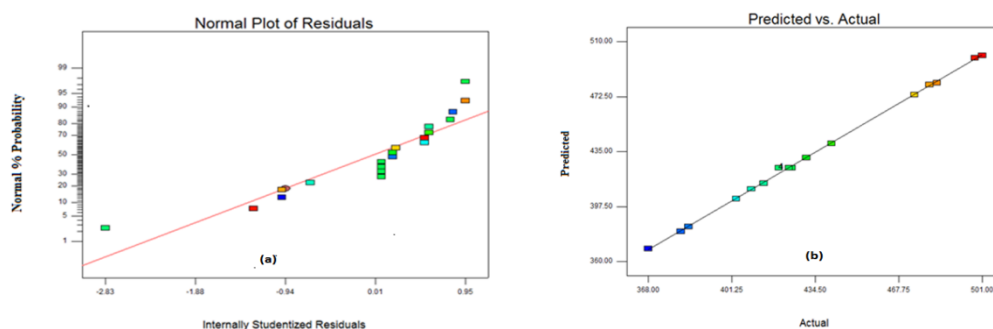


Fig. 5.3: showing tensile value for, a) Normal plot of residuals, b) predicted v/s actual

The effectiveness of the model was evaluated using the ANOVA method. The analysis of variance (ANOVA) results for tensile strength are shown in Table 5.2. The results include the sum of squares (SS), degree of freedom (DOF), and mean square (MS), which is calculated as the product of the SS and DOF, F-value, P-value, and percent contribution. The F-value is the proportion of variance within a factor to variation between factors. The probability, or P-value, should be less than 0.05. Contribution is the proportion of weight that the independent variables have in determining the outcomes. This shows how sensitive that aspect is. The results of the analysis of variance show the importance of the input factors and their interactions at 95% of the certified level. The quadratic model was indicated in the Design Summary, and the ANOVA accepted the model with significant results.

Table 5. 2 ANOVA Table for full quadratic for Tensile Strength							
Source	Sum of Squares	Df	Mean Square	F Value	P Value	Contribution (%)	
Model	27036.95	9	3004.11	1390.79	< 0.0001		significant
A- Welding time	24108.10	1	24108.10	11161.16	< 0.0001	49.10	
B-Slurry weight	115.60	1	115.60	53.52	< 0.0001	3.40	
C- Powder size	1822.50	1	1822.50	843.75	< 0.0001	-13.50	
AB	12.50	1	12.50	5.79	0.0370	1.25	
AC	40.50	1	40.50	18.75	0.0015	2.25	
BC	12.50	1	12.50	5.79	0.0370	1.25	
A ²	222.75	1	222.75	103.12	<0.0001	9.00	

B ²	33.69	1	33.69	15.60	0.0027	3.50	
C ²	24.75	1	24.75	11.46	0.0069	3.00	
Residual	21.60	1	2.16				
Lack of Fit	6.10	5	1.22	0.39	0.8354		Not significant
Pure Error	15.50	5	3.10				
Cor Total	27058.55	19			R*R	0.9992	
SD		1.47			Adjusted R*R	0.9985	
MEAN		431.65			Predicted R*R	0.9968	
C.V%		0.34			Adequate Precision	127.017	

The P-value denotes the probability factor, which should be less than 0.05 [15]. The model's significant F-value is 1390.79. Prob > F specifies model terms that may have values lower than 0.0500. The current analysis shows that every model term (A, B, C, AB, AC, BC, A², B², and C²) is relevant and that every model term is within the range (less than 0.1000). The lack of fit for F-data is 0.39. The ANOVA tables demonstrate that lack of fit is not significant because its P-value is more than 0.1. Welding duration has a greater influence on the value of tensile strength (49.10 percent) than powder size (13.50 percent) or slurry weight (3.40 percent) due to higher F-values and lower P-values (0.0001).

The response's coefficient of determination (R*R), which is used to assess how well the model fits the data, was 0.9992. The aforementioned figure demonstrates that

there is 99.92% likelihood that experimental data will match model predictions. Due to the model's accuracy, this model produces R^2 values that are less than 1 and that always fall between 0 and 1. The adjusted determination coefficient value should be high for the model to be more significant, and this model supports that value (adj. $R^2 = 0.9985$). Pred. R^2 's score of 0.9968 makes it clear that the model can foresee future outcomes while explaining 99.6% of the variation. This model's low (0.34) result for the coefficient of variance suggests that there is less divergence between the experimental and predicted values.

The value of acceptable precision in this inquiry is 127.017, while values over 4 denote desirability. As can be seen in the ANOVA table, adequate precision measures the desired signal-to-noise ratio (S/N), which is more than 4. A 95% confidence level was used to determine the significance of the created model. A ratio greater than 4 that exhibits an acceptable signal is preferred. The values of anticipated R^2 and adjusted R^2 are reasonably agreed upon for all response parameters. How closely the projected R^2 and modified R^2 values match determines how many points can fit along the regression line. The assumption that any one variable can fully explain the variance in the dependent variable is the main contrast between predicted R^2 and adjusted R^2 . The adjusted R^2 , which explains the degree of variation, only reveals the independent variables that actually have an effect on the dependent variable.

5.3.3 Effect of Process Parameter on Tensile Strength

The effect of process parameter on tensile strength discussed below in detail.

5.3.3.1 Welding Time effects on Tensile Value

The tensile value of the joint material increases as the welding time goes from least to greatest. As the welding process lasts longer, more heat is transferred from the nickel slurry to the material contact through the charcoal to the substance. The material's heat and mass transmission properties will determine how long it takes to heat the material. More welding time is always preferred within the allowable range for improved tensile strength. Figure 5.4 show that when welding time goes from the minimum to the maximum, the metal's tensile strength increases.

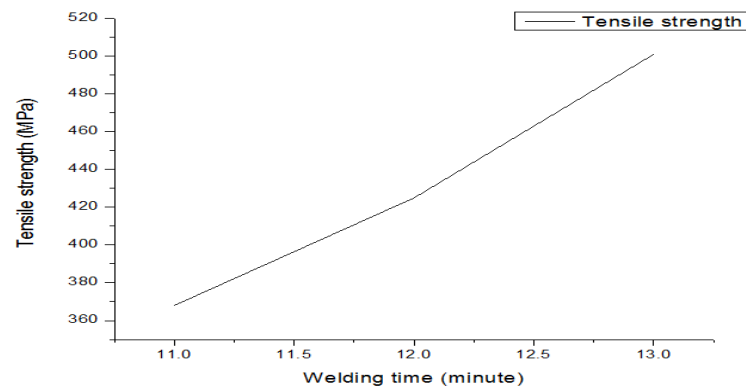


Fig.5. 4: Welding time effect on tensile strength

5.3.3.2 Effect of Powder Size on Tensile Strength

Figure 5.5 makes it obvious that the material's tensile strength decreases as the powder size increases. As particle size decreases from its highest value to its smallest value, more heat is absorbed over a shorter period of time. As a result, the microstructure of the welded connection becomes finer, increasing its tensile strength.

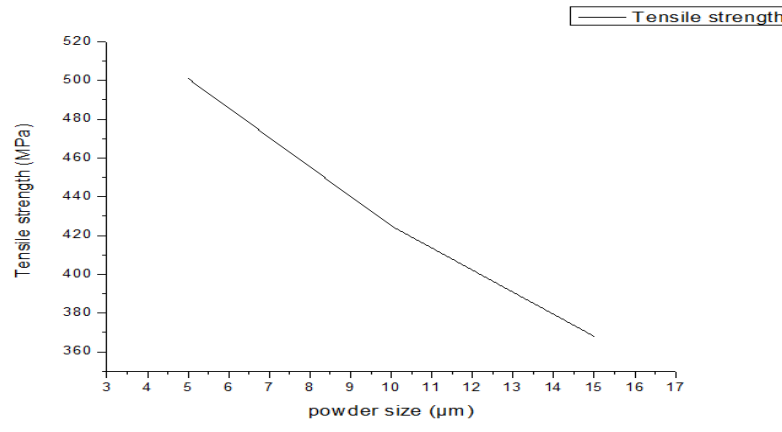


Fig.5.5: Powder size effects on tensile strength

5.3.3.3 Effect of Slurry Weight on Tensile Strength

According to figure 5.6, the value of tensile strength of the welded specimen slightly increases as slurry weight increases because more nickel particles are visible inside the joint area as the weight of the interfacing material increases, which is responsible for the increased value of tensile strength.

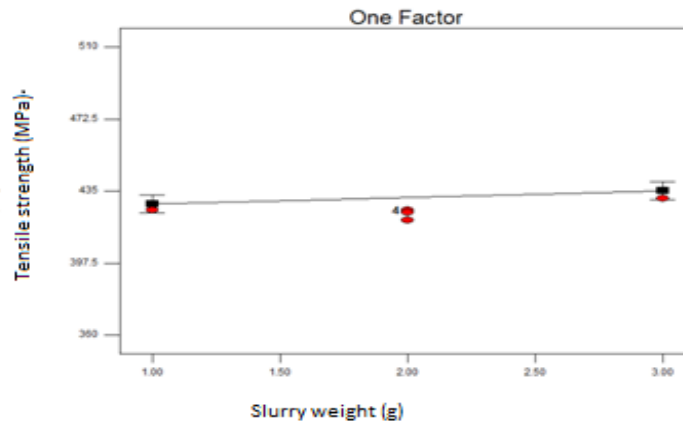


Fig.5.6: Slurry weight effects on tensile strength

5.3.3.4 RSM and Contour Effect of Input Variable on Tensile Strength

Response surfaces and contour plots are used to: 1) represent the interaction/dependence of the components; 2) show the stationary spots; and 3) accurately and sufficiently reflect the optimal value of the intended response. Tensile strength response surfaces and contour plots are shown in Figures 5.1 to 5.9. The tensile value is used as the response in the response surfaces and contour plots, respectively, while the other two independent components are preserved at the centre points of each graph. The design points are denoted by red dots in the aforementioned response surfaces and contour plots.

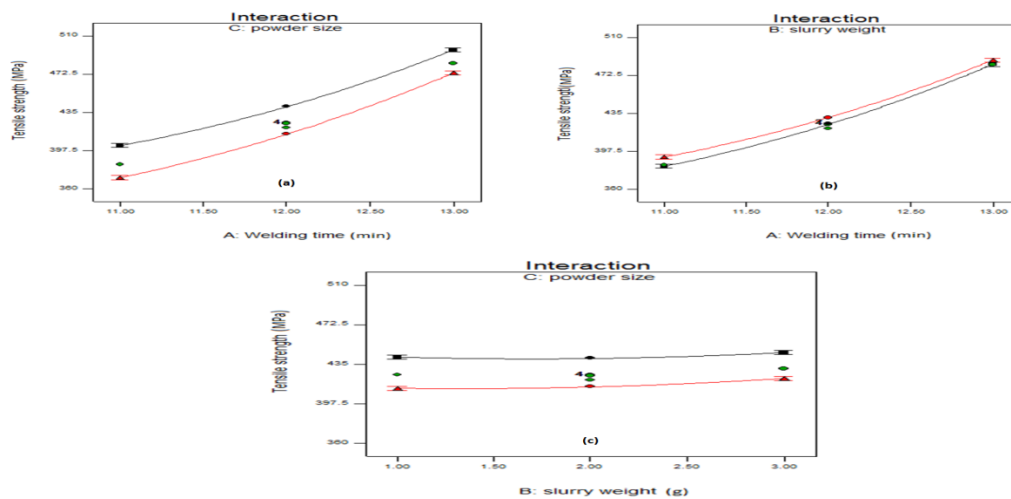


Fig.5.7: (a), (b), (c) Showing interaction effects of input parameters on tensile strength

The relationship between welding time, powder size, slurry weight, and tensile strength is shown in a graph. The impact of welding time on the tensile value of powder with a particle size of 5 microns meter and 15 microns meter, respectively, is shown by two lines in graph 5.7 (a). The graph indicates that the tensile strength of the specimen increases as the welding time goes from the lowest value to the highest

value. The upper and lower lines in graph 5.7(b) show the effects of welding time on tensile value for slurry weights of 1 g and 3 g, respectively. As powder particle size increases, the value of tensile strength decreased, which is the opposite of what is shown in graph 5.7 (c). From the graphs, it can be inferred that welding time has a greater influence on tensile value than powder size and slurry weight.

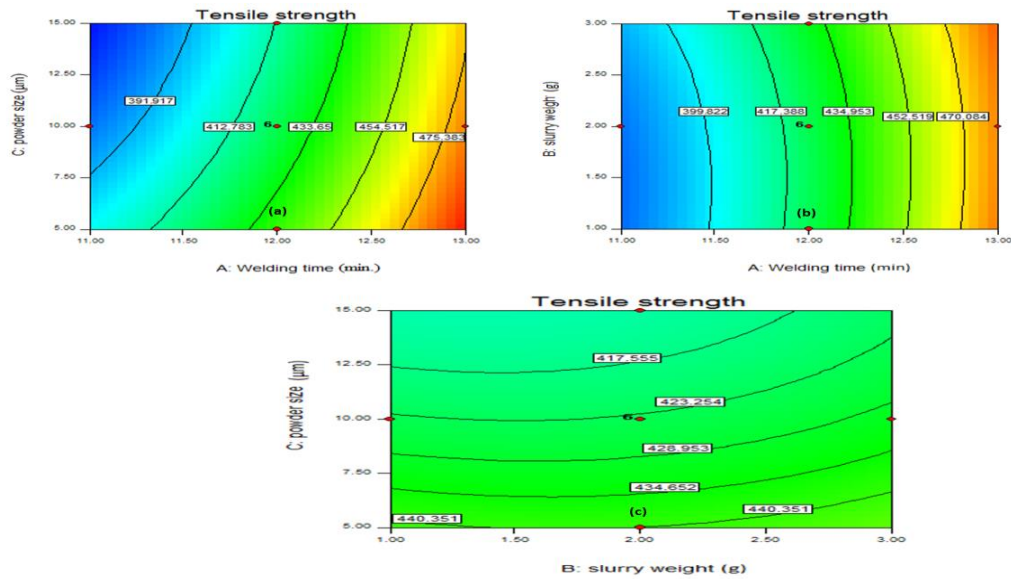


Fig.5.8: (a), (b), (c) Showing contour effect of input parameters for tensile strength

Local maxima are visible near the centre of the response surfaces and contour plots in Figures 5.8 and 5.9, but the maximum value of the response is highlighted in red in both diagrams. The contour plot for two dimensions is shown in Fig. 5.8 (a), (b), and (c), with the highest and minimum tensile strength values, 501 MPa and 368 MPa, respectively, kept at the centre point value. The effects of welding time and powder size on tensile strength are depicted in Fig. 5.8 (a) while maintaining a 10g slurry weight. The effects of welding time and slurry weight at 10 micron powder size are

depicted in Fig. 5.8 (b). The effects of powder size and slurry weight on tensile strength during a 12-minute welding time are depicted in Fig. 5.8 (c).

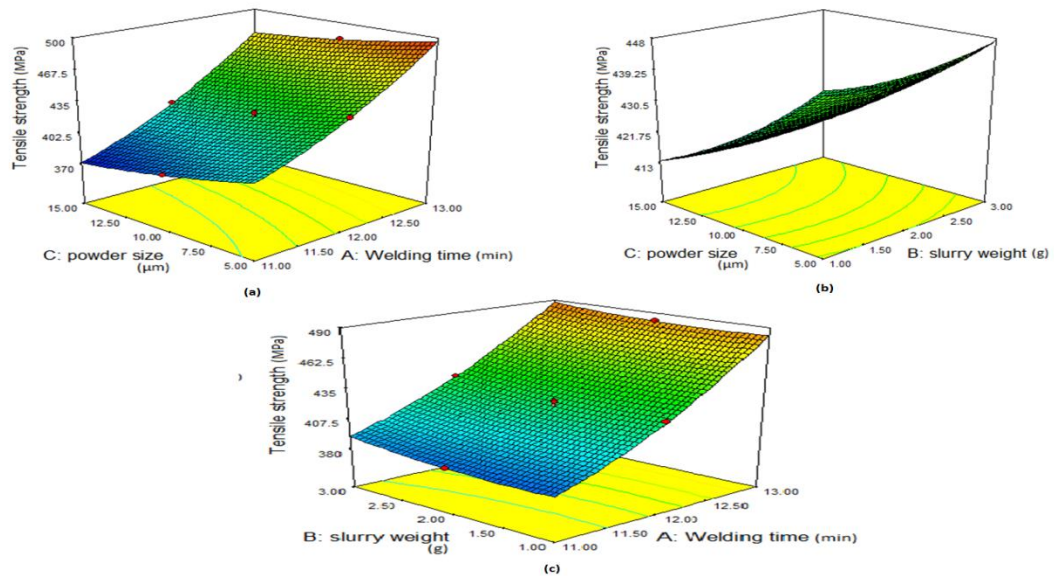


Fig.5.9: (a), (b), (c) showing 3D effect of input parameters for tensile strength

The three-dimensional effects of input parameters at the default tilt ($h=450$, $v=700$) are depicted in Figures 5.9 (a), (b), and (c). As shown in fig. 5.9 (a), the tensile strength of the joint increases as welding time increases, while the opposite is true as particle size increases. From fig. 5.9 (b), it can be seen that the tensile value increases somewhat as slurry weight increases but decreases when powder size increases. It is evident from fig. 5.9 (c) that when welding time and slurry weight are increased, so tensile strength increases.

5.4 Experimental Results for Microhardness

The cross section of joints that had undergone microwave processing was tested for Vicker's microhardness. The tests were run with a 300 gram load and a dwell period of 20 sec. The microhardness test findings showed that the joint region has greater hardness than the micro hardness of base metal; this is because hard phases such as

intermetallic and carbides that are present in the joint area precipitated there during the welding process. The experiment design matrix and associated data for the micro hardness of the weld joint region are shown in Table 5.3.

Table 5. 3 Experimental Results for Microhardness					
Std	Run	Welding Time (minute)	Slurry weight (grams)	Powder size (μm)	Micro hardness (Hv)
1	6	11	1	5	328
2	8	13	1	5	450
3	20	11	3	5	329
4	4	13	3	5	454
5	18	11	1	15	308
6	14	13	1	15	414
7	1	11	3	15	312
8	7	13	3	15	426
9	15	11	2	10	320
10	16	13	2	10	438
11	13	12	1	10	370
12	19	12	3	10	376
13	12	12	2	5	380
14	9	12	2	15	352
15	10	12	2	10	369
16	2	12	2	10	372

17	17	12	2	10	366
18	11	12	2	10	371
19	3	12	2	10	371
20	5	12	2	10	370

5.4.1 Mathematical Model for Microhardness

Mathematical model for microhardness was developed with the help of design expert software as shown in equation 5.3.

$$\text{Microhardness} = +369.94 + 58.50*A + 2.70*B - 12.90*C + 1.38*A*B - 3.37*A*C + 1.38*B*C + 8.91*A^2 + 2.91*B^2 - 4.09*C^2 \quad (5.3)$$

Mathematical model for microhardness in terms of parameters as shown in equation 5.4.

$$\begin{aligned} \text{Microhardness} = & + 924.01818 - 151.31818*\text{Welding time} - 28.18636*\text{Slurry weight} + \\ & 8.24273*\text{Powder size} + 1.37500*\text{Welding time}*\text{Slurry weight} - 0.67500*\text{Welding} \\ & \text{time}*\text{Powder size} + 0.27500*\text{Slurry weight}*\text{Powder size} + 8.90909*\text{Welding time}^2 \\ & + 2.90909*\text{Slurry weight}^2 - 0.16364*\text{Powder size} \end{aligned} \quad (5.4)$$

5.4.2 Checking the Adequacy of the Model for Microhardness

The projected vs real response for micro hardness is shown in Fig. 5.10, and the nearly perfect agreement between the two indicates the model's significance. The model's acceptability may be determined using the normal plot of the residual analysis. It displays the values' departure from the typical straight line. Values should be close to the straight line to improve the model. A graph between the anticipated and actual values was also created to examine the model's suitability. From the graph,

it can be deduced that the error distribution is normal and that all values are in order and sit roughly around the centre line. A graph between the residual and the input parameter can be used to examine the fluctuation of a single input parameter. From the graph, it can be concluded that variations are within the range.

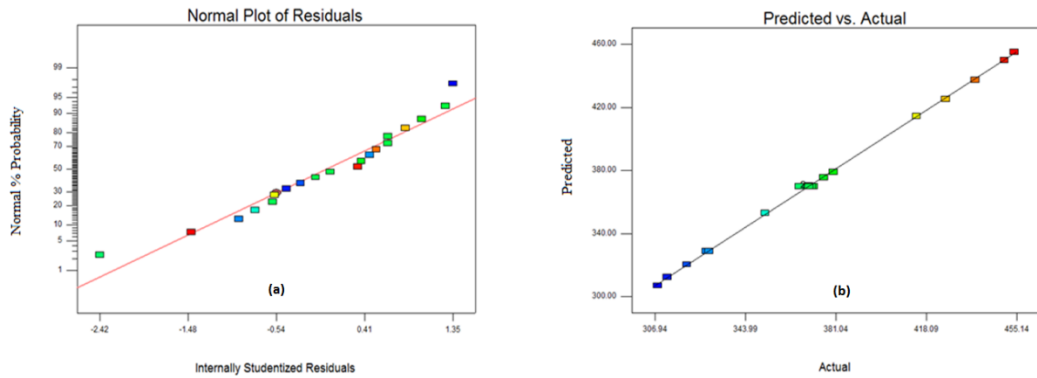


Fig. 5.10: Showing microhardness value for, a) Normal plot of residuals, b) predicted v/s actual

The effectiveness of the model was evaluated using the ANOVA method. The analysis of variance (ANOVA) results for micro hardness are presented in Table 5.4. The F-value for model 1348.36 reveals the model's importance. The P values must be less than 0.0500 for the model to be considered valid. All values (A, B, C, AB, AC, BC, A², B², and C²) from the model are below 0.0500. If there are more unimportant model terms, it may be necessary to reduce the model's support.

Table 5. 4 ANOVA Table for Full Quadratic for Micro hardness							
Source	Sum of Square	Df	Mean Square	F-value	p-value Prob > F	Contribution %	
Model	36469.15	9	4052.13	1348.36	< 0.0001		Significant
A-Weldin	34222.50	1	34222.50	11387.66	< 0.0001	58.50	

g time							
B- Slurry weight	72.90	1	72.90	24.26	0.0006	2.70	
C- Powder size	1664.1 0	1	1664.10	553.74	< 0.0001	-12.90	
AB	15.13	1	15.13	5.03	0.0487	1.38	
AC	91.13	1	91.13	30.32	0.0003	-3.37	
BC	15.13	1	15.13	5.03	0.0487	1.38	
A ²	218.27	1	218.27	72.63	<0.0001	8.91	
B ²	23.27	1	23.27	7.74	0.0194	2.91	
C ²	46.02	1	46.02	15.31	0.0029	-4.09	
Residu al	30.05	10	3.01				
Lack of Fit	7.22	5	1.44	0.32	0.8840		Not significa nt
Pure Error	22.83	5	4.57				
Cor Total	36499. 20		19				
SD			1.73		R*R	0.9992	
MEAN			373.80		Adjusted R*R	0.9984	
C.V%			0.46		Predicted R*R	0.9963	
					Adequate Precision	120.90	

Due to larger F-values and lower P-values (0.0001), welding time has a greater influence on the value of micro hardness (58.50%) compared to powder size (12.90%)

and slurry weight (2.70). The response's coefficient of determination (R^2), which is used to assess how well the model fits the data, was 0.9992. The aforementioned figure demonstrates that there is 99.92% likelihood that experimental data will match model predictions. Due to the model's accuracy, this model produces R^2 values that are less than 1 and that always fall between 0 and 1. The adjusted determination coefficient value should be high for the model to be more significant, and this model supports that value (adj. $R^2 = 0.9984$). The predicted R^2 value is 0.9963. The value of acceptable precision in this inquiry is 120.90, while values over 4 denote desirability. As can be seen in the ANOVA table 5.4, A 95% confidence level was used to determine the significance of the created model.

5.4.3 Effect of Process Parameter on Microhardness

The effects of process parameter on microhardness of joint discussed below in detail.

5.4.3.1 Welding time effects on micro hardness value

As welding time increases, the melting capacity of Ni particles also increases, and, as a result, the strength of the joint increases. As can be seen in Fig. 5.11, the hardness of the welded material increases sharply as welding time increases from the lowest value to the highest value.

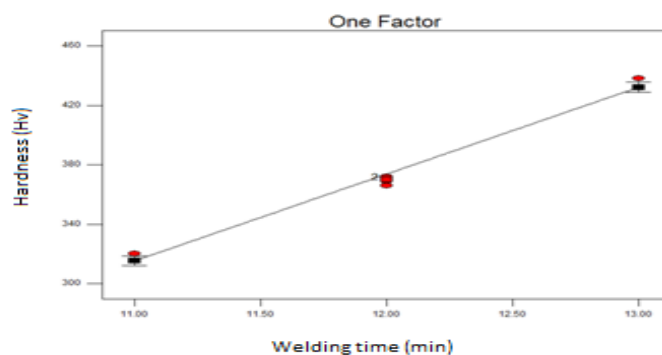


Fig.5.11: Welding time effect on micro hardness value

5.4.3.2 Effect of powder size on hardness

Since more heat is absorbed at a faster rate as the powder size increases, it is expected from figure 5.12 that the joint area hardness would decrease. These features can be seen when particle size declines from its greatest value to its minimum value. As a result, the microstructure of the welded connection becomes finer, raising the joint area's hardness value.

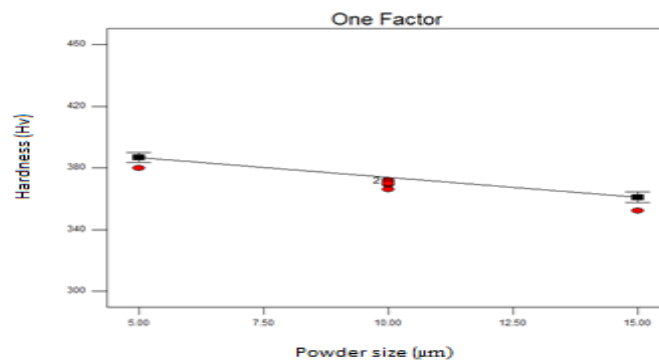


Fig.5.12: Powder size effect on micro hardness value

5.4.3.3 Effect of slurry weight on microhardness

According to fig. 5.13, there is a little increase in the welded specimen's hardness value because more Ni particles are present in the welding zone as the slurry weight rises, increasing the hardness value in the joint region.

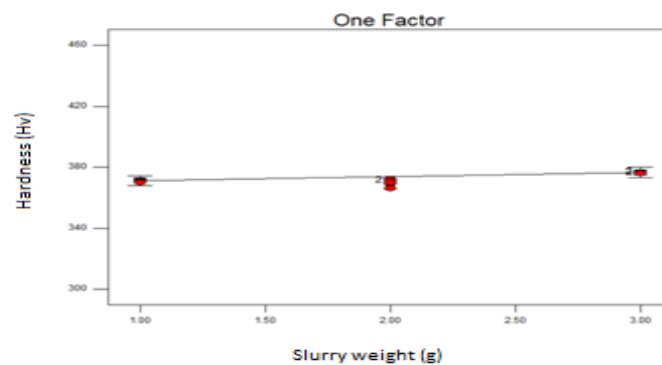


Fig.5.13: Slurry weight effect on micro hardness value

5.4.3.4 Interactive effect of input variable on microhardness

The relationship between welding time, slurry weight, and particle size is represented via an interactive graph. According to graph 5.14, microhardness increases along with welding time and slurry weight, and the opposite is true as powder particle size increases.

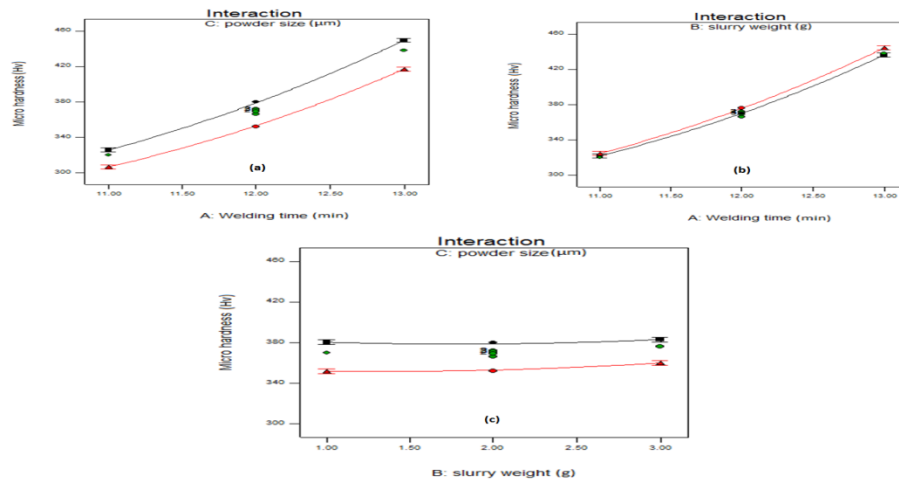


Fig.5.14: (a), (b), (c) interaction effects of input parameters on microhardness

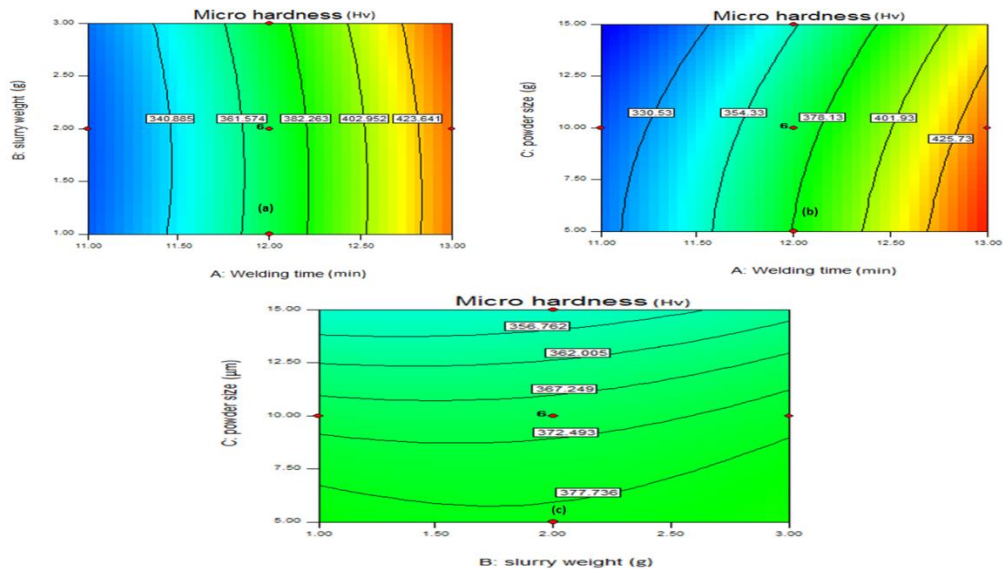


Fig.5.15: (a), (b), (c) Showing contour effect of input parameters on microhardness

The contour plot for two dimensions is shown in Fig. 5.15 (a), (b), and (c). The effects of welding time and slurry weight on microhardness at a powder size of 10 microns are shown in Fig. 5.15 (a). The effects of welding time and powder size at 2g slurry weight are shown in Fig. 5.15 (b). The effects of powder size and slurry weight on microhardness during a 12-minute welding time are shown in Fig. 5.15 (c).

The three-dimensional effects of input parameters are depicted in Figures 5.16 (a), (b), and (c). Figure 5.16 (a) makes it abundantly evident that while the tensile strength of the joint grows as welding time increases, the opposite effect occurs when powder size increases. It is evident from fig. 5.16 (b) that when welding time and slurry weight are increased, tensile strength increases. According to fig. 5.16 (c), the tensile value of joint increases somewhat as its slurry weight increases, but it decreases as the size of the powder particle increases.

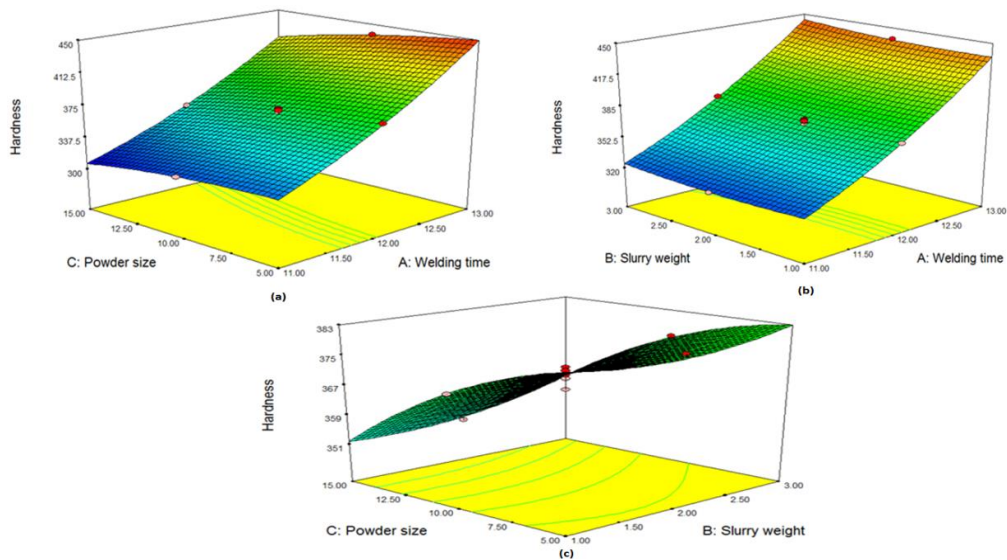


Fig.5.16: (a), (b), (c) showing 3D effect of input parameters on microhardness

5.5 Experimental Results for Surface Temperature

An infrared temperature gun (thermometer) of Mextech brand with range (50 to 2200⁰c) was used to measure the temperature in the weld joint region and the noted values are depicted in table 5.5.

Table 5. 5 Experimental Results for Surface Temperature					
Std	Run	Welding Time (minute)	Slurry weight (grams)	Powder size (µm)	Surface Temperature (Degree Celsius)
1	6	11	1	5	797
2	8	13	1	5	923
3	20	11	3	5	796
4	4	13	3	5	932
5	18	11	1	15	769
6	14	13	1	15	870
7	1	11	3	15	776
8	7	13	3	15	891
9	15	11	2	10	777
10	16	13	2	10	896
11	13	12	1	10	826
12	19	12	3	10	845
13	12	12	2	5	852
14	9	12	2	15	815
15	10	12	2	10	826
16	2	12	2	10	828

17	17	12	2	10	824
18	11	12	2	10	828
19	3	12	2	10	827
20	5	12	2	10	831

5.5.1 Mathematical Model for surface temperature

Mathematical model for surface temperature was developed with the help of design expert software as shown in equation 5.5.

$$\text{Surface Temperature} = + 828.29 + 59.70*A + 5.50*B - 17.90*C + 3.00*A*B - 5.75*A*C + 2.50*B*C + 6.77*A^2 + 5.77*B^2 + 3.77*C^2 \quad (5.5)$$

Mathematical model for surface temperature in terms of parameters as shown in equation 5.6.

$$\text{Surface Temperature} = +1094.14545 - 97.34545*Welding\ time - 58.59091*slurry\ weight + 6.20182*powder\ size + 3.00000*Welding\ time*slurry\ weight - 1.15000*Welding\ time*powder\ size + 0.50000*slurry\ weight*powder\ size + 6.77273*Welding\ time^2 + 5.77273*slurry\ weight^2 + 0.15091*powder\ size^2 \quad (5.6)$$

5.5.2 Checking the Adequacy of the Model for Surface Temperature

The projected vs real response for micro hardness is shown in Fig. 5.17, and the nearly perfect agreement between the two indicates the model's significance. The model's acceptability may be determined using the normal plot of the residual analysis. It displays the values' departure from the typical straight line. Values should be close to the straight line to improve the model. A graph between the anticipated and actual values was also created to examine the model's suitability. From the graph,

it can be deduced that the error distribution is normal and that all values are in order and sit roughly around the centre line. A graph between the residual and the input parameter can be used to examine the fluctuation of a single input parameter. From the graph, it can be concluded that variations are within the range.

Table 5. 6 ANOVA Table for full quadratic for Surface Temperature							
Source	Sum of Squares	df	Mean Square	F Value	p-value Prob > F	Contribution %	
Model	40519.70	9	4502.19	504.47	<0.0001		significant
A-Welding time	35640.90	1	35640.90	3993.58	<0.0001	59.70	
B-slurry weight	302.50	1	302.50	33.90	0.0002	5.50	
C-powder size	3204.10	1	3204.10	359.02	<0.0001	-17.90	
AB	72.00	1	72.00	8.07	0.0175	3.00	
AC	264.50	1	264.50	29.64	0.0003	-5.75	
BC	50.00	1	50.00	5.60	0.0395	2.50	
A ²	126.14	1	126.14	14.13	0.0037	6.77	
B ²	91.64	1	91.64	10.27	0.0094	5.77	
C ²	39.14	1	39.14	4.39	0.0627	3.77	
Residual	89.25	10	8.92				
Lack of Fit	61.91	5	12.38	2.27	0.1952		not significant
Pure Error	27.33	5	5.47				

Cor Total	40608.9 5	19					
SD	2.99			R-Squared	0.9978		
MEAN	836.45			Adj R-Squared	0.9958		
C.V%	0.36			Pred R-Squared	0.9882		
PRESS	479.13			Adeq Precision	78.678		

The model is suggested to be significant by the model F-value of 504.47. In this, important model terms were A, B, C, AB, AC, BC, A^2 , and B^2 . Model terms are not significant if the value is higher than 0.1000. According to the "Lack of Fit F-value" of 2.27, the lack of fit is not significant in comparison to pure error.

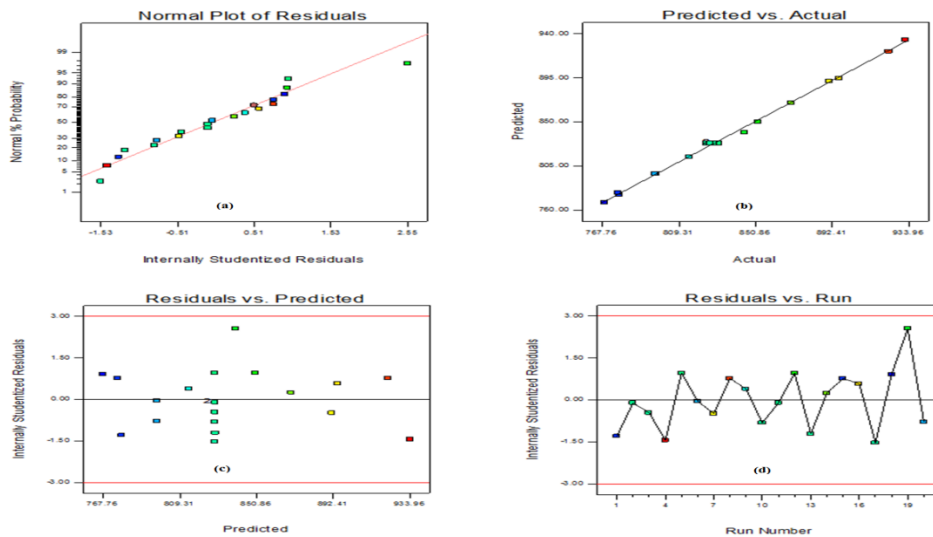


Fig. 5.17: showing a) normal plot of residuals, b) predicted v/s actual values, c) residuals v/ predicted values, d) residuals v/s run

Figure 5.17 shows a plot of normal probability (percent) against UTS residuals that have been externally studentized (a). The graphic serves as verification that the residual for the response surface temperature follows the normal distribution. The predicted against real plot, shown in Figure 5.17 (b), compares the null model to the model's effect. The figure makes it evident that every point is located near to the centre line, demonstrating an excellent fit. The plot of residuals against rising expected response values is shown in Figure 5.17 (c), and the residuals should be randomly dispersed and devoid of any pattern. Figure 5.17(d) plots the residuals against the sequence of the experimental runs to look for hidden factors that might affect the experiment's response and should display random dispersion.

5.5.3 Effect of Process Parameter on Surface Temperature

Figure 5.18 (a), (b), and (c) make it evident that the surface temperature of the treated joint increases with increasing welding time. Figure 5.18 (b) shows the same influence on slurry weight, although the fluctuation range is quite small. Figure 5.18 (c) illustrates the opposite effect, wherein the surface temperature of the joint area decreases as the particle size is increased due to the presence of coarse particles as opposed to fine particles.

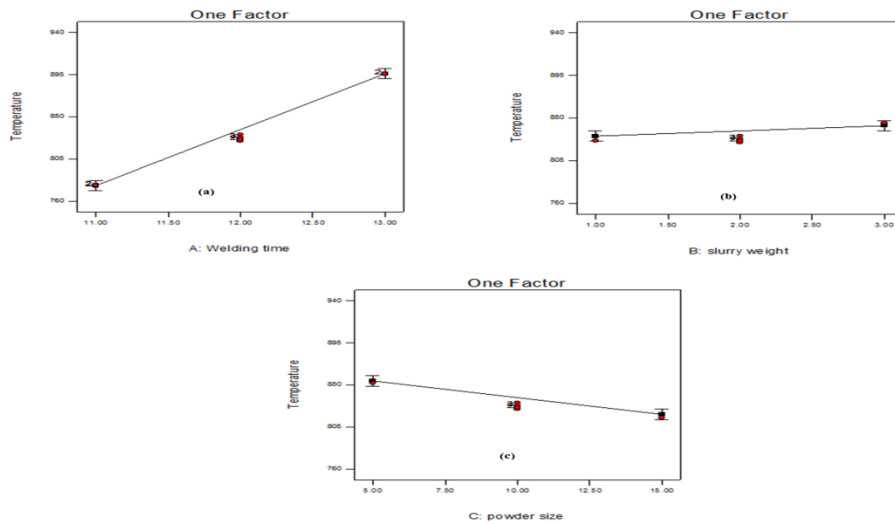


Fig.5.18: showing a) welding time effects, b) slurry weight effects and c) powder size effects on surface temperature

5.5.3.1 Interaction parameter effects on surface temperature value

Figure 5.19 illustrates the interaction between welding time, slurry weight, and powder size on surface temperature.

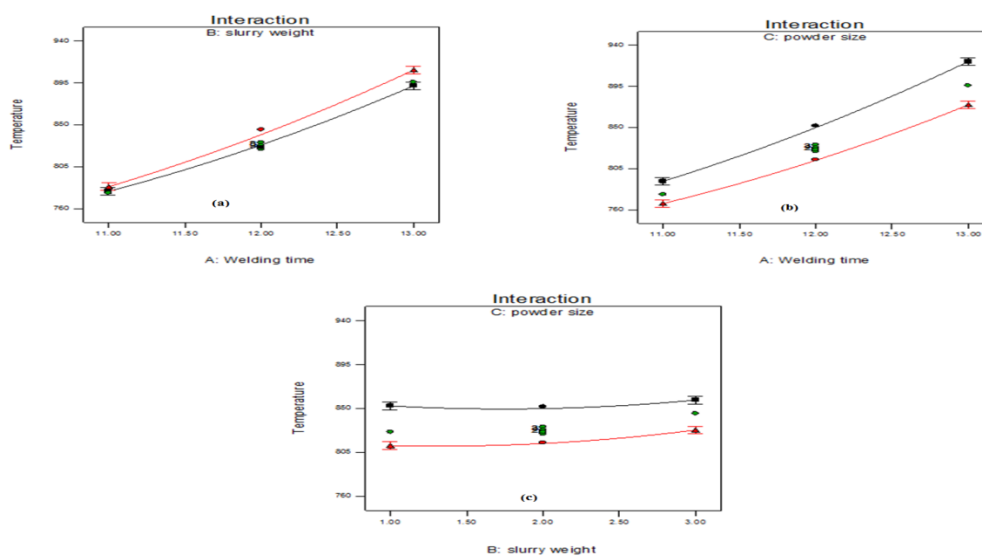


Fig.5.19: showing interaction effects of a) welding time & slurry weight, b) welding time & powder size and c) powder size & slurry weight, on surface temperature

Figures 5.19 (b) and (c) show a greater difference between the lines than in Figure (a), which makes it clear that welding time and powder size particle have greater effects on surface temperature than slurry weight. The red line and black line in Fig. 5.19 (a) represent the welding effects at 1g and 3g of slurry weight, respectively, whereas the intermediate value of powder size and the red dot represent the design point. The surface temperature increases as values increase for both lines. The effects of welding time and powder size on surface temperature are shown in Fig. 5.19 (b). Both lines demonstrate a rise in surface temperature as welding time increases; the top line displays data at powder sizes of 5 microns meter while the bottom line displays values at 15 microns meter. The response value increases slightly when the slurry weight increases from 1 g to 3 g, as shown in fig. 5.19(c). Lower line values are shown at a 15 micron scale, while the upper line impacts on reaction are shown at a 5 micron level.

5.5.3.2 Contour Plot on Surface Temperature

Figure 5.20 (a, b, c) illustrates contour impacts on surface temperature in a 2D interactive manner while retaining the third input parameter at the centre. The effects of welding time and slurry weight on surface temperature are shown in Fig. 5.20 (a) while maintaining a median value for powder size. Surface temperature increases when welding time and slurry weight are increased. Figure 5.20 (b) depicts the highest surface temperature for greater welding time and smaller powder particle sizes. Surface temperature exhibits its highest response at lower levels of powder size and maximum levels of slurry weight; although the influence of both input parameters was minimal (Fig. 5.20 (c)) if welding time was kept at a moderate value.

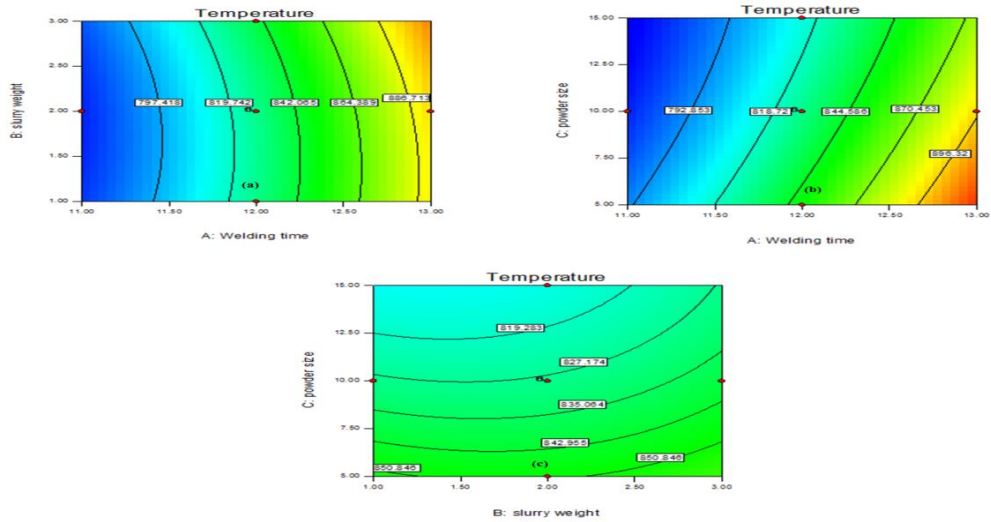


Fig.5.20: (a), (b), (c) Showing contour effects on surface temperature

Fig. 5.21 (a), (b), and (c) illustrate how input parameters affect response in three dimensions at the rotation's default value ($h=450$, $v=700$). The temperature of the joint increases as welding time and slurry weight increase, as can be observed in fig. 5.21 (a), but when welding time and powder size increases; the opposite effect can be seen in fig. 5.21 (b). From fig. 5.21 (c), it can be seen that temperature values somewhat increased as slurry weight increases but decreases when powder size increases.

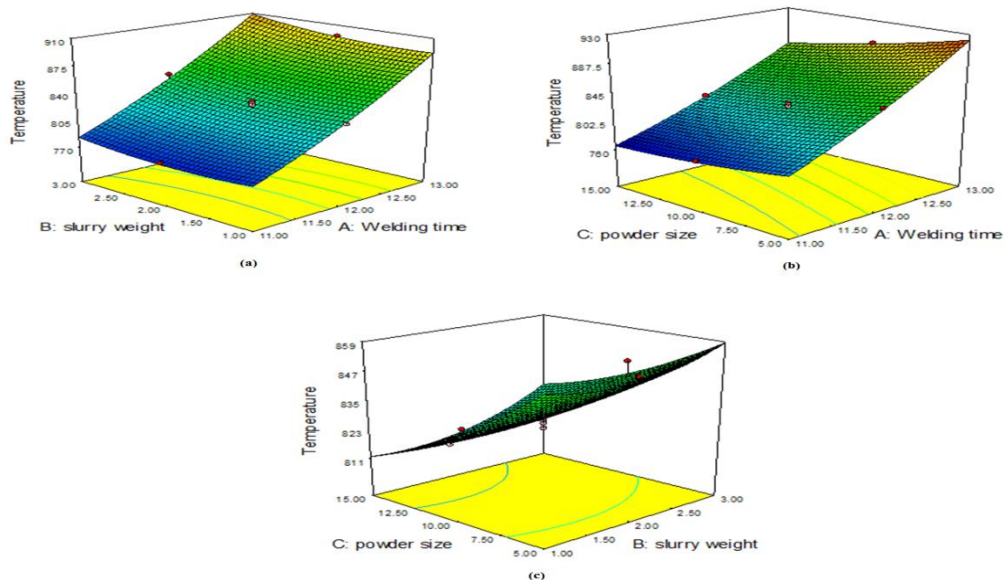


Fig.5.21: (a), (b), (c) Showing 3D effect of input parameters on surface temperature

5.6 X-Ray Diffraction

Phase identification is accomplished using the material characterization technique known as X-ray diffraction (XRD). It is composed of X-rays that are incident on the sample surface and are monochromatic. A cathode ray tube is the source of these X-rays, which are further filtered to produce monochromatic radiation. As the sample and detector spin at angles of 2θ ranging from ten to seventy degrees, the quantity of diffracted X-rays is continuously recorded.

The XRD analysis was finished using two distinct software tools called Origin and Xpert High Score. XRD analysis produced three peaks with various Miller indices. The XRD peaks' high intensity denotes a high degree of crystallinity.

Fig 5.22 (a), (b), (c) shows the X- ray diffraction of 5μ , 10μ and 15μ nickel powder. The powder primarily contains nickel, with minor amounts of other elements.

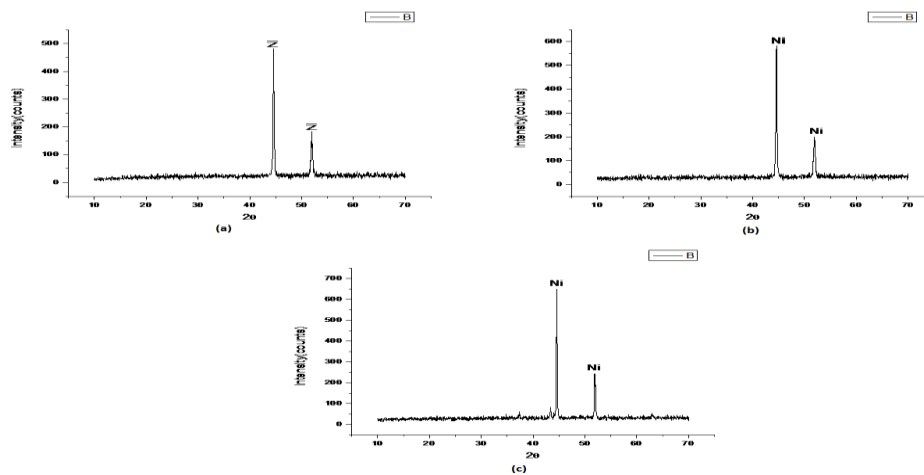


Fig. 5.22: (a), (b), (c) showing xrd pattern of 5μ , 10μ and 15μ respectively

Fig 5.23 (a), (b) and (c) shows the xrd spectra of the joint region for maximum, medium and minimum value of outcomes respectively, revealed the formation of some intermetallics of iron & nickel, such as NiSi, FeNi, and carbides of chromium, and iron, such as Cr_3C_2 and Fe_2C in the joint zone. At high temperatures, various

possible reactions between the elements might have favoured the formation of these intermetallic phases. These phases are thought to have formed as a result of the sandwich layer made of nickel heating up quickly and the melt pool abruptly cooling to room temperature at the end of the irradiation cycle. The formation of nickel silicide (NiSi) elements because of presence of more nickel elements in the powder and substrate also and as a result of the diffusion process the nickel powder melts with a thin layer of substrate. It's possible that the intermixing of substrate material and nickel powder in the joint region is what causes the presence of iron phases (FeNi) in the weld region. Because there was free carbon in the graphite sheet (separator), which interacted with the substrate during microwave heating, carbides (Cr_3C_2 and Fe_2C) may have been present.

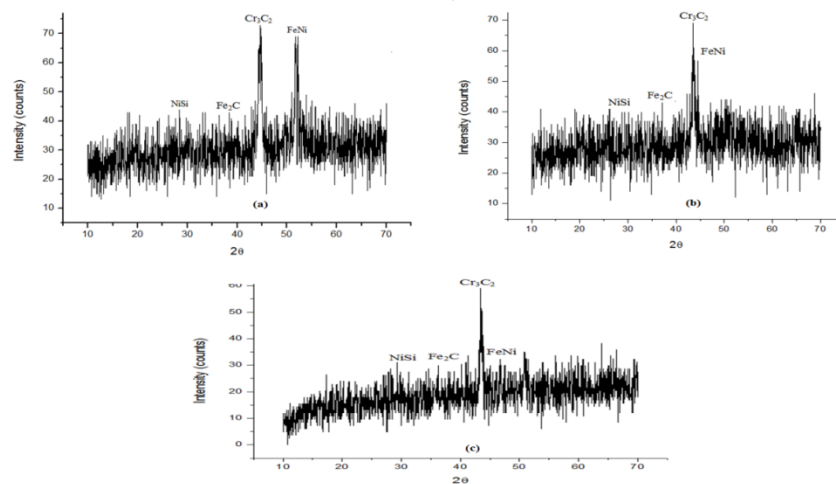


Fig.5.23: (a), (b) and (c) showing xrd pattern of joint area for maximum, medium and minimum value of outcomes respectively

The peak corresponding to $2\theta \sim 28.998^\circ$ indicates the formation of nickel silicides (NiSi), Peaks of iron nickel (FeNi) corresponding to 2θ of 50.96° ; are observed. Similarly, at an elevated temperature chromium reacts with carbon to form chromium

carbides (Cr_3C_2) corresponding to 2θ of 43.76° and iron of substrate to form iron carbide (Fe_2C) at 38.42° .

5.7 Microstructural Characterization of Welding

Olympus GX41 compact inverted metallurgical microscope is used for microstructural images. The completed weld was then sliced transversely, polished with various emery paper grades, and for best results, polished with velvet paper. Prior to doing a thorough investigation of the microstructure, the sample was etched using an acidic solution made by combining 45 gram of ferric chloride with 150 millilitres of hydrochloric acid and 75 millilitres of distilled water. The polished workpiece was briefly immersed in solution.

Fig. 5.24, 5.25 and 5.26 shows the microstructural images from optical microscope for minimum value of outcomes [of Run 5], medium value of outcomes [of run 17] and maximum value of outcomes [of Run 4] respectively. Figures 5.24 (a), 5.25(a), and 5.26 (a) shows the microstructure for base metal, Figure 5.24 (b), 5.25(b), and 5.26 (b) microstructure of joint area at 100X magnification scale and Figure 5.24 (c), 5.25(c), and 5.26 (c) microstructure of joint area at 200X magnification scale. In all three experiments, the interface slurry was correctly attached to the substrate interfaces.

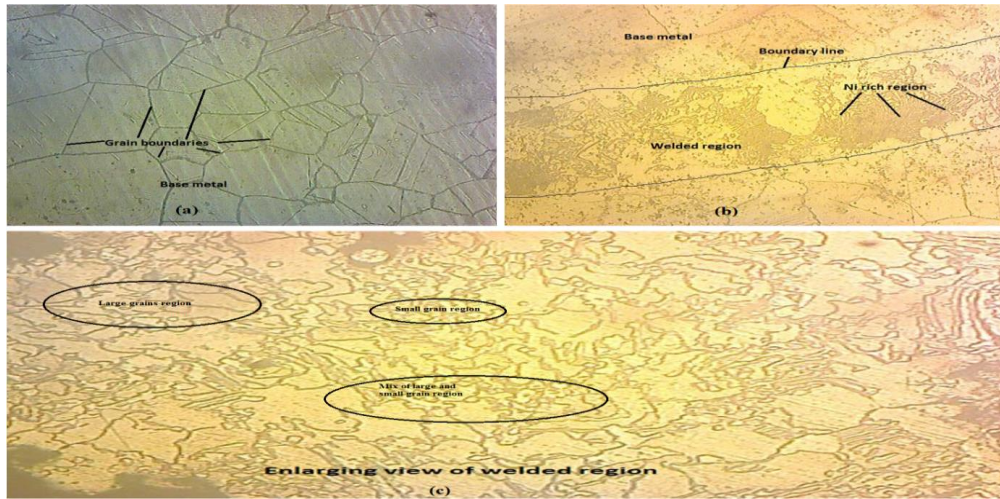


Fig.5.24: Shows microstructural images of a) base metal, b) at 100x, c) at 200x for minimum value of outcomes

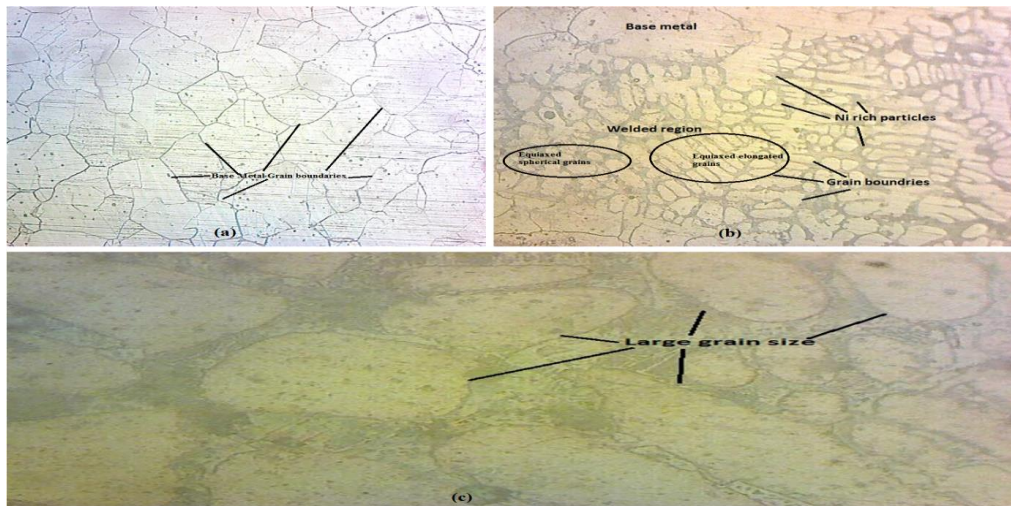


Fig.5.25: Shows microstructural images of a) base metal, b) at 100x, c) at 200x for medium value of outcomes

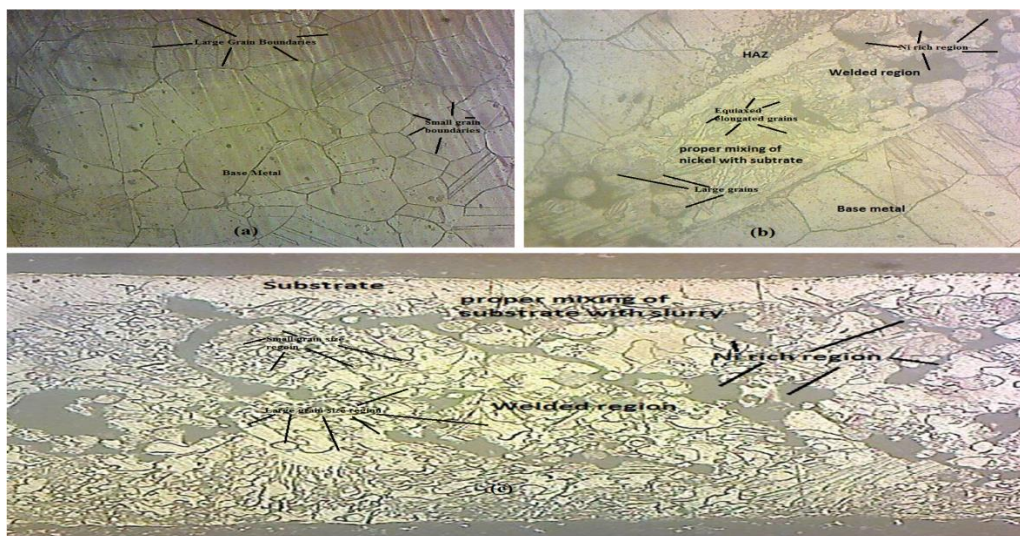


Fig.5.26: Shows microstructural images of a) base metal, b) at 100x, c) at 200x for maximum value of outcomes

Typical optical micrographs for maximum, medium, and minimum output values are given in Figs. 5.24, 5.25, and 5.26, respectively. These images clearly show needle-like structures in the joint zone, primarily closer to the base metals. This could be because of the development of a martensitic structure at the weld interface, which is connected to a quicker cooling rate since the base material is nearby. The greater microhardness seen closer to the interface zones is also related to this martensitic structure. Although there are carbide precipitates in the joint zone's core, the highest value of outcome obviously has a larger degree of carbide precipitation and the smallest grain boundaries when compared to the other two outcomes, as shown in Fig. 5.26. The emergence of carbides is crucial for improving the joint's mechanical strength. Figure 5.24, on the other hand, shows elongated grains with broad grain borders. According to the research, improved mechanical results are caused by small boundaries.

5.8 Field Emission Scanning Electron Microscope Analysis

Fig. 5.27 (a) depicts the FE-SEM image of the joint region, which shows a small defect at the weld joint with a wavy interface. With less porosity present in the interface area, a negligibly heat-affected zone is readily visible. The thermal gradients existing in the melt pool as a result of microwaves' inverse heating profile are what create the convection currents that cause the wavy interface to form in the area. These currents cause the substrate and powder particles to mix together. According to the XRD diffraction patterns in Fig. 5.23, this cause various iron and carbide phases to develop. The SEM image makes the carbide precipitation along the grains quite obvious. The SEM image shows the carbide precipitation along the grains.

Microwave heating is mostly limited to nickel powder, but as the nickel metal weld diffuses and solidifies, heat is transported to low-heated areas, towards the bulk metal.

The SEM picture demonstrates the substrate's metallurgical coupling with the powder particle after it has completely melted. There are no pores or fissures in the joint. At the joint, a uniform, thick structure develops. The volumetric heating of the material is what causes the joint's apparent uniformity. Heat may be produced via the volume of the material, leading to volumetric heating since microwaves can directly transfer energy to the substance by penetrating through the material. As a susceptor for the microwave's first connection, charcoal powder was employed. After absorbing microwave energy, charcoal powder is heated to a high temperature, and then, using a graphite sheet utilised as a separator in this experiment, it transmits heat to a layer of nickel powder. The powder begins to absorb microwaves at a high temperature, which causes its temperature to increase enough for the powder to melt. The interfacing surfaces get moist from the molten powder, which causes the interfacing surfaces to melt.

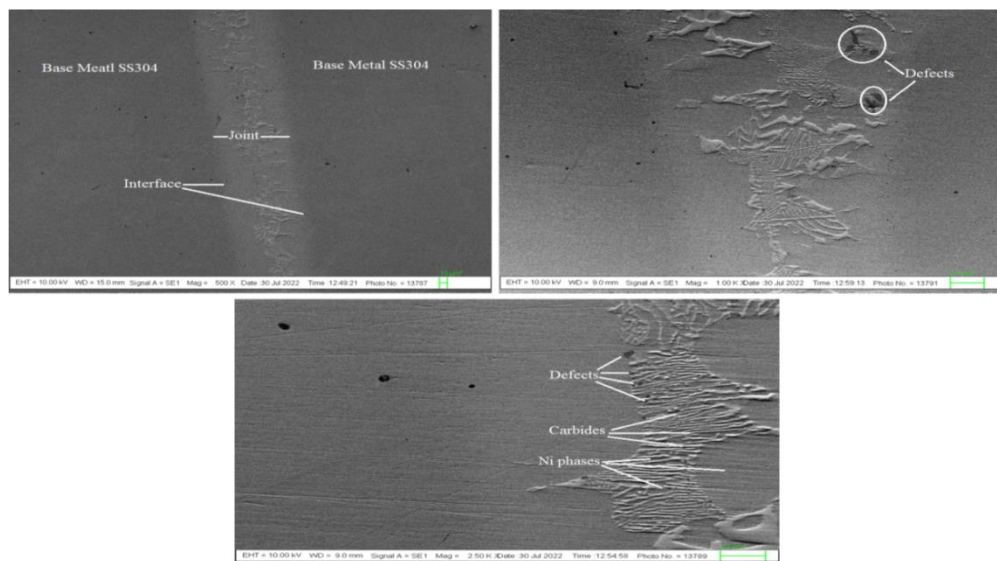


Fig.5.27: shows FESEM images of joint area a) at X20, b) at 150X, c) at 5000X for minimum value of outcomes

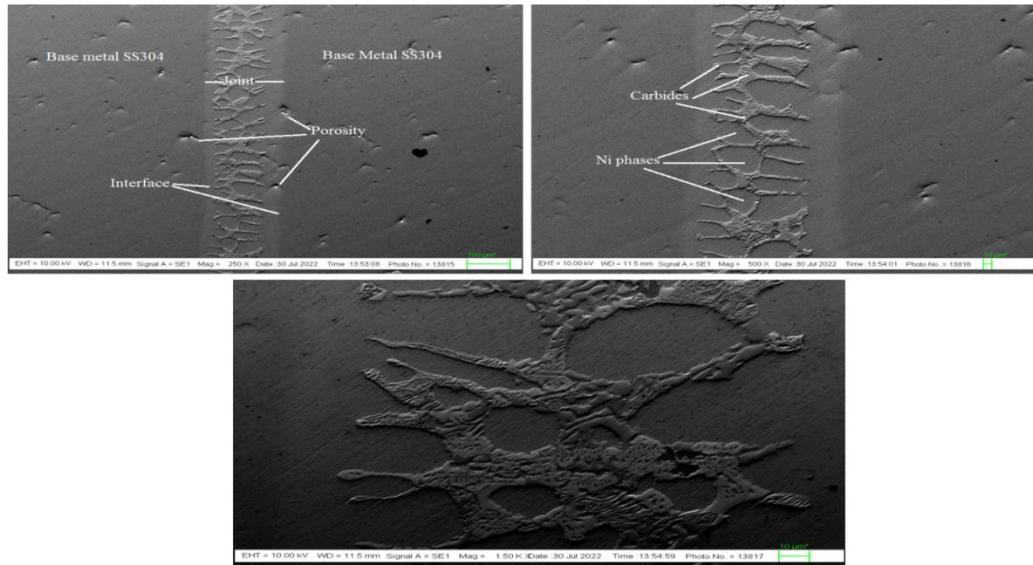


Fig.5.28: shows FESEM images of joint area a) at X20, b)at 150X, c)at 5000X, for medium value of outcomes

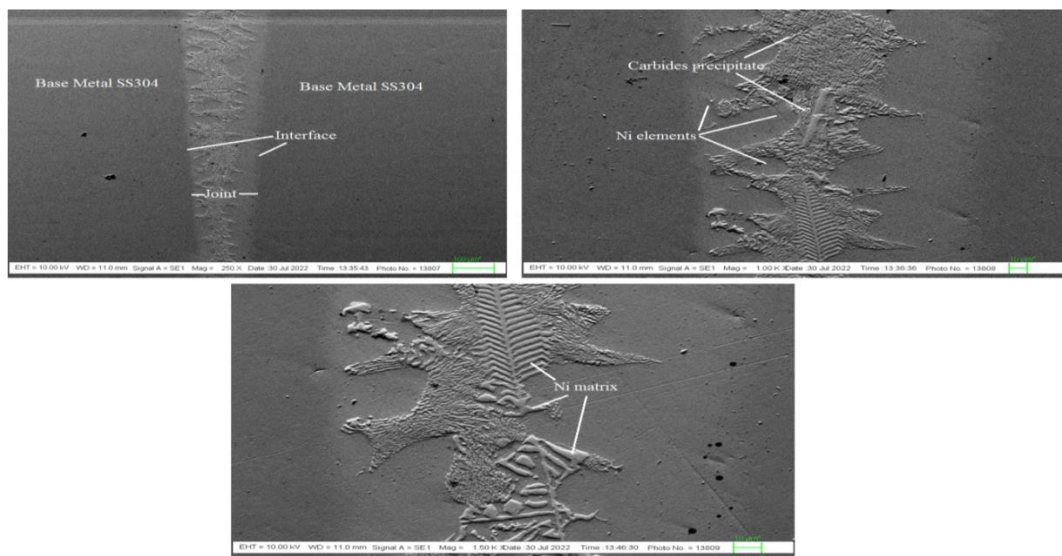


Fig.5.29: shows FESEM images of joint area a) at X20, b) at 150X, c) at 5000X for maximum value of outcomes

The SEM images revealed that the microstructure for maximum value of outcomes having of equiaxed grains in joint with less pores on the surfaces compared with FESEM images for medium and minimum value of outcomes. The volumetric heating properties of microwaves cause the development of equiaxed grains, which decreases

the dendritic transitions from equiaxed or cellular structures [Hebbale and Srinath (2016)]. Additionally, the solidification takes place as a consequence of heat being transferred from the core to the cavity walls after the microwave radiation has stopped. It has frequently been observed that equiaxed structures expand in the direction of heat flow, that is, from the core to the outer surface. It is evident that the nickel reinforcement particles are firmly lodged in the matrix grains, and the interfaces are devoid of flaws and fractures to ensure the best possible results.

At the joint section, carbides of chromium and iron, and in particular (Cr_3C_2 and Fe_2C), are formed. This occurs as a result of the joint's wide grain boundaries, which allow for easy diffusion of Cr and Fe from the base and carbon from the graphite sheet at high temperatures. This chromium and iron combines with carbon at a high temperature during the heating and fusing process, creating chromium carbide and iron carbide as a result. It is evident that two atoms of carbon consume three atoms of chromium, during the synthesis of the intermetallic complex Cr_3C_2 , some carbon is joined with a large quantity of chromium and two atoms of iron consume one atom of carbon for the synthesis of the Fe_2C . These intermetallics are brittle and hard by nature.

The matrix deforms plastically as the tensile stress is applied. However, these hard particles (carbides and intermetallics), which are predominately present in the grain boundary zone; prevent the dislocation movement, which limits the matrix's plastic deformation. As a result, an elongation occurs at the joint zone that is restrained by the hard particles and results in the material failing largely in a ductile manner, as seen by the creation of a lip (cone) in the SEM picture of fractured joint. Due to the base metal's structure being created by numerous re-crystallizations of hot wrought

steel, it shows direction-based qualities to a significant amount, which accounts for the difference in tensile properties between the base metal and weld metal. But at the joint zone, the weld zone is made up of hard particles like carbides and resolidified metallic material.

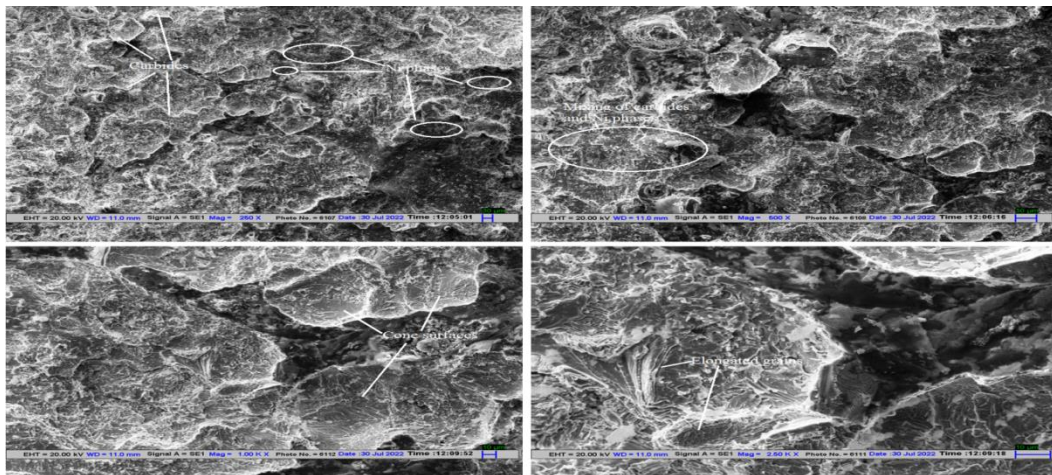


Fig.5.30: Shows FESEM images of fractured joint

The fragments of the broken tensile specimens that were further examined using FESEM are depicted in Fig. 5.30. The illustration shows that along the crystallographic planes, ductile fracture of the material occurs more often. The fractograph makes the cone formation quite evident. The shattered surfaces of the joint are depicted in Figures 5.30 at scales of 250X, 500X, 1000X, and 2500X. The graphic makes it obvious that the joint failed due to a mixed mode of failure. As seen by the abrupt separation (brittle failure) and plastic deformation (cone formation) in the ductile mode failure, both brittle and ductile modes of failure were seen during the joint fracture. Brittle failure results from the presence of carbide phases in the material, while ductile failure is caused by the presence of a comparatively soft matrix made up of solidified Ni powder. The matrix deforms plastically when a force is applied, but these carbide precipitates cannot keep up with the matrix deformation.

The brittle phases (carbide particles) cleave when a certain load value is attained. As a result, the joint fracture involves both ductile and brittle failure.

5.9 Energy Dispersive X-Ray Spectroscopy Analysis

The element distribution was done by the EDS analysis on the joint at various locations; namely on the base metal (1), at the interface joint (2), and on the welded joint (3). Fig. 5.31 shows the findings for the greatest output values; Fig. 5.32 shows the results for the intermediate output values; and Fig. 5.33 shows the results for the minimum output values. The results for base metal at point 1 indicate that stainless steel 304 has a larger percentage of iron than other constituents like chromium, nickel, silicon, and carbon. When the data for the interface boundary were shown at point 2, the percentages of nickel and carbon increased while the proportion of iron decreased, indicating that the nickel powder had properly fused with the base metal. The findings for the joint section are shown at point 3, where there is a larger concentration of nickel and chromium, as well as a predominance of carbon, silicon, and iron on the grain surfaces.

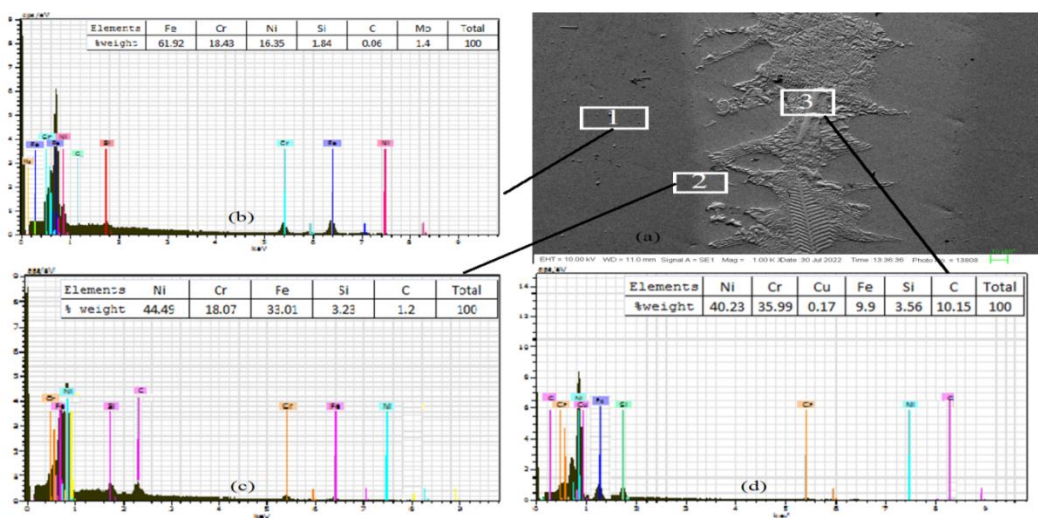


Fig.5.31: Shows EDS analysis for maximum value of outcomes at different portions

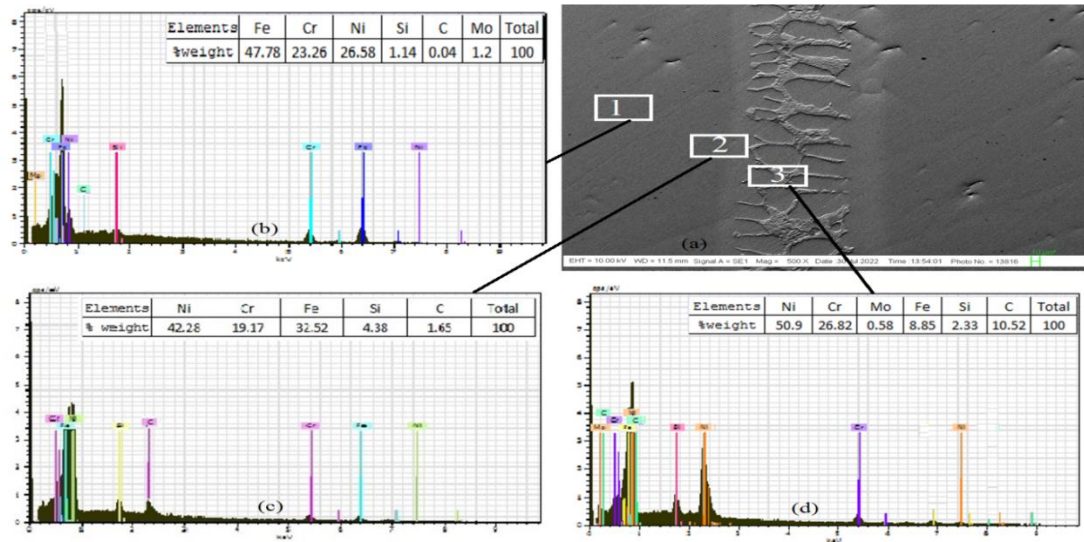


Fig.5.32: Shows EDS analysis for middle value of outcomes at different portions

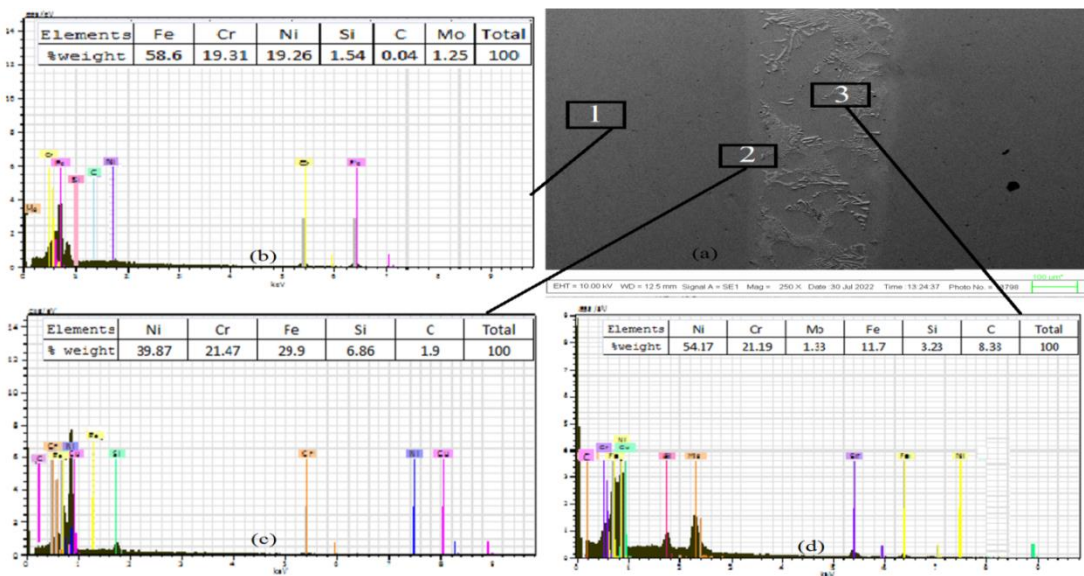


Fig.5.33: Shows EDS analysis for minimum value of outcomes at different portions

According to the EDS analysis for the maximum output values (fig. 5.31), intermediate output values (fig. 5.32) and minimum output values (fig. 5.33), the joint section's chromium and carbon content will be higher for the maximum output values than for the intermediate value and minimum output values, which will result in the mechanical values being at their highest for the maximum value of the process parameter. Due to exposure to direct heat transfer and temperature increase, melting

of the nickel metal powder and layers of the metal joining interface occurs as a result of the filler metallic powders being subjected to microwave radiation. The connecting portion develops a strong metallic carbide formation pathway as a result of the infiltration of various elements, which keeps the welded parts together. The prolonged precipitation of chromium carbides at the grain boundaries during microwave processing is what causes the higher levels of chromium and carbon to be present at the joint. The explanation for the creation of strong bonds is justified by the production of iron and chromium carbides at the joint. Nickel and intermetallics of nickel and iron make up the majority of the grains' composition. In XRD analysis, the production of these intermetallics has already been covered.

5.10 Summary

In this chapter, according to the DOE listed in table 3.3, welding for butt-positioned metal produced utilising microwave hybrid heating was carried out. The welding process input parameters (welding time, slurry weight, and powder size) have a significant impact on the joint characterization. For best results, joint areas should be clear of debris, flaws, faulty fusion, etc. Because these characteristics not only affect the joint but also revealed information about the mechanical and metallurgical integrity, direct impacts as well as interaction effects were also investigated in this study project. To provide optimal welding settings and improve welding quality, mathematical modelling is done using RSM. The importance of the model for the DOE is assessed using the Central Composite Face Centred Design (CCFCD). ANOVA used to investigate how process factors affect the weld joint and how each parameter affects the output responses (tensile strength, micro hardness, and surface temperature). In order to make the model meaningful and the lack of fit- not significant, quadratic model equations are created.

After process parameter tuning, this chapter shows the findings of several metallurgical and mechanical characterizations of microwave treated welding. Graphs are used to describe the impacts of process parameters as well as the consequences of their interactions. In order to explore distinct phases, compounds, elements present, and their distribution, metallurgical characterizations of so-developed welding have been carried out in various capacities using XRD methods. Weld microstructure was first examined using an optical microscope, and then in greater detail using a field emission scanning electron microscope (FESEM). Energy Dispersive x-ray spectroscopy (EDS) analysis also done at various locations of joint for elemental weight in percentage. Vickers microhardness tests and tensile tests were used to characterise the various welding processes mechanically. An infrared gun was used to measure the joint section's surface temperature.

CHAPTER 6: CONCLUSIONS AND SCOPE FOR FUTURE WORK

Precise conclusions have been reported in this chapter. Second section of the chapter outlines potential follow-up research that might build on the study's findings.

6.1 Conclusions

The main goal of the current study was to use a domestic microwave oven operating at a frequency of 2.45 GHz and a maximum power output of 900 W to melt nickel particles and create joints using microwave hybrid heating. The key findings of the current work are outlined below.

- The development of green manufacturing technologies will be facilitated by the low energy needs for microwave material processing and the reduction in pollutants.
- This study examined the integrated effects of welding time, slurry weight, and powder size on the tensile strength, microhardness, and surface temperature of microwave processed welding of stainless steel 304. Experiments were conducted using a rotatable central composite design.
- For tensile strength, microhardness, and surface temperature, mathematical models have been developed. Using CCDFC of RSM, the models were analysed.
- ANOVA is used to investigate how process factors affect the weld joint and how each parameter affects the output responses (tensile strength, microhardness, and surface temperature).

- In order to make the model meaningful and the lack of fit insignificant, quadratic model equations are created.

6.1.1 Mechanical Characterizations of Microwave Processed welding

- As welding time and slurry weight increases, tensile strength, microhardness, and surface temperature of the welded material all increases, but as particle size increases, all three output variables decreases.
- The greatest values of tensile strength (501MPa), microhardness (454Hv), and surface temperature (926.3⁰C) in the welded region are obtained using experimental settings of 13 minutes of welding time, 3 gram of slurry weight, and 5 microns meter of powder size.

6.1.2 Effects of Process Parameter on Tensile Strength

- According to the ANOVA table for tensile strength, welding time is the most important factor among the three input parameters, contributing 49.10 percent of the total, followed by powder particle size, which contributed 13.50 percent in the opposite direction, and slurry weight, which contributed 3.40 percent.
- The tensile strength of the joint material increases as the welding time increases because of improved heat transfer qualities that improve the microstructural property. Therefore, higher welding times are always preferred within the permitted range for improved tensile strength.
- The tensile strength of the material is decreases as the powder size increases because more heat is absorbed at a faster rate when the particle size drops from its highest value to its minimum value. As a result, the microstructure of the welded connection becomes finer, increasing its tensile strength.

- The value of the tensile strength of the welded specimen slightly increases as the weight of the slurry increases because more nickel particles are seen within the joint region as the weight of the interface material increases, which is responsible for the higher value of tensile strength.
- The relationship between the welding time, powder size, slurry weight, and tensile strength is represented on a graph. The graph indicates that tensile strength increases together with welding time and slurry weight. On tensile strength, welding time has a greater impact than slurry weight.

6.1.3 Effects of Process Parameter on Microhardness

- From the lowest number to the greatest value, welding time increases together with the hardness of the welded material. As the welding time increases, more heat is delivered to the nickel powder, increasing the melting capacity of the nickel particles and, as a result, increased the joint's strength.
- It is anticipated that the hardness of the joint region will decrease as particle size increases. Because less grain size absorbs more heat, which causes the microstructure of the welded joint to be finer and raises the joint area's hardness value.
- The value of the welded specimen's hardness increases as the slurry weight increases because more nickel particles are melted, increasing the value of hardness in the joint.
- The relationship between welding time, slurry weight, and particle size is represented via an interactive graph. The graph shows that as welding time and slurry weight increases, the values of microhardness of the joint increase, while both the output values decreases when particle size increases.

6.1.4 Effects of Process Parameters on Surface Temperature

- It is noticeable that when the welding time for processed joints is longer, the surface temperature of the joint area is more because the welded surface is able to absorb more heat, which raises the surface temperature of the joint area.
- Slurry weight has the same impact, although the fluctuation range is relatively small.
- When the particle size is increased, the surface temperature of the joint region decreases because there are more coarse particles present, which absorb less heat as compared with fine particles.
- Due to the fact that the difference between the lines for the maximum and minimum value of welding time is greater than that of the other two input parameters, it is evident from the interactive effects plots of welding time, slurry weight, and powder size on surface temperature that the latter two clearly have more of an impact on the temperature (slurry weight and powder size).

6.1.5 Characterizations of the Microwave-Processed welded joint by XRD, Microstructure, FESEM and EDS

The following are the main deductions made from the results:

- The high microwave heating caused a variety of intermetallics to develop, according to the XRD examination. Carbides and phases of iron and nickel (Cr_3C_2 , Fe_2C , NiSi , and FeSi) are detected in the research using XRD analysis at 2 theta values (70 degrees). The existence of additional nickel elements in the powder and substrate also contributes to the creation of these elements,

and as a result of the diffusion process, the nickel powder melts with a thin layer of substrate. Iron phases present in the weld zone because nickel powder and substrate material were mixed together. The presence of carbides caused by the free carbon that was present in the graphite sheet (separator) and charcoal powder that combined with the nickel powder during microwave heating.

- The FESEM picture demonstrates the substrate's metallurgical coupling with the powder particle after it has completely melted. According to the findings of the microstructure and FESEM studies, microwave processing resulted in superior microstructures with fewer flaws at the maximum value of the process parameter than at lower input values. Absolute fusion of flaying surfaces and appropriate metallurgical bonding with metal are achieved by volumetric and uniform heating throughout the joint.
- The fragments of the broken tensile specimens examined using FESEM. The graphic makes that the joint failed due to a mixed mode of failure. As seen by the abrupt separation (brittle failure) and plastic deformation (cone formation) in the ductile mode failure, both brittle and ductile modes of failure were seen during the joint fracture. Brittle failure results from the presence of carbide phases in the material, while ductile failure is caused by the presence of a comparatively soft matrix made up of solidified Ni powder.
- According to the EDS analysis for the maximum, intermediate and minimum output values, the joint section's chromium and carbon content will be higher for the maximum output values than for the intermediate value and minimum output values, which will result in the mechanical values being at their highest for the maximum value of the input parameter.

6.2 Scope for Future Work

Due to the inherent benefits of microwave radiation in material processing, researchers have continued to study sintering, coatings, claddings, surface treatments, joining, heat treatment, heating optimization, and other related topics. Many investigations into the advancement and characterization of microwave processed welding were conducted with the help of the current study. Below are a few ideas for the next work:

- In the current study, a domestic microwave oven operating at 2.45 GHz with a 900 W output was employed. Industrial microwave applicators with variable frequency and increased power can be utilised to shorten processing times.
- It is possible to investigate the potential of hybrid processing technologies that combine microwaves with other heating sources, such as laser beams.
- The establishment of rational and empirical relations for determining the heat flow rate into and out of the target materials, susceptor, and specimens for theoretical modelling of the microwave joining process can be done.
- To properly forecast joining process parameters such as heat production rate, heat flow rate, time needed for joining, etc., software-based simulation of the microwave joining process may be investigated.
- For microwave joining, mostly rectangular and circular cross-sections have been studied. For the purpose of this technique, other cross-sections can also be investigated and evaluated for efficacy.
- The insulating boxes and refractory bricks used in this method only last for two to three cycles before they must be thrown away owing to wear and tear from frequent use. It is necessary to look into better, longer-lasting materials for bricks and boxes.

REFERENCES

- [1] Adachi S. and Ueda N. (2013). Surface hardness improvement of plasma-sprayed AISI 316L stainless steel coating by low temperature plasma carburizing. *Advanced Powder Technology*, 24, 818–823.
- [2] Adak D. K., Mukherjee M. and Pal T. K. (2015). Development of a direct correlation of bead geometry, grain size and HAZ width with the GMAW process parameters on bead-on-plate welds of mild steel. *Transactions of the Indian Institute of Metals*, 68(5), 839-849.
- [3] Agrawal D. (2006). Microwave sintering, brazing and melting of metallic materials. *Sohn International Symposium*, TMS, 4, 184–192.
- [4] Agrawal, D. (2013). Microwave Sintering of Metal Powders: Metals and Surface Engineering: Advances in Powder Metallurgy; Wood head publishing: UK, ISBN: 9780857094209.
- [5] Ahmed A. and Siores E. (2001). Microwave joining of 48% alumina– 32% zirconia–20% silica ceramics. *Journal of Material Process Technology*, 118, 88–95.
- [6] Almeida F.J.M., Martinelli J.R. and Partiti C.S.M. (2007). Characterization of iron phosphate glasses prepared by microwave heating. *Journal of Non-Crystalline Solids*, 353:4783- 4791.
- [7] Appleton T.J., Colder R.I., Kingman S.W. Lowndes I.S. and Read A.G. (2005). Microwave technology for energy-efficient processing of waste. *Applied Energy*, 81(1):85- 113.
- [8] Aravindan S. and Krishnamurthy R. (1999). Joining of ceramic composites by microwave heating. *Material Letters*, 38, 245–249.
- [9] Badiger R. I., Narendranath S. and Srinath M. S. (2015). Joining of inconel-625 alloy through microwave hybrid heating and its characterization. *Journal of Manufacturing Processes*, 18, 117–123.
- [10] Bagha L., Sehgal S. and Thakur A. (2016). Comparative analysis of microwave based joining/welding of SS304-SS304 using different interfacing materials. *MATEC Web Conference*, 57 (3001), 1–4.

- [11] Bagha L., Sehgal S., Thakur A. and Kumar H. (2017). Effects of powder size of interface material on selective hybrid carbon microwave joining of SS304–SS304. *Journal of Manufacturing Processes*, 25, 290–295.
- [12] Bagha L., Sehgal S., Thakur A., and Kumar H. and Goyal D. (2019). Low cost joining of SS304-SS304 through microwave hybrid heating without filler-powder, *Engineering Research Express*, 1(2), doi: 10.1088/2631-8695/ab551d.
- [13] Balanis CA. (1989). Advanced engineering electromagnetics. *New York: John Wiley & Sons, Inc.*
- [14] Bansal A., Sharma A. K. and Das S. (2013). Metallurgical and mechanical characterization of mild steel-mild steel joint formed by microwave hybrid heating process. *Sadhana - Academy Proceedings in Engineering Science*, 38 (4), 679–686.
- [15] Bansal A., Sharma A. K., Das S. and Kumar P. (2015). On microstructure and strength properties of microwave welded Inconel 718/stainless steel (SS-316L). *Proceedings of the Institution of Mechanical Engineers, Part L: Journal of Materials: Design and Applications*, 230 (5), 939–948.
- [16] Bansal A., Sharma A. K., Kumar P. and Das S. (2012). Application of electromagnetic energy for joining inconel 718 plates. *Journal on Mechanical Engineering*, 2 (4), 18–24.
- [17] Bansal A., Sharma A. K., Kumar P. and Das S. (2012). Joining of mild steel plates using microwave energy. *Advanced Materials Research*, 585, 465–469.
- [18] Bansal A., Sharma A. K., Kumar P. and Das S. (2014). Characterization of bulk stainless steel joints developed through microwave hybrid heating. *Materials Characterization*, 91, 34–41.
- [19] Bansal A., Sharma A. K., Kumar P. and Das S. (2014). Investigation on microstructure and mechanical properties of the dissimilar weld between mild steel and stainless steel-316 formed using microwave energy. *Proceedings of the Institution of Mechanical Engineers, Part B: Journal of Engineering Manufacture*, 230 (3), 439–448.
- [20] Bansal A., Sharma A. K., Kumar P. and Das S. (2015). Structure–property correlations in microwave joining of inconel 718. *Journal of Minerals, Metals and Materials Society*, 67 (9), 2087–2098.

- [21] Bao R. and Yi J. (2014). Densification and alloying of microwave sintering WC-8 wt.%Co composites. *International Journal of Refractory Metals and Hard Materials*, 43, 269–275.
- [22] Bao R., Yi J., Peng Y. and Zhang H. (2013). Effects of microwave sintering temperature and soaking time on microstructure of WC - 8Co. *Transactions of Nonferrous Metals Society of China*, 23, 372–376.
- [23] Benavente R., Salvador M.D., Penaranda-Foix F.L., Pallone E. and Borrell A. (2014). Mechanical properties and microstructural evolution of alumina–zirconia nanocomposites by microwave sintering. *Ceramics International*, 40, 11291–11297
- [24] Benedetto A. and Calvi A. (2013). A pilot study on microwave heating for production and recycling of road pavement materials. *Construction and Building Materials*, 44, 351–359.
- [25] Ben-Lalli A., Meot J.M., Collignan A. and Bohuon P. (2011). Modelling heat-disinfestation of dried fruits on biological model larvae *Ephestiakuehniella* (Zeller). *Food Research International*, 44(1):156-166.
- [26] Bian H., Yang Y., Wang Y., Tian W., Jiang H. Hu, Z. and Yu W. (2012). Alumina—titania ceramics prepared by microwave sintering and conventional pressure-less sintering. *Journal of Alloys and Compounds*, 525, 63–67.
- [27] Bobicki E.R., Liu Q. and Xu Z. (2014). Microwave heating of ultramafic nickel ores and mineralogical effects. *Minerals Engineering*, 58, 22–25.
- [28] Boromei I., Casagrande A., Tarterini F., Poli G., Verones, P. and Rosa R. (2010). Ni-Al-Ti coatings obtained by microwave assisted SHS: oxidation behaviour in the 750–900°C range. *Surface and Coatings Technology*, 204, 1793–1799.
- [29] Brosnan K.H., Messing G.L. and Agrawal D. (2003). Microwave sintering of alumina at 2.45 GHz. *Journal of the American Ceramic Society*, 86(8), 1307–1312.
- [30] Bruce R.W., Fliflet, A.W., Huey H.E. and Stephenson C. (2010). Microwave sintering and melting of titanium powder for low-cost processing. *Key Engineering Materials*, 436, 131–140.
- [31] Bykov Y.V., Egorov S.V., Eremeev A.G., Holoptsev V.V., Plotnikov I.V., Rybakov K.I., Semenov V.E. and Sorokin A.A. (2014). Temperature profile

- optimization for microwave sintering of bulk Ni–Al₂O₃ functionally graded materials. *Journal of Materials Processing Technology*, 214, 210–216.
- [32] Bykov Y.V., Rybakov K.I. and Semenov V.E. (2001). High-temperature microwave processing of materials, *Journal of Physics D: Applied Physics*, 34, R55–R75.
- [33] Cammarota G.P., Casagrande A., Poli G. and Veronesi P. (2009). Ni–Al–Ti coatings obtained by microwave assisted SHS: effect of annealing on microstructural and mechanical properties. *Surface and Coatings Technology*, 203, 1429–1437.
- [34] Cao R., Feng Z., Lin Q. and Chen J.H. (2014). Study on cold metal transfer welding– brazing of titanium to copper. *Materials and Design*, 56, 165–173.
- [35] Chanda A., Dasgupta S., Bose S., and Bandyopadhyay A. (2009). Microwave sintering of calcium phosphate ceramics. *Materials Science and Engineering: C*, 29(4), 1144–1149.
- [36] Chandel R. S., Seow H. P. and Cheong F. L. (1997). Effect of increasing deposition rate on the bead geometry of submerged arc welds. *Journal of materials processing technology*, 72(1), 124–128.
- [37] Chandrasekaran S., Basak T. and Ramanathan S. (2011). Experimental and theoretical investigation on microwave melting of metals. *Journal of Materials Processing Technology*, 211, 482–487.
- [38] Chen L., Tang C.Y. and Ku H.S. (2014). Microwave sintering and characterization of polypropylene/multi-walled carbon nanotube/hydroxyapatite composites. *Composites Part B: Engineering*, 56, 504–511.
- [39] Cheng J., Roy R. and Agrawal, D. (2002). Radically different effects on materials by separated microwave electric and magnetic fields. *Material Research Innovation* 5, 170–177.
- [40] Cherradi A., Marinel S., Lakhdari G., Desgardin G., Provost J., Raveau B. (1994). A symmetric cavity that saves energy during microwave processing of materials. *Microwave Journal*, 41(2).
- [41] Clark D. E., and Sutton W. H. (1996). Microwave Processing of Materials. *Annual Review of Materials Science*, 26 (1) 299–331.
- [42] Clark D.E. and Sutton W.H. (1999). Microwave processing of materials, *Annu. Rev. Mater. Composites: Part A-Applied Science and Manufacturing*, 30(9):1055-1071.

- [43] Cravotto G., Di Carlo S., Ondruschka B., Tumiatti V. and Roggero C.M. (2007). Decontamination of soil containing POPs by the combined action of solid Fenton-like reagents and microwaves. *Chemosphere*, 69(8):1326-1329.
- [44] Das S., Bansal A. and Sharma A.K. (2012). Theory of welding of metallic parts in microwave cavity applicator. *Fundamental of Journal Modern Physics*, 3(2), 125–155.
- [45] Das S., Mukhopadhyay A.K., Datta S., Das G.C. and Basu D. (2008). Hard glass-ceramic coating by microwave processing. *Journal of the European Ceramic Society*, 28(4):729- 738.
- [46] Demirskyi D., Agrawal D. and Ragulya A. (2013). Comparisons of grain size-density trajectory during microwave and conventional sintering of titanium nitride. *Journal of Alloys and Compounds*, 581, 498–501.
- [47] Deng H., Li G.X., Yang H.B., Tang J.P. and Tang J.Y. (2010). Preparation of activated carbons from cotton stalk by microwave assisted KOH and K₂CO₃ activation. *Chemical Engineering Journal*. 163(3):373-381.
- [48] Duval D.J., Phillips B.L., Terjak M.J.E. and Risbud S.H. (1997). Reversible color changes and structural implications of microwave melting ion-conducting glasses. *Journal of Solid State Chemistry*.131(1):173-176.
- [49] Dwivedi S. P. and Sharma S. (2014). Effect of process parameters on tensile strength of 1018 mild steel joints fabricated by microwave welding. *Metallography, Microstructure and Analysis*, 3 (1), 58–69.
- [50] Egerton R. F. (2005). Physical principles of electron microscopy: *An Introduction to TEM, SEM, and AEM*. New York: Springer.
- [51] Fang Y., Agrawal D., Roy R. and Jayan P.S. (2000). Continuous microwave sintering of alumina abrasive grit. *Journal of Materials Processing Technology*, 108, 26–29.
- [52] Fang Y., Cheng J. and Roy R. (1997). Enhancing densification of zirconia-containing ceramic-matrix composites by microwave processing. *Journal Material Science*, 32: 4925–4930.
- [53] Gautam U. and Vipin. (2018). overview of Welding using Microwave Radiation, *International journal of Advanced Production and Industrial Engineering*, IJAPIE-2018-10-422, 3(4), pages 11-14, ISSN 2455–8419.

- [54] Gautam U. and Vipin. (2021). Joining of Metals Using Microwave Energy, *Lecture Notes in Mechanical Engineering*, pp. 1035–1039, http://doi:10.1007/978-981-15-5463-6_92, ISBN978-981-15-5462-9.
- [55] Gautam U., Asgar M. E., Singh K., A review on materials processing using microwave radiation. *Materials Today: Proceedings*.2214-7853,<https://doi.org/10.1016/j.matpr.2022.10.249>.
- [56] Gautam U. and Vipin. (2022). Effect of Process Parameter on Tensile Strength and Hardness of SS 304 Processed by Microwave Radiation, *Transactions of Indian Institute of Metals*, volume 75, Issue 3, pages 653-662, <https://doi.org/10.1007/s12666-021-02440-1>.
- [57] Gautam U. and Vipin. (2022). Joint Characterization of SS 304 Processed by Microwave Radiation, *Journal of Engineering Research*, special issue, 135-143, <http://doi:10.36909/jer.ICAPIE.15047>.
- [58] Giberson R.T. and Sanders M. (2009). The real benefits of microwave-assisted processing go beyond time savings. *Microscopy and Microanalysis*, 15, 926–927.
- [59] Gnyusov S.F. and Tarasov S.Y. (2014). The microstructural aspects of abrasive wear resistance in composite electron beam clad coatings. *Applied Surface Science*, 293, 318–325.
- [60] Granastein V.L., Parker R.K. and Armstrong C.M. (1999). Vacuum Electronics at the dawn of the Twenty-First Century, *P. IEEE*, 87, 702–716.
- [61] Gronwald F. and Nitsch J. (2001). The structure of the electromagnetic field as derived from first principles, *IEEE Antennas Propagation Magazine*, 43, 64-79.
- [62] Gunaraj V. and Murugan N. (2002). Prediction of heat-affected zone characteristics in submerged arc welding of structural steel pipes. *Welding Journal-New York-*, 81(3), 45-s.
- [63] Guo J.F., Chen H.C., Sun C.N., Bi G., Sun Z. and Wei J. (2014). Effects of process parameters Friction stir welding of dissimilar materials between AA6061 and AA7075 Al alloys. *Materials and Design*, 56, 185–192.
- [64] Gupta D. and Sharma A.K. (2010). A method of cladding/coating of metallic and non-metallic powders on metallic substrate by microwave irradiation. *Patent 527/Del/2010*, India.
- [65] Gupta D. and Sharma A.K. (2011). Copper coating on austenitic stainless steel using microwave hybrid heating. *Proceedings of the Institution of Mechanical*

- Engineers, Part E: Journal of Process Mechanical Engineering [PIE]*, 226, 132–141.
- [66] Gupta D. and Sharma A.K. (2011). Investigation on sliding wear performance of WC10Co2Ni cladding developed through microwave irradiation. *Wear*, 271, 1642–1650.
- [67] Gupta D. and Sharma A.K. (2011). Microwave cladding: a new surface engineering technique for developing uniform microstructure. *i-manager's Journal on Mechanical Engineering*, 1, 17–23.
- [68] Gupta D. and Sharma A.K. (2011). The Minerals, M. & M.S. (TMS): Development of Copper Coating on Austenitic Stainless Steel through Microwave Hybrid Heating; *Supplemental Proceedings; John Wiley & Sons: Hoboken, NJ, USA*, pp. 263–270.
- [69] Gupta D. and Sharma A.K. (2012). Microstructural characterisation of cermet cladding on austenitic stainless steel developed through microwave irradiation. *Journal of Materials Engineering and Performance*, 21, 2165- 2172.
- [70] Gupta D. and Sharma A.K. (2014). Microwave cladding: A new approach in surface engineering. *Journal of Manufacturing Process*, 16(2), 176–182.
- [71] Gupta D., Bhovi P.M., Sharma A.K. and Dutta S. (2012) Development and characterization of microwave composite cladding. *Journal of Manufacturing Processes*, 14(3), 243–249.
- [72] Gupta D., Sharma A.K., Link G. and Thumm M. (2012). Investigation on Microstructural Characterization of Microwave Cladding, Processing and Properties of Advanced Ceramics and Composites IV; *Ceramic Transactions: Wiley*, , pp 133–143. ISBN: 978-1-1184-9183-6.
- [73] Gupta M. and Wong W.L.E. (2005). Enhancing overall mechanical performance of metallic materials using two directional microwaves assisted rapid sintering. *Scripta Material*; 52: 479–483.
- [74] Gupta M., Wong W. L.E. (2007). *Microwaves and metals*. Singapore: John Wiley & Sons (Asia). *Wiley online library*.
- [75] Gupta P. and Kumar S. (2014). Investigation of stainless steel joint fabricated through microwave energy. *Materials Manufacturing Process*, 29(8), 910–915.
- [76] Gupta P., Kumar S. and Kumar A. (2013). Study of joint formed by tungsten carbide bearing alloy through microwave welding. *Materials and Manufacturing Processes*, 28 (5), 601–604.

- [77] Guy A.W. (1984). History of Biological Effects and Medical Applications of Microwave Energy, *IEEE T. Microwave Theory*, 32, 1182–1200.
- [78] H. Matsumoto. (2002). Research on solar power satellites and microwave power transmission in Japan. *IEEE Microwave Magazine*, 3(4), 36-45.
- [79] Hajiannia I., Shamanian M. and Kasiri M. (2013). Microstructure and mechanical properties of AISI 347 stainless steel/A335 low alloy steel dissimilar joint produced by gas tungsten arc welding. *Materials and Design*, 50, 566–573.
- [80] Handbook series N 9014, Design guidelines for selection and use of stainless steel, distributed by Nickel Development Institute.
- [81] He W.D., Pan C.Y. and Lu T. (2001). Soapless emulsion polymerization of butyl methacrylate through microwave heating. *Journal of Applied Polymer Science*, 80(13):2455- 2459.
- [82] Heddleson R.A and Doores S. (1994). Factors affecting microwave-heating of foods and microwave-induced destruction of food borne pathogens - a review. *Journal of Food Protection*, 57(11):1025-1037.
- [83] Hemono N., Chenu S., Lebullenger R., Rocherulle J., Keryvin V. and Wattiaux A. (2010). Microwave synthesis and physical characterization of tin (II) phosphate glasses. *Journal of Materials Science*, 45, 2916-2920.
- [84] Holcombe C.E., Dykes N.L. (1991). Microwave sintering of titanium diboride. *Journal of Materials Science*, 26, 3730–3738.
- [85] Horikoshi S., Sumi T. and Serpone N. (2013). A hybrid microreactor/ microwave high-pressure flow system of a novel concept design and its application to the synthesis of silver nanoparticles. *Chem Eng Process: Process Intensif*; 73, 59–66.
- [86] Huang Z., Gotoh M., Hirose Y. (2009). Improving sinterability of ceramics using hybrid microwave heating. *Journal of Materials Processing Technology*, 209, 2446–2452.
- [87] Ishii T.K. (Ed.) (1995). Handbook of Microwave Technology Vol. 2 Applications, *Academic Press*, London.
- [88] Ishizaki K., Nagata K. and Hayashi T. (2006). Production of pig iron from magnetite ore–coal composite pellets by microwave heating. *ISIJ Int*; 46, 1403–1409.
- [89] Jayalakshmi S., Sahu S., Sankaranarayanan S., Gupta S. and Gupta M. (2014). Development of novel Mg–Ni₆₀Nb₄₀ amorphous particle reinforced composites

- with enhanced hardness and compressive response. *Materials and Design*, 53, 849–855.
- [90] Jou M. (2003). Experimental study and modeling of GTA welding process. *Journal of Manufacturing Science Engineer*, 125(4), 801-808.
- [91] Kawala Z. and Atamanczuk T. (1998). Microwave-enhanced thermal decontamination of soil. *Environmental Science and Technology*, 32(17), 2602-2607.
- [92] Kharissova O.V., Kharisov B.I., Valdes J.J.R. (2010). Review: The use of microwave irradiation in the processing of glasses and their composites. *Industrial and Engineering Chemistry Research*, 49(4):1457-1466.
- [93] Komarneni S., Rajha R.K., Katsuki H. (1999). Microwave hydrothermal processing of titanium dioxide. *Materials Chemistry and Physics*, 61, 50–54.
- [94] Kumar P., Ingle A. and Jhavar S. (2019). Parametric review of microwave-based materials, *Journal of Materials Research Technology*, 8(3), 3306–3326.
- [95] Kumar S., Sehgal S., Singh S. and Bagha A. K. (2020). Investigations on material characterization of joints produced using microwave hybrid heating, *Materials today: proceedings*, 28, <https://doi.org/10.1016/j.matpr.2020.04.588>.
- [96] Kumar V. and Sehgal S. (2020). Joining of duplex stainless steel through selective microwave hybrid heating technique without using filler material, *Material Today Proceedings*, 28, 1314–1318, doi: 10.1016/j.matpr.2020.04.509.
- [97] Lai F.D., Wu T.I. and Wu J.K. (1993). Surface modification of Ti-6Al-4V alloy by salt cyaniding and nitriding. *Surface and Coatings Technology*, 58, 79–81.
- [98] Lee J. I. and Rhee S. (2000). Prediction of process parameters for gas metal arc welding by multiple regression analysis. *Proceedings of the Institution of Mechanical Engineers, Part B: Journal of Engineering Manufacture*, 214(6), 443-449.
- [99] Leonelli C., Veronesi P., Denti L., Gatto A. and Iuliano L. (2008). Microwave assisted sintering of green metal parts. *Journal of Materials Processing Technology*, 205, 489–496.
- [100] Lin L.H., Chen S.C., Wu C.Z., Hung J.M. and Ou, K.L. (2011). Microstructure and antibacterial properties of microwave plasma nitrided layers on biomedical stainless steels. *Applied Surface Science*, 257, 7375–7380.

- [101] Lin S. and Xiong W. (2012). Microstructure and abrasive behaviours of TiC-316L composites prepared by warm compaction and microwave sintering. *Advanced Powder Technology*, 23, 419–425.
- [102] Loupy A. (2004). Solvent-free microwave organic synthesis as an efficient procedure for green chemistry, *Comptes Rendus Chimie*, 7(2), 103-112, ISSN 1631-0748.
- [103] Lu J., Mu Y., Luo X. and Niu J. (2012). A new method for soldering particle-reinforced aluminum metal matrix composites. *Materials Science Engineering B*, 177, 1759–1763.
- [104] Mallia B. and Dearnley P.A. (2013). Exploring new W–B coating materials for the aqueous corrosion–wear protection of austenitic stainless steel. *Thin Solid Films*, 549, 204–215.
- [105] Mallon F.K. and Ray W.H. (1998). Enhancement of solid-state polymerization with microwave energy. *Journal of Applied Polymer Science*, 69(6), 1203-1212.
- [106] Mazur M., Szymanska M., Kalisz M., Kaczmarek D. and Domaradzki J. (2014). Surface and mechanical characterization of ITO coatings prepared by microwave-assisted magnetron sputtering process. *Surface and Interface Analysis*, 46, 827–831.
- [107] Mendez P.F., Barnes N., Bell K., Borle S.D., Gajapathi S.S., Guest S.D., Izadi H., Gol A.K. and Wood G. (2014). Welding processes for wear resistant overlays. *Journal of Manufacturing Processes*, 16, 4–25.
- [108] Menendez J.A., Inguanzo M., Pis J.J. (2002). Microwave-induced pyrolysis of sewage sludge. *Water Research*, 36(13), 3261-3264.
- [109] Menezes R.R. and Kiminami R.H.G.A. (2008). Microwave sintering of alumina–zirconia nanocomposites. *Journal of Materials Processing Technology*, 203, 513–517.
- [110] Menezes R.R., Souto P.M., Kiminami R.H.G.A. (2003). Microwave hybrid fast sintering of methacrylate under pulsed microwave irradiation. *European Polymer Journal*, 39(6): 1187-1193.
- [111] Mondal A., Upadhyaya A. and Agrawal D. (2009). Microwave sintering of W-18Cu and W-7Ni-3Cu alloys. *The Journal of Microwave Power and Electromagnetic Energy*, 43, 6–11.

- [112] Mondal A., Upadhyaya A. and Agrawal D. (2013).Effect of heating mode and copper content on the densification of W-Cu alloys. *Indian Journal of Materials Science*, 2013, 1–7.
- [113] National Research Council. Microwave Processing of Materials. New York: *National Academy Press*, 1994.
- [114] Nowotny S., Berger L.M., and Spatzier J. (2014). Coatings by Laser Cladding, *Material Science*.
- [115] Osepchuk J.M. (1984). A History of Microwave Heating Applications,' *IEEE T. Microwave Theory*, 32, 1200–1224.
- [116] Osepchuk J.M. (2002). Microwave Power Applications, *IEEE T. Microwave Theory*, 50, 975–985.
- [117] Ovadia D.Z., Walker C.E. (1995). Microwave baking of bread. *Journal of Microwave Power and Electromagnetic Energy*, 30(2), 81-89.
- [118] Padmavathi C., Upadhyaya A. and Agrawal D. (2012).Effect of sintering temperature and heating mode on consolidation of Al–7Zn–2 _5Mg–1Cu aluminum alloy. *Bulletin of Materials Science*, 35, 823–832.
- [119] Pal M., Kumar V., Sehgal S., Kumar H., Saxena K. K. and Bagha A. K. (2020). Microwave hybrid heating based optimized joining of SS304/SS316, *Material and Manufacturing Process*, 00, 1–7, doi: 10.1080/10426914.2020.1854469.
- [120] Panda S.S., Singh V., Upadhyaya A. and Agrawal D. (2006).Sintering response of austenitic (316L) and ferritic (434L) stainless steel consolidated in conventional and microwave furnaces. *ScriptaMaterialia*, 54, 2179–2183.
- [121] Patnaik N. and Rao R.B. (2004). Microwave energy in mineral processing – a review, *Inst. Eng. (India) J. – Mining*, 84, 56–61.
- [122] Plucknett K.P. and Wilkinson D.S. (1995). Microstructural characterization of a microwave-sintered silicon nitride based ceramic. *Journal of Materials Research*, 10, 1387–1396.
- [123] Rajkumar K. and Aravindan S. (2013). Tribological behavior of microwave processed copper–nanographite composites. *Tribology International*, 57, 282–296.
- [124] Ramesh P.D., Brandon D., Schachter L. (1999). Use of partially oxidized SiC particle bed for microwave sintering of low loss ceramics. *Materials Science and Engineering* , 266(1-2), 211- 220.

- [125] Rana V. and Sandhu C. S. (2015). Investigation on microstructural and micro hardness of microwave welded joint of EN-31. *International Journal of Latest Trends in Engineering and Technology*, 5 (1), 112–117.
- [126] Ravindran P., Manisekar K., Narayanasamy R. and Narayanasamy P. (2013). Tribological behaviour of powder metallurgy-processed aluminium hybrid composites with the addition of graphite solid lubricant. *Ceramics International*, 39, 1169–1182.
- [127] Ravindran P., Manisekar K., Rathika P. and Narayanasamy P. (2013). Tribological properties of powder metallurgy processed aluminium self-lubricating hybrid composites with SiC additions. *Materials and Design*, 45, 561–570.
- [128] Ren D. and Liu L. (2014) Interface microstructure and mechanical properties of arc spot welding Mg–steel dissimilar joint with Cu interlayer. *Materials and Design*, 59, 369–376.
- [129] Roberts C.J. and Williams P.M. (1999). Scanning Probe Microscopy, Applications, *Encyclopedia of Spectroscopy and Spectrometry*.
- [130] Roy R., Agarwal D., Cheng J., Gedavanishvili S. (1999). Full sintering powdered metal bodies in microwave field, *Nature*, 399, 401, 668-670.
- [131] Ryyanen S. (1995). The electromagnetic properties of food materials - A review of the basic principles. *Journal of Food Engineering*, 26(4), 409-429.
- [132] Saber N., Ju Y., Hsu H.Y. and Lee S.H. (2013). A feasibility study on the application of microwaves for online biofilm monitoring in the pipelines. *International Journal of Pressure Vessels and Piping*, 111–112, 99–105.
- [133] Saitou K. (2006). Microwave sintering of iron, cobalt, nickel, copper and stainless steel powders. *Scripta Materials*, 54, 875–879.
- [134] Salot S., Sehgal S., Pabla B. and Kumar H. (2017). Microwave joining of metals: a review, *Research Journal of Engineering Technology*. 8 (3) 282.
- [135] Satyanarayana V.V., Reddy M. G. and Mohandas T. (2005). Dissimilar metal friction welding of austenitic–ferritic stainless steels. *Journal of Materials Processing Technology*, 160, 128–137.
- [136] Saxena S., Bansal S., Deo R., and Khan S. (2014). Joining of bulk metallic pipes by microwave hybrid heating process under parametrical regulations. *International Organization of Scientific Research-Journal of Mechanical and Civil Engineering*; 11 (6), 62–69.

- [137] Schulz R.L., Folz D.C., Clark D.E. and Wicks G.G. (1994). Microwave energy for waste remediation applications. *Materials Research Society Symposium Proceedings*, 347, 401-406.
- [138] Sethi G., Upadhyaya A. and Agrawal D. (2003). Microwave and conventional sintering of premixed and prealloyed Cu- 12Sn bronze. *Science Sintering*, 35(2): 49–65.
- [139] Shannigrahi S.R., Pramoda K.P. and Nugroho F.A.A. (2012). Synthesis and characterizations of microwave sintered ferrite powders and their composite films for practical applications. *Journal of Magnetism and Magnetic Materials*, 324, 140–145.
- [140] Sharma A., Sehgal S. and Goyal D. (2020). Effects of process parameters in joining of Inconel-625 alloy through microwave hybrid heating, *Materials today: proceedings*, 28(3), 1323-1327.
- [141] Sharma A.K. and Gupta D. (2012). On microstructure and flexural strength of metal–ceramic composite cladding developed through microwave heating. *Applied Surface Science*, 258, 5583–5592.
- [142] Sharma A.K. and Krishnamurthy R. (2002). Microwave processing of sprayed alumina composite for enhanced performance. *Journal of the European Ceramic Society*, 22, 2849–2860.
- [143] Sharma A.K., Srinath M.S. and Kumar P. (2009). Microwave joining of metallic materials. *Patent application 1994/Del/ 2009*, India.
- [144] Singh K. and Sharma S. (2019). Fabrication and Investigation of Co-based and CeO₂-modified Microwave Coatings. *Protection of Metals and Physical Chemistry of Surfaces*, 55(2), 352-358.
- [145] Singh S., Suri N. M., and Belokar R. M. (2015). Characterization of joint developed by fusion of aluminum metal powder through microwave hybrid heating. *Materials Today: Proceedings*, 2 (4–5), 1340–1346.
- [146] Sinnwell S. and Ritter H. (2007). Recent advances in microwave-assisted polymer synthesis. *Australian Journal of Chemistry*, 60(10), 729-743.
- [147] Siores E., and Rego D., (1995). Microwave applications in materials joining. *Journal of Materials Processing Technology*, 48(1–4), 619–625.
- [148] Skolnik M. (2002). Role of Radar in Microwaves. *IEEE T. Microwave Theory*, 50, 625–632.

- [149] Sobol, H. and Tomiyasu, K. (2002). Milestones of Microwaves, *IEEE T. Microwave. Theory*, 50, 594–611.
- [150] Soni P., Sehgal S., Kumar H. and Singh A. P. (2018). Effect of Nickel nanopowder on joining SS316-SS316 through microwave hybrid heating. *Advanced Materials Manufacturing & Characterization*, 8(1).
- [151] Sosa-M. M.E, Valerio-J. L, Lopez-M. A, Garcia H.S. (2010). Dielectric properties of foods: Reported data in the 21st century and their potential applications. *LWT– Food Science and Technology*, 43(8), 1169-1179.
- [152] Sosnik A., Gotelli G. and Abraham G.A. (2011). Microwave-assisted polymer synthesis (MAPS) as a tool in biomaterials science: How new and how powerful. *Progress in Polymer Science*, 36, 1050–1078.
- [153] Sourav, Gautam U., Marwah A., Sharma A., and Lakshay, (2021), Microwave Welding of Mild Steel, *Lecture Notes in Mechanical Engineering*, 885–892, [http:// doi: 10.1007/978-981-15-5463-6_78](http://doi:10.1007/978-981-15-5463-6_78).
- [154] Srikant S.S., Mukherjee P.S. and Rao R.B. (2013). Effect of heat treatment in microwave furnace for placer ilmenite. *International Journal of Applied Science and Engineering*, 11, 245–250.
- [155] Srinath M. S., Sharma A. K. and Kumar P.(2011), Microwave processing of metallic joints and their Characterization. *I-manager’s Journal on Mechanical Engineering*, 11(1).
- [156] Srinath M. S., Sharma A. K., and Kumar P. (2011). A new approach to joining of bulk copper using microwave energy. *Materials and Design*, 32 (5), 2685–2694.
- [157] Srinath M. S., Sharma A. K., and Kumar P. (2011). A novel route for joining of austenitic stainless steel (SS-316) using microwave energy. *Proceedings of the Institution of Mechanical Engineers, Part B: Journal of Engineering Manufacture*, 225 (7), 1083–1091.
- [158] Srinath M. S., Sharma A. K., and Kumar P. (2011). Investigation on microstructural and mechanical properties of microwave processed dissimilar joints. *Journal of Manufacturing Processes*, 13 (2), 141–146.
- [159] Srivastava L. (2005). Ubiquitous Network Societies: The Case of Radio Frequency Identification, International Telecommunication Union Document UNS/04.

- [160] Stein D.F. (1994). Microwave Processing of Materials, Committee on Microwave Processing of Materials, *National Materials Advisory Board*. <https://doi.org/10.17226/2266>.
- [161] Sun Y. and Bell T. (2002). Dry sliding wear resistance of low temperature plasma carburized austenitic stainless steel. *Wear*, 253, 689–693.
- [162] Tajchakavit S, Ramaswamy HS, Fustier P. (1998). Enhanced destruction of spoilagemicroorganisms in apple juice during continuous flow microwave heating. *Food Research International*. 31(10), 713-722.
- [163] Tajchakavit S. and Ramaswamy H.S. (1997). Continuous-flow microwave inactivation kinetics of pectin methyl esterase in orange juice. *Journal of Food Processing and Preservation*. 21(5), 365-378.
- [164] Tamang S. and Aravindan S. (2019). 3D numerical modelling of microwave heating of SiC susceptor, *Applied Thermal Engineering*. 162 (114250).
- [165] Tang C.Y., Wong C.T., Zhang L.N., Choy M.T., Choy T.W., Chan K.C., Yue T.M. and Chen Q. (2013). In situ formation of Ti alloy/TiC porous composites by rapid microwave sintering of Ti6Al4V-MWCNTs powder. *Journal of Alloys and Compounds*, 557, 67–72.
- [166] Tao J., Shi X. (2012). Properties, phases and microstructure of microwave sintered W-20Cu composites from spray pyrolysis continuous reduction processed powders. *Journal of Wuhan University of Technology-Material Science Edition*, 27, 38–44.
- [167] Tata A. and Beone F. (1995). Hospital waste sterilization - A technical and economic comparison between radiation and microwaves treatments. *Radiation Physics and Chemistry*, 46(4-6), 1153-1157.
- [168] Thostenson E.T. and Chou T.-W. (1999). Microwave processing: fundamentals and applications, *Composites Part A Applied Science*, 30, 1055–1071.
- [169] Thuault A., Savary E., Bazin J. and Marinel S. (2014). Microwave sintering of large size pieces with complex shape. *Journal of Materials Processing Technology*, 214, 470.
- [170] Tong C.H. and Lund D.B. (1993). Microwave-heating of baked dough products with simultaneous heat and moisture transfer. *Journal of Food Engineering*. 19(4):319-339.
- [171] Upadhyaya A., Tiwari S.K. and Mishra P. (2007). Microwave sintering of W–Ni–Fe alloy. *Scripta Materialia*, 56, 5–8.

- [172] Upadhyaya D.D., Ghosh A., Dey G.K., Prasad R., Suri A.K. (2001). Microwave sintering of zirconia ceramics. *Journal of Materials Science*, 36, 4707–4710.
- [173] Varela P., Salvador A., Fiszman S.M. (2008). Methodological developments in crispness assessment: Effects of cooking method on the crispness of crusted foods. *LWT–Food Science and Technology*, 41(7), 1252–1259.
- [174] Vishwakarma V. and Uthaman S. (2020). Environmental impact of sustainable green concrete. *Smart Nanoconcretes and Cement-Based Materials*, 241–255.
- [175] Walkiewicz J.W., Kazonich G. and Macgill S.L. ((1988)). Microwave heating characteristics of selected minerals and compounds, *Minerals Metallurgy Process*, 39–42.
- [176] Wang J., Binner J., Pang Y. and Vaidhyanathan B. (2008). Microwave-enhanced densification of sol–gel alumina films. *Thin Solid Films*, 516, 5996–6001.
- [177] Weng F., Chen C. and Yu H. (2014). Research status of laser cladding on titanium and its alloys: a review. *Materials and Design*, 58, 412–425.
- [178] Wiesbrock F., Hoogenboom R. and Schubert U.S. (2004). Microwave-assisted polymer synthesis: State-of-the-art and future perspectives. *Macromolecular Rapid Communications*, 25(20), 1739–1764.
- [179] Wong W.L.E. and Gupta M. (2005). Development of metallic materials using hybrid microwave assisted rapid sintering. *Proceeding: ASME International Mechanical Engineering Congress and Exposition*, Orlando, Florida, USA.
- [180] Yadoji P., Peelamedu R. and Agrawal D. (2003). Microwave sintering of Ni-Zn ferrites: comparison with conventional sintering. *Materials Science Engineering B: Adv*, 98, 269–278.
- [181] Yang Y., He C. and Wu B. (2013). Non-destructive microwave evaluation of plasma sprayed TBCs porosity. *NDT & E International*, 59, 34–39.
- [182] Yarlagadda P.K.D.V., and Chai T.C. (1998). An investigation into welding of engineering thermoplastics using focused microwave energy. *Journal of Material Process Technology*, 74, 199–212.
- [183] Yarlagadda P.K.D.V., and Soon R.C.T. (1998). Characterisation of materials behaviour in microwave joining of ceramics. *Journal of Material Process Technology*, 84, 162–174.
- [184] Zafar S. and Sharma A.K. (2014). Development and characterisations of WC–12Co microwave clad. *Materials Characterization*, 96, 241–248.

- [185] Zafar S., Bansal A., Sharma A.K., Arora N. and Ramesh C.S. (2014). Dry erosion wear performance of Inconel 718 microwave clad. *Surface Engineering*, 30, 852–859.
- [186] Zafar S., Sharma A.K. and Arora N. (2013). Development and microstructural characterisation of Inconel cladding on stainless steel through microwave irradiation. *I-managers Journal Mechanical Engineers*, 3(1), 9–16.
- [187] Zanotto A., Luyt A.S., Spinella A. and Caponetti E. (2013). Improvement of interaction in and properties of PMMA-MWNT nanocomposites through microwave assisted acid treatment of MWNT. *European Polymer Journal*, 49, 61–69.
- [188] Zeng N., Lai L.M.C. and Russell A. (2003). Abuse-Tolerant Metallic Packaging Materials for Microwave Cooking. *US Patent 6552315 B2*.
- [189] Zhang H., Datta A.K., Taub I.A., Doona C. (2001). Electromagnetics, heat transfer, and thermokinetics in microwave sterilization. *AIChE Journal*, 47(9), 1957-1968.
- [190] Zhang M, Tang J, Mujumdar AS, Wang S. (2006). Trends in microwave-related drying of fruits and vegetables. *Trends in Food Science and Technology*, 17(10), 524-534.
- [191] Zheng R.R., Wu Y., Liao S.L., Wang W.Y., Wang W.B. and Wang A.H. (2014). Microstructure and mechanical properties of Al/(Ti,W)C composites prepared by microwave sintering. *Journal of Alloys and Compounds*, 590, 168–175.
- [192] Zhou H., Nabiyouni M. and Bhaduri S.B. (2013). Microwave assisted apatite coating deposition on Ti6Al4V implants. *Material Science Engineering C*, 33, 4435–4443.
- [193] Zhu X.L., Chen J.Y., Cheng Z.P., Lu J.M. and Zhu J. (2003). Emulsion polymerization of styrene under pulsed microwave irradiation. *Journal of Applied Polymer Science*, 89(1), 28-35.

LIST OF PUBLICATIONS

List of papers Published in SCI/SCIE journals

- **Uma Gautam and Vipin** [March, 2022], Effect of Process Parameter on Tensile Strength and Hardness of SS304 processed by Microwave Radiation, Transactions of Indian Institute of Metals, Volume 75, Issue 3, Pages 653-662, <https://doi.org/10.1007/s12666-021-02440-1>.
- **Uma Gautam and Vipin** [March 2022], Joint Characterization of SS 304 Processed by Microwave Radiation, Journal of Engg. Research, special issue pp. 135-143, ISSN 2307-1877, online ISSN 2307-1885, <https://doi.org/10.36909/jer.ICAPIE.15047>.

List of papers Accepted in SCI/SCIE journals

- **Uma Gautam and Vipin**, Influence of Input Parameters on Joint Characterization of SS 304 using Hybrid Microwave Welding, Protection of Metals and Physical Chemistry of Surfaces.
- **Uma Gautam and Vipin**, Influence of processing parameters on Joint Characterization of SS 304 using Microwave Hybrid Heating, Journal of Process Mechanical Engineering.

List of papers communicated in SCI/SCIE journals

- **Uma Gautam and Vipin**, Optimization of Multi Response Process Parameters in Microwave Processed Joints of SS304 using Grey Relational Analysis, IJEMS.

Research Work presented at Conferences

- **Uma Gautam and Vipin** [5-6 October, 2018], overview of welding using Microwave Radiation International conference on Advanced Production and Industrial Engineering, organized by Delhi Technological University.
- **Uma Gautam and Vipin** [26-27 July 2019], Material Joining using Microwave Hybrid Heating ,International Conference on Emerging Trends in Electro-Mechanical Technologies & Management, organized by HMR Institute of Technology and Management.